Sandor, B.I.; Roloff, R; et. al. “Mechanics of Solids”
Mechanical Engineering Handbook
Ed. Frank Kreith
Boca Raton: CRC Press LLC, 1999

Mechanics of Solids

Bela I. Sandor
University of Wisconsin-Madison

Ryan Roloff
Allied Signal Aerospace

Stephen M. Birn
Allied Signal Aerospace

Maan H. Jawad
Nooter Consulting Services

Michael L. Brown
A.O. Smith Corp.

1.1 Introduction

Bela I. Sandor

Engineers use the concepts and methods of mechanics of solids in designing and evaluating tools, machines, and structures, ranging from wrenches to cars to spacecraft. The required educational background for these includes courses in statics, dynamics, mechanics of materials, and related subjects. For example, dynamics of rigid bodies is needed in generalizing the spectrum of service loads on a car, which is essential in defining the vehicle's deformations and long-term durability. In regard to structural

FIGURE 1.1.1 Artist's concept of a moving stainless steel roadway to drive the suspension system through a spinning, articulated wheel, simulating three-dimensional motions and forces. (MTS Systems Corp., Minneapolis, MN. With permission.) Notes: Flat-Trac® Roadway Simulator, R&D100 Award-winning system in 1993. See also Color Plate 1.*

integrity and durability, the designer should think not only about preventing the catastrophic failures of products, but also of customer satisfaction. For example, a car with gradually loosening bolts (which is difficult to prevent in a corrosive and thermal and mechanical cyclic loading environment) is a poor product because of safety, vibration, and noise problems. There are sophisticated methods to assure a product's performance and reliability, as exemplified in Figure 1.1.1. A similar but even more realistic test setup is shown in Color Plate 1.

It is common experience among engineers that they have to review some old knowledge or learn something new, but what is needed at the moment is not at their fingertips. This chapter may help the reader in such a situation. Within the constraints of a single book on mechanical engineering, it provides overviews of topics with modern perspectives, illustrations of typical applications, modeling to solve problems quantitatively with realistic simplifications, equations and procedures, useful hints and reminders of common errors, trends of relevant material and mechanical system behaviors, and references to additional information.

The chapter is like an emergency toolbox. It includes a coherent assortment of basic tools, such as vector expressions useful for calculating bending stresses caused by a three-dimensional force system on a shaft, and sophisticated methods, such as life prediction of components using fracture mechanics and modern measurement techniques. In many cases much more information should be considered than is covered in this chapter.

* Color Plates 1 to 16 follow page 1-131.

1.2 Statics

Bela I. Sandor

Vectors. Equilibrium of Particles. Free-Body Diagrams

Two kinds of quantities are used in engineering mechanics. A scalar quantity has only magnitude (mass, time, temperature, …). A vector quantity has magnitude and direction (force, velocity, ...). Vectors are represented here by arrows and bold-face symbols, and are used in analysis according to universally applicable rules that facilitate calculations in a variety of problems. The vector methods are indispensable in three-dimensional mechanics analyses, but in simple cases equivalent scalar calculations are sufficient.

Vector Components and Resultants. Parallelogram Law

A given vector **F** may be replaced by two or three other vectors that have the same net effect and representation. This is illustrated for the chosen directions *m* and *n* for the components of **F** in two dimensions (Figure 1.2.1). Conversely, two concurrent vectors **F** and **P** of the same units may be combined to get a resultant **R** (Figure 1.2.2).

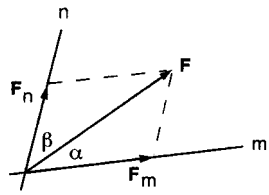

FIGURE 1.2.1 Addition of concurrent vectors **F** and **P**.

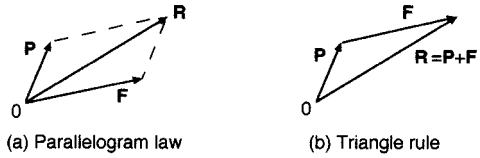

FIGURE 1.2.2 Addition of concurrent, coplanar vectors **A**, **B**, and **C**.

Any set of components of a vector **F** must satisfy the *parallelogram law.* According to Figure 1.2.1, the law of sines and law of cosines may be useful.

$$\frac{F_n}{\sin\alpha} = \frac{F_m}{\sin\beta} = \frac{F}{\sin\left[180^\circ - (\alpha+\beta)\right]}$$
$$F^2 = F_n^2 + F_m^2 - 2F_nF_m\cos\left[180^\circ - (\alpha+\beta)\right] \qquad (1.2.1)$$

Any number of concurrent vectors may be summed, mathematically or graphically, and in any order, using the above concepts as illustrated in Figure 1.2.3.

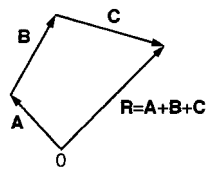

FIGURE 1.2.3 Addition of concurrent, coplanar vectors **A**, **B**, and **C**.

Unit Vectors

Mathematical manipulations of vectors are greatly facilitated by the use of unit vectors. A unit vector **n** has a magnitude of unity and a defined direction. The most useful of these are the unit coordinate vectors **i**, **j**, and **k** as shown in Figure 1.2.4.

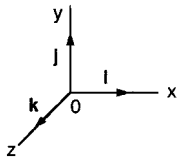

FIGURE 1.2.4 Unit vectors in Cartesian coordinates (the same **i**, **j**, and **k** set applies in a parallel $x'y'z'$ system of axes).

The three-dimensional components and associated quantities of a vector **F** are shown in Figure 1.2.5. The unit vector **n** is collinear with **F**.

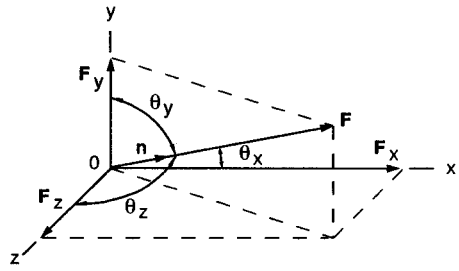

FIGURE 1.2.5 Three-dimensional components of a vector **F**.

The vector **F** is written in terms of its scalar components and the unit coordinate vectors,

$$\mathbf{F} = F_x\mathbf{i} + F_y\mathbf{j} + F_z\mathbf{k} = F\mathbf{n} \tag{1.2.2}$$

where

$$F_x = F\cos\theta_x \quad F_y = F\cos\theta_y \quad F_z = F\cos\theta_z$$

$$F = \sqrt{F_x^2 + F_y^2 + F_z^2}$$

$$n_x = \cos\theta_x \quad n_y = \cos\theta_y \quad n_z = \cos\theta_z$$

$$n_x^2 + n_y^2 + n_z^2 = 1$$

$$\frac{n_x}{F_x} = \frac{n_y}{F_y} = \frac{n_z}{F_z} = \frac{1}{F}$$

The unit vector notation is convenient for the summation of concurrent vectors in terms of scalar or vector components:

Scalar components of the resultant **R**:

$$R_x = \sum F_x \qquad R_y = \sum F_y \qquad R_z = \sum F_z \tag{1.2.3}$$

Vector components:

$$\mathbf{R}_x = \sum \mathbf{F}_x = \sum F_x \mathbf{i} \qquad \mathbf{R}_y = \sum \mathbf{F}_y = \sum F_y \mathbf{j} \qquad \mathbf{R}_z = \sum \mathbf{F}_z = \sum F_z \mathbf{k} \tag{1.2.4}$$

Vector Determination from Scalar Information

A force, for example, may be given in terms of its magnitude F, its sense of direction, and its line of action. Such a force can be expressed in vector form using the coordinates of any two points on its line of action. The vector sought is

$$\mathbf{F} = F_x \mathbf{i} + F_y \mathbf{j} + F_z \mathbf{k} = F\mathbf{n}$$

The method is to find $\mathbf{n}$ on the line of points $A(x_1, y_1, z_1)$ and $B(x_2, y_2, z_2)$:

$$\mathbf{n} = \frac{\text{vector A to B}}{\text{distance A to B}} = \frac{d_x \mathbf{i} + d_y \mathbf{j} + d_z \mathbf{k}}{\sqrt{d_x^2 + d_y^2 + d_z^2}}$$

where $d_x = x_2 - x_1$, $d_y = y_2 - y_1$, $d_z = z_2 - z_1$.

Scalar Product of Two Vectors. Angles and Projections of Vectors

The scalar product, or dot product, of two concurrent vectors $\mathbf{A}$ and $\mathbf{B}$ is defined by

$$\mathbf{A} \cdot \mathbf{B} = AB\cos\phi \tag{1.2.5}$$

where A and B are the magnitudes of the vectors and ϕ is the angle between them. Some useful expressions are

$$\mathbf{A} \cdot \mathbf{B} = \mathbf{B} \cdot \mathbf{A} = A_x B_x + A_y B_y + A_z B_z$$

$$\phi = \arccos \frac{A_x B_x + A_y B_y + A_z B_z}{AB}$$

The projection F' of a vector $\mathbf{F}$ on an arbitrary line of interest is determined by placing a unit vector $\mathbf{n}$ on that line of interest, so that

$$F' = \mathbf{F} \cdot \mathbf{n} = F_x n_x + F_y n_y + F_z n_z$$

Equilibrium of a Particle

A particle is in **equilibrium** when the resultant of all forces acting on it is zero. In such cases the algebraic summation of rectangular scalar components of forces is valid and convenient:

$$\sum F_x = 0 \qquad \sum F_y = 0 \qquad \sum F_z = 0 \tag{1.2.6}$$

Free-Body Diagrams

Unknown forces may be determined readily if a body is in equilibrium and can be modeled as a particle. The method involves **free-body diagrams**, which are simple representations of the actual bodies. The appropriate model is imagined to be isolated from all other bodies, with the significant effects of other bodies shown as force vectors on the free-body diagram.

Example 1

A mast has three guy wires. The initial tension in each wire is planned to be 200 lb. Determine whether this is feasible to hold the mast vertical (Figure 1.2.6).

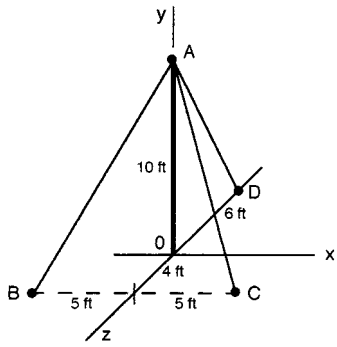

FIGURE 1.2.6 A mast with guy wires.

Solution.

$$\mathbf{R} = \mathbf{T}_{AB} + \mathbf{T}_{AC} + \mathbf{T}_{AD}$$

The three tensions of known magnitude (200 lb) must be written as vectors.

$$\mathbf{T}_{AB} = (\text{tension } AB)(\text{unit vector } A \text{ to } B) = 200 \text{ lb } \mathbf{n}_{AB} = 200 \text{ lb } \frac{\left(d_x\mathbf{i} + d_y\mathbf{j} + d_z\mathbf{k}\right)}{d}$$

$$= \frac{200 \text{ lb}}{\sqrt{5^2 + 10^2 + 4^2}}\left(-5\mathbf{i} - 10\,\mathbf{j} + 4\mathbf{k}\right)\frac{\text{ft}}{\text{ft}} = -84.2 \text{ lb } \mathbf{i} - 168.4 \text{ lb } \mathbf{j} + 67.4 \text{ lb } \mathbf{k}$$

$$\mathbf{T}_{AC} = \frac{200 \text{ lb}}{11.87 \text{ ft}}\left(5\mathbf{i} - 10\,\mathbf{j} + 4\mathbf{k}\right) \text{ ft} = 84.2 \text{ lb } \mathbf{i} + 168.4 \text{ lb } \mathbf{j} + 67.4 \text{ lb } \mathbf{k}$$

$$\mathbf{T}_{AD} = \frac{200 \text{ lb}}{11.66 \text{ ft}}\left(0\mathbf{i} - 10\,\mathbf{j} + 6\mathbf{k}\right) \text{ ft} = -171.5 \text{ lb } \mathbf{j} - 102.9 \text{ lb } \mathbf{k}$$

The resultant of the three tensions is

$$\mathbf{R} = \sum F_x\mathbf{i} + \sum F_y\mathbf{j} + \sum F_z\mathbf{k} = (-84.2 + 84.2 + 0) \text{ lb } \mathbf{i} + (-168.4 - 168.4 - 171.5) \text{ lb } \mathbf{j}$$

$$+ (67.4 + 67.4 - 102.9) \text{ lb } \mathbf{k} = 0 \text{ lb } \mathbf{i} - 508 \text{ lb } \mathbf{j} + 31.9 \text{ lb } \mathbf{k}$$

There is a horizontal resultant of 31.9 lb at *A*, so the mast would not remain vertical.

Forces on Rigid Bodies

All solid materials deform when forces are applied to them, but often it is reasonable to model components and structures as rigid bodies, at least in the early part of the analysis. The forces on a rigid body are generally not concurrent at the center of mass of the body, which cannot be modeled as a particle if the force system tends to cause a rotation of the body.

Moment of a Force

The turning effect of a force on a body is called the moment of the force, or torque. The moment M_A of a force **F** about a point A is defined as a scalar quantity

$$M_A = Fd \tag{1.2.7}$$

where d (the moment arm or lever arm) is the nearest distance from A to the line of action of **F**. This nearest distance may be difficult to determine in a three-dimensional scalar analysis; a vector method is needed in that case.

Equivalent Forces

Sometimes the equivalence of two forces must be established for simplifying the solution of a problem. The necessary and sufficient conditions for the equivalence of forces **F** and **F′** are that they have the same magnitude, direction, line of action, and moment on a given rigid body in static equilibrium. Thus,

$$\mathbf{F} = \mathbf{F}' \quad \text{and} \quad M_A = M'_A$$

For example, the ball joint A in Figure 1.2.7 experiences the same moment whether the vertical force is pushing or pulling downward on the yoke pin.

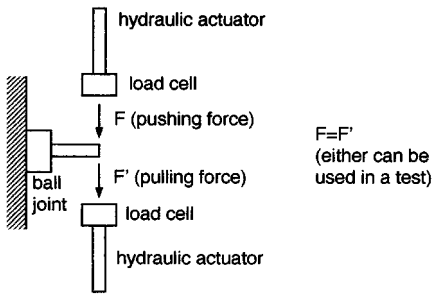

FIGURE 1.2.7 Schematic of testing a ball joint of a car.

Vector Product of Two Vectors

A powerful method of vector mechanics is available for solving complex problems, such as the moment of a force in three dimensions. The *vector product* (or cross product) of two concurrent vectors **A** and **B** is defined as the vector $\mathbf{V} = \mathbf{A} \times \mathbf{B}$ with the following properties:

1. **V** is perpendicular to the plane of vectors **A** and **B**.
2. The sense of **V** is given by the right-hand rule (Figure 1.2.8).
3. The magnitude of **V** is $V = AB \sin\theta$, where θ is the angle between **A** and **B**.
4. $\mathbf{A} \times \mathbf{B} \neq \mathbf{B} \times \mathbf{A}$, but $\mathbf{A} \times \mathbf{B} = -(\mathbf{B} \times \mathbf{A})$.
5. For three vectors, $\mathbf{A} \times (\mathbf{B} + \mathbf{C}) = \mathbf{A} \times \mathbf{B} + \mathbf{A} \times \mathbf{C}$.

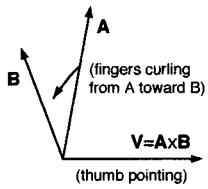

FIGURE 1.2.8 Right-hand rule for vector products.

The vector product is calculated using a determinant,

$$\mathbf{V} = \begin{vmatrix} \mathbf{i} & \mathbf{j} & \mathbf{k} \\ A_x & A_y & A_z \\ B_x & B_y & B_z \end{vmatrix} = A_y B_z \mathbf{i} + A_z B_x \mathbf{j} + A_x B_y \mathbf{k} - A_y B_x \mathbf{k} - A_x B_z \mathbf{j} - A_z B_y \mathbf{i} \tag{1.2.8}$$

Moment of a Force about a Point

The vector product is very useful in determining the moment of a force **F** about an arbitrary point *O*. The vector definition of moment is

$$\mathbf{M}_O = \mathbf{r} \times \mathbf{F} \tag{1.2.9}$$

where **r** is the position vector from point *O* to any point on the line of action of **F**. A double arrow is often used to denote a moment vector in graphics.

The moment $\mathbf{M}_O$ may have three scalar components, M_x, M_y, M_z, which represent the turning effect of the force **F** about the corresponding coordinate axes. In other words, a single force has only one moment about a given point, but this moment may have up to three components with respect to a coordinate system,

$$\mathbf{M}_O = M_x \mathbf{i} + M_y \mathbf{j} + M_z \mathbf{k}$$

Triple Products of Three Vectors

Two kinds of products of three vectors are used in engineering mechanics. The *mixed triple product* (or scalar product) is used in calculating moments. It is the dot product of vector **A** with the vector product of vectors **B** and **C**,

$$\mathbf{A} \cdot (\mathbf{B} \times \mathbf{C}) = \begin{vmatrix} A_x & A_y & A_z \\ B_x & B_y & B_z \\ C_x & C_y & C_z \end{vmatrix} = A_x \left(B_y C_z - B_z C_y \right) + A_y \left(B_z C_x - B_x C_z \right) + A_z \left(B_x C_y - B_y C_x \right) \tag{1.2.10}$$

The *vector triple product* $(\mathbf{A} \times \mathbf{B}) \times \mathbf{C} = \mathbf{V} \times \mathbf{C}$ is easily calculated (for use in dynamics), but note that

$$(\mathbf{A} \times \mathbf{B}) \times \mathbf{C} \neq \mathbf{A} \times (\mathbf{B} \times \mathbf{C})$$

Moment of a Force about a Line

It is common that a body rotates about an axis. In that case the moment M_ℓ of a force F about the axis, say line ℓ, is usefully expressed as

$$\mathbf{M}_\ell = \mathbf{n} \cdot \mathbf{M}_O = \mathbf{n} \cdot (\mathbf{r} \times \mathbf{F}) = \begin{vmatrix} n_x & n_y & n_z \\ r_x & r_y & r_z \\ F_x & F_y & F_z \end{vmatrix} \tag{1.2.11}$$

where **n** is a unit vector along the line ℓ, and **r** is a position vector from point *O* on ℓ to a point on the line of action of **F**. Note that M_ℓ is the projection of $\mathbf{M}_O$ on line ℓ.

Special Cases

1. The moment about a line ℓ is zero when the line of action of **F** intersects ℓ (the moment arm is zero).
2. The moment about a line ℓ is zero when the line of action of **F** is parallel to ℓ (the projection of $\mathbf{M}_O$ on ℓ is zero).

Moment of a Couple

A pair of forces equal in magnitude, parallel in lines of action, and opposite in direction is called a *couple*. The magnitude of the moment of a couple is

$$M = Fd$$

where d is the distance between the lines of action of the forces of magnitude F. The moment of a couple is a free vector **M** that can be applied anywhere to a rigid body with the same turning effect, as long as the direction and magnitude of **M** are the same. In other words, a couple vector can be moved to any other location on a given rigid body if it remains parallel to its original position (equivalent couples). Sometimes a curled arrow in the plane of the two forces is used to denote a couple, instead of the couple vector **M**, which is perpendicular to the plane of the two forces.

Force-Couple Transformations

Sometimes it is advantageous to transform a force to a force system acting at another point, or vice versa. The method is illustrated in Figure 1.2.9.

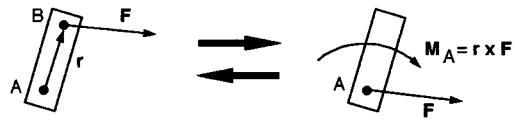

FIGURE 1.2.9 Force-couple transformations.

1. A force **F** acting at B on a rigid body can be replaced by the same force **F** acting at A and a moment $\mathbf{M}_A = \mathbf{r} \times \mathbf{F}$ about A.
2. A force **F** and moment $\mathbf{M}_A$ acting at A can be replaced by a force **F** acting at B for the same total effect on the rigid body.

Simplification of Force Systems

Any force system on a rigid body can be reduced to an equivalent system of a resultant force **R** and a resultant moment $\mathbf{M}_R$. The **equivalent force-couple system** is formally stated as

$$\mathbf{R} = \sum_{i=1}^{n} \mathbf{F}_i \quad \text{and} \quad \mathbf{M}_R = \sum_{i=1}^{n} \mathbf{M}_i = \sum_{i=1}^{n} \left(\mathbf{r}_i \times \mathbf{F}_i \right) \tag{1.2.12}$$

where $\mathbf{M}_R$ depends on the chosen reference point.

Common Cases

1. The resultant force is zero, but there is a resultant moment: $\mathbf{R} = 0$, $\mathbf{M}_R \neq 0$.
2. Concurrent forces (all forces act at one point): $\mathbf{R} \neq 0$, $\mathbf{M}_R = 0$.
3. Coplanar forces: $\mathbf{R} \neq 0$, $\mathbf{M}_R \neq 0$. $\mathbf{M}_R$ is perpendicular to the plane of the forces.
4. Parallel forces: $\mathbf{R} \neq 0$, $\mathbf{M}_R \neq 0$. $\mathbf{M}_R$ is perpendicular to **R**.

Example 2

The torque wrench in Figure 1.2.10 has an arm of constant length L but a variable socket length $d = OA$ because of interchangeable tool sizes. Determine how the moment applied at point O depends on the length d for a constant force **F** from the hand.

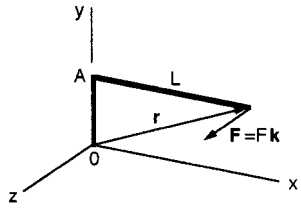

FIGURE 1.2.10 Model of a torque wrench.

Solution. Using $\mathbf{M}_O = \mathbf{r} \times \mathbf{F}$ with $\mathbf{r} = L\mathbf{i} + d\mathbf{j}$ and $\mathbf{F} = F\mathbf{k}$ in Figure 1.2.10,

$$\mathbf{M}_O = (L\mathbf{i} + d\mathbf{j}) \times F\mathbf{k} = Fd\mathbf{i} - FL\mathbf{j}$$

Judgment of the Result

According to a visual analysis the wrench should turn clockwise, so the –**j** component of the moment is justified. Looking at the wrench from the positive x direction, point A has a tendency to rotate counterclockwise. Thus, the **i** component is correct using the right-hand rule.

Equilibrium of Rigid Bodies

The concept of equilibrium is used for determining unknown forces and moments of forces that act on or within a rigid body or system of rigid bodies. The equations of equilibrium are the most useful equations in the area of statics, and they are also important in dynamics and mechanics of materials. The drawing of appropriate free-body diagrams is essential for the application of these equations.

Conditions of Equilibrium

A rigid body is in static equilibrium when the equivalent force-couple system of the external forces acting on it is zero. In vector notation, this condition is expressed as

$$\sum \mathbf{F} = 0$$
$$\sum \mathbf{M}_O = \sum (\mathbf{r} \times \mathbf{F}) = 0 \tag{1.2.13}$$

where O is an arbitrary point of reference.

In practice it is often most convenient to write Equation 1.2.13 in terms of rectangular scalar components,

$$\sum F_x = 0 \qquad \sum M_x = 0$$
$$\sum F_y = 0 \qquad \sum M_y = 0$$
$$\sum F_z = 0 \qquad \sum M_z = 0$$

Maximum Number of Independent Equations for One Body

1. One-dimensional problem: $\sum F = 0$
2. Two-dimensional problem:

$$\sum F_x = 0 \quad \sum F_y = 0 \quad \sum M_A = 0$$

$$\text{or} \quad \sum F_x = 0 \quad \sum M_A = 0 \quad \sum M_B = 0 \quad (x \text{ axis not} \perp \text{AB})$$

$$\text{or} \quad \sum M_A = 0 \quad \sum M_B = 0 \quad \sum M_C = 0 \quad (AB \text{ not} \parallel \text{BC})$$

3. Three-dimensional problem:

$$\sum F_x = 0 \quad \sum F_y = 0 \quad \sum F_z = 0$$

$$\sum M_x = 0 \quad \sum M_y = 0 \quad \sum M_z = 0$$

where *xyz* are orthogonal coordinate axes, and *A*, *B*, *C* are particular points of reference.

Calculation of Unknown Forces and Moments

In solving for unknown forces and moments, always draw the free-body diagram first. Unknown external forces and moments must be shown at the appropriate places of action on the diagram. The directions of unknowns may be assumed arbitrarily, but should be done consistently for systems of rigid bodies. A negative answer indicates that the initial assumption of the direction was opposite to the actual direction. Modeling for problem solving is illustrated in Figures 1.2.11 and 1.2.12.

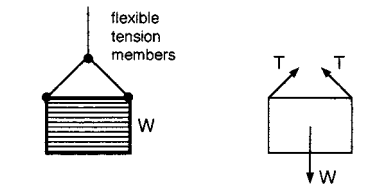

FIGURE 1.2.11 Example of two-dimensional modeling.

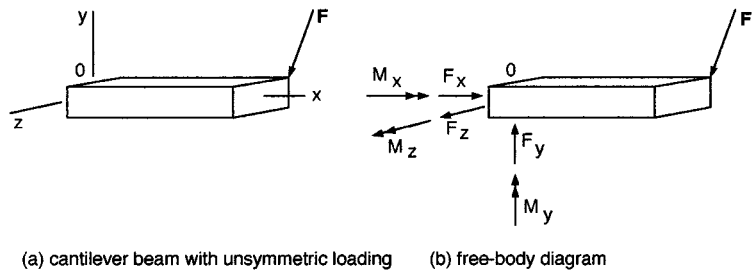

FIGURE 1.2.12 Example of three-dimensional modeling.

Notes on Three-Dimensional Forces and Supports

Each case should be analyzed carefully. Sometimes a particular force or moment is possible in a device, but it must be neglected for most practical purposes. For example, a very short sleeve bearing cannot

support significant moments. A roller bearing may be designed to carry much larger loads perpendicular to the shaft than along the shaft.

Related Free-Body Diagrams

When two or more bodies are in contact, separate free-body diagrams may be drawn for each body. The mutual forces and moments between the bodies are related according to Newton's third law (action and reaction). The directions of unknown forces and moments may be arbitrarily assumed in one diagram, but these initial choices affect the directions of unknowns in all other related diagrams. The number of unknowns and of usable equilibrium equations both increase with the number of related free-body diagrams.

Schematic Example in Two Dimensions (Figure 1.2.13)

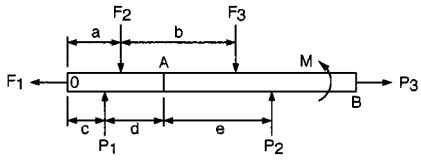

FIGURE 1.2.13 Free-body diagram.

Given: F_1, F_2, F_3, M
Unknowns: P_1, P_2, P_3, and forces and moments at joint A (rigid connection)

Equilibrium Equations

$$\sum F_x = -F_1 + P_3 = 0$$

$$\sum F_y = P_1 + P_2 - F_2 - F_3 = 0$$

$$\sum M_O = P_1 c + P_2 (c + d + e) + M - F_2 a - F_3 (a + b) = 0$$

Three unknowns (P_1, P_2, P_3) are in three equations.

Related Free-Body Diagrams (Figure 1.2.14)

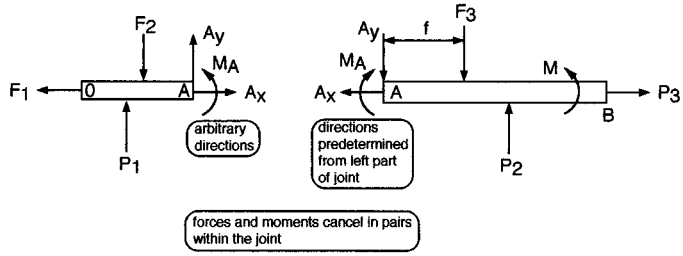

FIGURE 1.2.14 Related free-body diagrams.

Dimensions *a*, *b*, *c*, *d*, and *e* of Figure 1.2.13 are also valid here.

New Set of Equilibrium Equations

Left part: (OA)

$$\sum F_x = -F_1 + A_x = 0$$

$$\sum F_y = P_1 + A_y - F_2 = 0$$

$$\sum M_O = P_1 c + A_y (c + d) + M_A - F_2 a = 0$$

Right side: (AB)

$$\sum F_x = -A_x + P_3 = 0$$

$$\sum F_y = P_2 - A_y - F_3 = 0$$

$$\sum M_A = -M_A + P_2 e + M - F_3 f = 0$$

Six unknowns (P_1, P_2, P_3, A_x, A_y, M_A) are in six equations.

Note: In the first diagram (Figure 1.2.13) the couple M may be moved anywhere from O to B. M is not shown in the second diagram (O to A) because it is shown in the third diagram (in which it may be moved anywhere from A to B).

Example 3

The arm of a factory robot is modeled as three bars (Figure 1.2.15) with coordinates A: (0.6, –0.3, 0.4) m; B: (1, –0.2, 0) m; and C: (0.9, 0.1, –0.25) m. The weight of the arm is represented by $\mathbf{W}_A$ = –60 N**j** at A, and $\mathbf{W}_B$ = –40 N**j** at B. A moment $\mathbf{M}_C$ = (100**i** – 20**j** + 50**k**) N · m is applied to the arm at C. Determine the force and moment reactions at O, assuming that all joints are temporarily fixed.

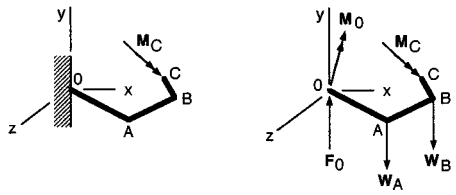

FIGURE 1.2.15 Model of a factory robot.

Solution. The free-body diagram is drawn in Figure 1.2.15b, showing the unknown force and moment reactions at O. From Equation 1.2.13,

$$\sum \mathbf{F} = 0$$

$$\mathbf{F}_O + \mathbf{W}_A + \mathbf{W}_B = 0$$

$$\mathbf{F}_O - 60\ \text{N}\ \mathbf{j} - 40\ \text{N}\ \mathbf{j} = 0$$

$$\mathbf{F}_O = 100\ \text{N}\,\mathbf{j}$$

$$\sum M_O = 0$$

$$\mathbf{M}_O + \mathbf{M}_C + (\mathbf{r}_{OA} \times \mathbf{W}_A) + (\mathbf{r}_{OB} \times \mathbf{W}_B) = 0$$

$$\mathbf{M}_O + (100\mathbf{i} - 20\,\mathbf{j} + 50\mathbf{k})\ \text{N}\cdot\text{m} + (0.6\mathbf{i} - 0.3\mathbf{j} + 0.4\mathbf{k})\ \text{m} \times (-60\ \text{N}\,\mathbf{j}) + (\mathbf{i} - 0.2\,\mathbf{j})\ \text{m} \times (-40\ \text{N}\,\mathbf{j}) = 0$$

$$\mathbf{M}_O + 100\ \text{N}\cdot\text{m}\,\mathbf{i} - 20\ \text{N}\cdot\text{m}\,\mathbf{j} + 50\ \text{N}\cdot\text{m}\,\mathbf{k} - 36\ \text{N}\cdot\text{m}\,\mathbf{k} + 24\ \text{N}\cdot\text{m}\,\mathbf{i} - 40\ \text{N}\cdot\text{m}\,\mathbf{k} = 0$$

$$\mathbf{M}_O = (-124\mathbf{i} + 20\,\mathbf{j} + 26\mathbf{k})\ \text{N}\cdot\text{m}$$

Example 4

A load of 7 kN may be placed anywhere within *A* and *B* in the trailer of negligible weight. Determine the reactions at the wheels at *D*, *E*, and *F*, and the force on the hitch *H* that is mounted on the car, for the extreme positions *A* and *B* of the load. The mass of the car is 1500 kg, and its weight is acting at *C* (see Figure 1.2.16).

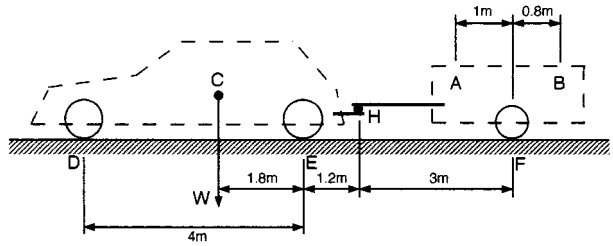

FIGURE 1.2.16 Analysis of a car with trailer.

Solution. The scalar method is best here.

Put the load at position *A* first
For the trailer alone, with *y* as the vertical axis
$\sum M_F = 7(1) - H_y(3) = 0$, $H_y = 2.33$ kN
On the car
$H_y = 2.33$ kN ↓Ans.
$\sum F_y = 2.33 - 7 + F_y = 0$, $F_y = 4.67$ kN ↑Ans.
For the car alone
$\sum M_E = -2.33(1.2) - D_y(4) + 14.72(1.8) = 0$
$D_y = 5.93$ kN ↑Ans.
$\sum F_y = 5.93 + E_y - 14.72 - 2.33 = 0$
$E_y = 11.12$ kN ↑Ans.

Put the load at position *B* next
For the trailer alone
$\sum M_F = 0.8(7) - H_y(3) = 0$, $H_y = -1.87$ kN
On the car
$H_y = 1.87$ kN ↓Ans.
$\sum F_y = -1.87 - 7 + E_y = 0$
$E_y = 8.87$ kN ↑Ans.
For the car alone
$\sum M_E = -(1.87)(1.2) - D_y(4) + 14.72(1.8) = 0$
$D_y = 7.19$ kN ↑Ans.
$\sum F_y = 7.19 + E_y - 14.72 - (-1.87) = 0$
$E_y = 5.66$ kN ↑Ans.

Forces and Moments in Beams

Beams are common structural members whose main function is to resist bending. The geometric changes and safety aspects of beams are analyzed by first assuming that they are rigid. The preceding sections enable one to determine (1) the external (supporting) reactions acting on a statically determinate beam, and (2) the internal forces and moments at any cross section in a beam.

Classification of Supports

Common supports and external reactions for two-dimensional loading of beams are shown in Figure 1.2.17.

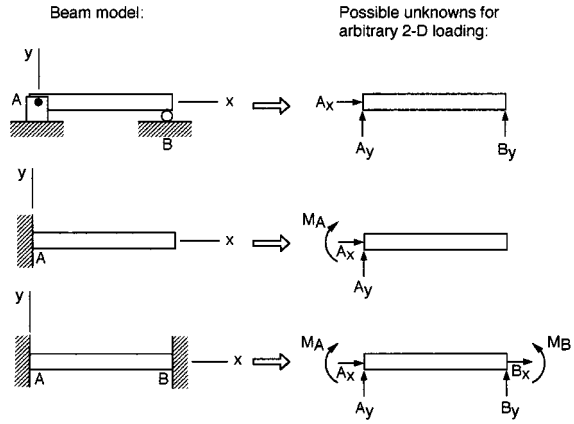

FIGURE 1.2.17 Common beam supports.

Internal Forces and Moments

The internal force and moment reactions in a beam caused by external loading must be determined for evaluating the strength of the beam. If there is no torsion of the beam, three kinds of internal reactions are possible: a horizontal normal force H on a cross section, vertical (transverse) shear force V, and bending moment M. These reactions are calculated from the equilibrium equations applied to the left or right part of the beam from the cross section considered. The process involves free-body diagrams of the beam and a consistently applied system of signs. The modeling is illustrated for a cantilever beam in Figure 1.2.18.

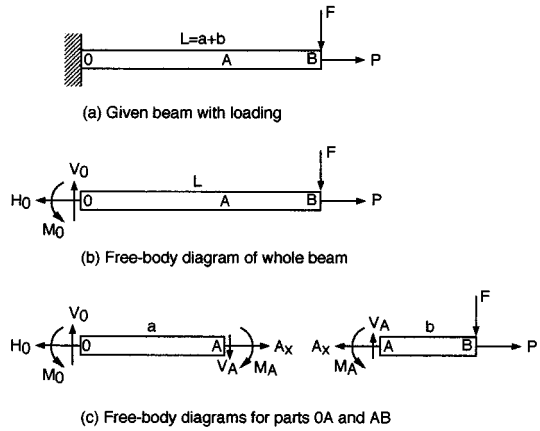

FIGURE 1.2.18 Internal forces and moments in a cantilever beam.

Sign Conventions. Consistent sign conventions should be used in any given problem. These could be arbitrarily set up, but the following is slightly advantageous. It makes the signs of the answers to the equilibrium equations correct for the directions of the shear force and bending moment.

A moment that makes a beam concave upward is taken as positive. Thus, a clockwise moment is positive on the left side of a section, and a counterclockwise moment is positive on the right side. A

shear force that acts upward on the left side of a section, or downward on the right side, is positive (Figure 1.2.19).

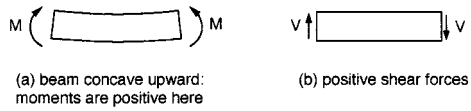

FIGURE 1.2.19 Preferred sign conventions.

Shear Force and Bending Moment Diagrams

The critical locations in a beam are determined from shear force and bending moment diagrams for the whole length of the beam. The construction of these diagrams is facilitated by following the steps illustrated for a cantilever beam in Figure 1.2.20.

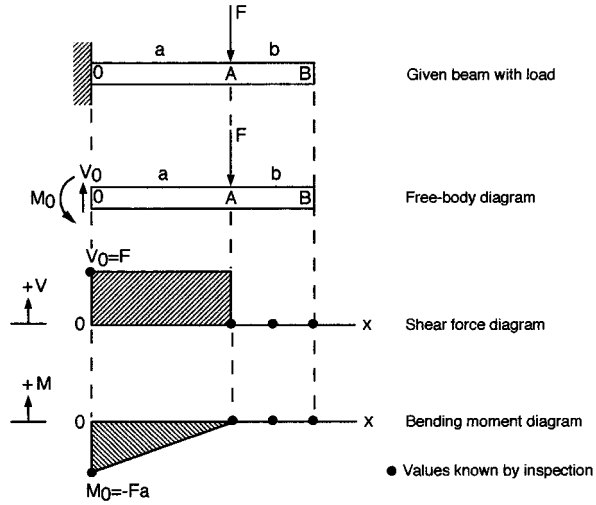

FIGURE 1.2.20 Construction of shear force and bending moment diagrams.

1. Draw the free-body diagram of the whole beam and determine all reactions at the supports.
2. Draw the coordinate axes for the shear force (V) and bending moment (M) diagrams directly below the free-body diagram.
3. Immediately plot those values of V and M that can be determined by inspection (especially where they are zero), observing the sign conventions.
4. Calculate and plot as many additional values of V and M as are necessary for drawing reasonably accurate curves through the plotted points, or do it all by computer.

Example 5

A construction crane is modeled as a rigid bar AC which supports the boom by a pin at B and wire CD. The dimensions are AB = 10ℓ, BC = 2ℓ, BD = DE = 4ℓ. Draw the shear force and bending moment diagrams for bar AC (Figure 1.2.21).

Solution. From the free-body diagram of the entire crane,

$$\sum F_x = 0 \qquad \sum F_y = 0 \qquad \sum M_A = 0$$

$$A_x = 0 \qquad -P + A_y = 0 \qquad -P(8\ell) + M_A = 0$$

$$A_y = P \qquad M_A = 8P\ell$$

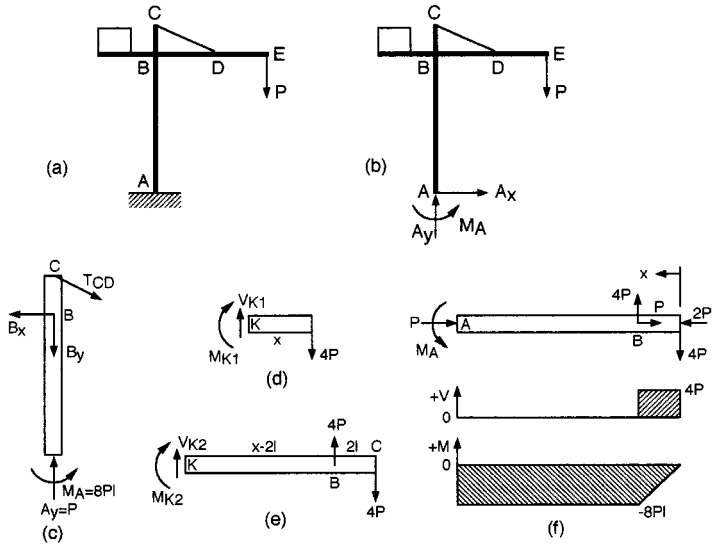

FIGURE 1.2.21 Shear force and bending moment diagrams of a component in a structure.

Now separate bar AC and determine the forces at B and C.

$$\sum F_x = 0 \qquad \sum F_y = 0 \qquad \sum M_A = 0$$

$$-B_x + T_{CD_x} = 0 \qquad P - B_y - T_{CD_y} = 0 \qquad -\frac{2}{\sqrt{5}} T_{CD}(12\ell) + B_x(10\ell) + M_A = 0$$

$$\text{(a)}\ \ B_x = \frac{2}{\sqrt{5}} T_{CD} \qquad \text{(b)}\ \ B_y = P - \frac{1}{\sqrt{5}} T_{CD} \qquad -\frac{24\ell}{\sqrt{5}} T_{CD} + \frac{20\ell}{\sqrt{5}} T_{CD} = -8P\ell$$

$$\text{(c)}\ \ T_{CD} = \frac{8\sqrt{5}}{4} P = 2\sqrt{5}P$$

From (a) and (c), $B_x = 4P$ and $T_{CD_x} = 4P$. From (b) and (c), $B_y = P - 2P = -P$ and $T_{CD_y} = 2P$.

Draw the free-body diagram of bar AC horizontally, with the shear force and bending moment diagram axes below it. Measure x from end C for convenience and analyze sections $0 \le x \le 2\ell$ and $2\ell \le x \le 12\ell$ (Figures 1.2.21b to 1.2.21f).

1. $0 \le x \le 2\ell$

$$\sum F_y = 0 \qquad \sum M_K = 0$$

$$-4P + V_{K_1} = 0 \qquad M_{K_1} + 4P(x) = 0$$

$$V_{K_1} = 4P \qquad M_{K_1} = -4Px$$

2. $2\ell \le x \le 12\ell$

$$\sum F_y = 0 \qquad \sum M_K = 0$$

$$4P - 4P + V_{K_2} = 0 \qquad M_{K_2} - 4P(x - 2\ell) + 4P(x) = 0$$

$$V_{K_2} = 0 \qquad M_{K_2} = -8P\ell$$

At point *B*, $x = 2\ell$, $M_{K_1} = -4P(2\ell) = -8P\ell = M_{K_2} = M_A$. The results for section *AB*, $2\ell \le x \le 12\ell$, show that the combined effect of the forces at *B* and *C* is to produce a couple of magnitude $8P\ell$ on the beam. Hence, the shear force is zero and the moment is constant in this section. These results are plotted on the axes below the free-body diagram of bar *A*-*B*-*C*.

Simple Structures and Machines

Ryan Roloff and Bela I. Sandor

Equilibrium equations are used to determine forces and moments acting on statically determinate simple structures and machines. A simple structure is composed solely of two-force members. A machine is composed of multiforce members. The method of joints and the method of sections are commonly used in such analysis.

Trusses

Trusses consist of straight, slender members whose ends are connected at joints. Two-dimensional *plane trusses* carry loads acting in their planes and are often connected to form three-dimensional *space trusses*. Two typical trusses are shown in Figure 1.2.22.

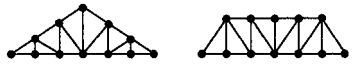

FIGURE 1.2.22 Schematic examples of trusses.

To simplify the analysis of trusses, assume frictionless pin connections at the joints. Thus, all members are two-force members with forces (and no moments) acting at the joints. Members may be assumed weightless or may have their weights evenly divided to the joints.

Method of Joints

Equilibrium equations based on the entire truss and its joints allow for determination of all internal forces and external reactions at the joints using the following procedure.

1. Determine the support reactions of the truss. This is done using force and moment equilibrium equations and a free-body diagram of the entire truss.
2. Select any arbitrary joint where only one or two unknown forces act. Draw the free-body diagram of the joint assuming unknown forces are tensions (arrows directed away from the joint).
3. Draw free-body diagrams for the other joints to be analyzed, using Newton's third law consistently with respect to the first diagram.
4. Write the equations of equilibrium, $\sum F_x = 0$ and $\sum F_y = 0$, for the forces acting at the joints and solve them. To simplify calculations, attempt to progress from joint to joint in such a way that each equation contains only one unknown. Positive answers indicate that the assumed directions of unknown forces were correct, and vice versa.

Example 6

Use the method of joints to determine the forces acting at A, B, C, H, and I of the truss in Figure 1.2.23a. The angles are $\alpha = 56.3°$, $\beta = 38.7°$, $\phi = 39.8°$, and $\theta = 36.9°$.

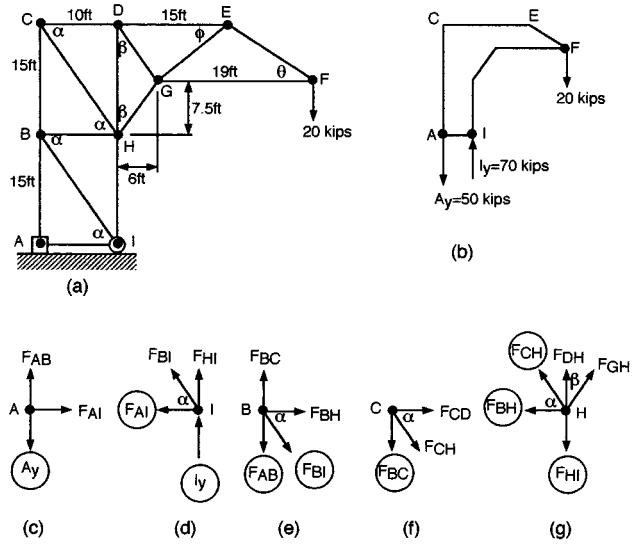

FIGURE 1.2.23 Method of joints in analyzing a truss.

Solution. First the reactions at the supports are determined and are shown in Figure 1.2.23b. A joint at which only two unknown forces act is the best starting point for the solution. Choosing joint A, the solution is progressively developed, always seeking the next joint with only two unknowns. In each diagram circles indicate the quantities that are known from the preceding analysis. Sample calculations show the approach and some of the results.

Joint A:

$$\sum F_x = 0 \qquad \sum F_y = 0$$

$$F_{AI} = 0 \qquad F_{AB} - A_y = 0$$

$$F_{AB} - 50 \text{ kips} = 0$$

$$F_{AB} = 50 \text{ kips (tension)}$$

Joint H:

$$\sum F_x = 0 \qquad \sum F_y = 0$$

$$F_{GH}\sin\beta - F_{CH}\cos\alpha - F_{BH} = 0 \qquad F_{CH}\sin\alpha + F_{DH} + F_{GH}\cos\beta - F_{HI} = 0$$

$$F_{GH}(0.625) + (60.1 \text{ kips})(0.555) - 0 = 0 \qquad -(60.1 \text{ kips})(0.832) + F_{DH} - (53.4 \text{ kips})(0.780) + 70 \text{ kips} = 0$$

$$F_{GH} = -53.4 \text{ kips (compression)} \qquad F_{DH} = 21.7 \text{ kips (tension)}$$

Method of Sections

The method of sections is useful when only a few forces in truss members need to be determined regardless of the size and complexity of the entire truss structure. This method employs any section of the truss as a free body in equilibrium. The chosen section may have any number of joints and members in it, but the number of unknown forces should not exceed three in most cases. Only three equations of equilibrium can be written for each section of a plane truss. The following procedure is recommended.

1. Determine the support reactions if the section used in the analysis includes the joints supported.

2. Section the truss by making an imaginary cut through the members of interest, preferably through only three members in which the forces are unknowns (assume tensions). The cut need not be a straight line. The sectioning is illustrated by lines *l-l*, *m-m*, and *n-n* in Figure 1.2.24.
3. Write equations of equilibrium. Choose a convenient point of reference for moments to simplify calculations such as the point of intersection of the lines of action for two or more of the unknown forces. If two unknown forces are parallel, sum the forces perpendicular to their lines of action.
4. Solve the equations. If necessary, use more than one cut in the vicinity of interest to allow writing more equilibrium equations. Positive answers indicate assumed directions of unknown forces were correct, and vice versa.

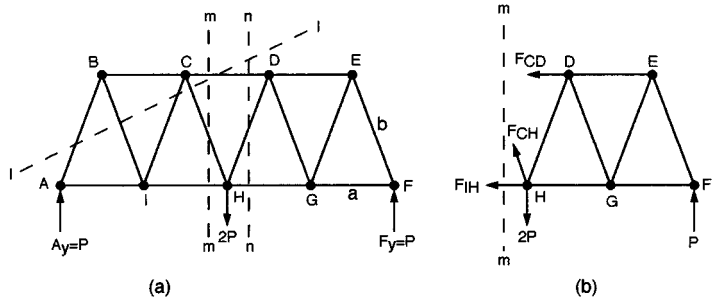

FIGURE 1.2.24 Method of sections in analyzing a truss.

Space Trusses

A space truss can be analyzed with the method of joints or with the method of sections. For each joint, there are three scalar equilibrium equations, $\sum F_x = 0$, $\sum F_y = 0$, and $\sum F_z = 0$. The analysis must begin at a joint where there are at least one known force and no more than three unknown forces. The solution must progress to other joints in a similar fashion.

There are six scalar equilibrium equations available when the method of sections is used: $\sum F_x = 0$, $\sum F_y = 0$, $\sum F_z = 0$, $\sum M_x = 0$, $\sum M_y = 0$, and $\sum M_z = 0$.

Frames and Machines

Multiforce members (with three or more forces acting on each member) are common in structures. In these cases the forces are not directed along the members, so they are a little more complex to analyze than the two-force members in simple trusses. Multiforce members are used in two kinds of structure. *Frames* are usually stationary and fully constrained. *Machines* have moving parts, so the forces acting on a member depend on the location and orientation of the member.

The analysis of multiforce members is based on the consistent use of related free-body diagrams. The solution is often facilitated by representing forces by their rectangular components. Scalar equilibrium equations are the most convenient for two-dimensional problems, and vector notation is advantageous in three-dimensional situations.

Often, an applied force acts at a pin joining two or more members, or a support or connection may exist at a joint between two or more members. In these cases, a choice should be made of a single member at the joint on which to assume the external force to be acting. This decision should be stated in the analysis. The following comprehensive procedure is recommended.

Three independent equations of equilibrium are available for each member or combination of members in two-dimensional loading; for example, $\sum F_x = 0$, $\sum F_y = 0$, $\sum M_A = 0$, where A is an arbitrary point of reference.

1. Determine the support reactions if necessary.
2. Determine all two-force members.

3. Draw the free-body diagram of the first member on which the unknown forces act assuming that the unknown forces are tensions.
4. Draw the free-body diagrams of the other members or groups of members using Newton's third law (action and reaction) consistently with respect to the first diagram. Proceed until the number of equilibrium equations available is no longer exceeded by the total number of unknowns.
5. Write the equilibrium equations for the members or combinations of members and solve them. Positive answers indicate that the assumed directions for unknown forces were correct, and vice versa.

Distributed Forces

The most common distributed forces acting on a body are parallel force systems, such as the force of gravity. These can be represented by one or more concentrated forces to facilitate the required analysis. Several basic cases of distributed forces are presented here. The important topic of stress analysis is covered in mechanics of materials.

Center of Gravity

The center of gravity of a body is the point where the equivalent resultant force caused by gravity is acting. Its coordinates are defined for an arbitrary set of axes as

$$\bar{x} = \frac{\int x\, dW}{W} \qquad \bar{y} = \frac{\int y\, dW}{W} \qquad \bar{z} = \frac{\int z\, dW}{W} \tag{1.2.14}$$

where x, y, z are the coordinates of an element of weight dW, and W is the total weight of the body. In the general case $dW = \gamma\, dV$, and $W = \int \gamma\, dV$, where γ = specific weight of the material and dV = elemental volume.

Centroids

If γ is a constant, the center of gravity coincides with the centroid, which is a geometrical property of a body. Centroids of lines L, areas A, and volumes V are defined analogously to the coordinates of the center of gravity,

$$\text{Lines:} \quad \bar{x} = \frac{\int x\, dL}{W} \qquad \bar{y} = \frac{\int y\, dL}{L} \qquad \bar{z} = \frac{\int z\, dL}{L} \tag{1.2.15}$$

$$\text{Areas:} \quad \bar{x} = \frac{\int x\, dA}{A} \qquad \bar{y} = \frac{\int y\, dA}{A} \qquad \bar{z} = \frac{\int z\, dA}{A} \tag{1.2.16}$$

$$\text{Volumes:} \quad \bar{x} = \frac{\int x\, dV}{V} \qquad \bar{y} = \frac{\int y\, dV}{V} \qquad \bar{z} = \frac{\int z\, dV}{V} \tag{1.2.17}$$

For example, an area A consists of discrete parts A_1, A_2, A_3, where the centroids x_1, x_2, x_3 of the three parts are located by inspection. The x coordinate of the centroid of the whole area A is $\bar{x}$ obtained from $A\bar{x} = A_1x_1 + A_2x_2 + A_3x_3$.

Surfaces of Revolution. The surface areas and volumes of bodies of revolution can be calculated using the concepts of centroids by the theorems of Pappus (see texts on Statics).

Distributed Loads on Beams

The distributed load on a member may be its own weight and/or some other loading such as from ice or wind. The external and internal reactions to the loading may be determined using the condition of equilibrium.

External Reactions. Replace the whole distributed load with a concentrated force equal in magnitude to the area under the load distribution curve and applied at the centroid of that area parallel to the original force system.

Internal Reactions. For a beam under a distributed load $w(x)$, where x is distance along the beam, the shear force V and bending moment M are related according to Figure 1.2.25 as

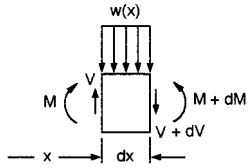

FIGURE 1.2.25 Internal reactions in a beam under distributed loading.

$$w(x) = -\frac{dV}{dx} \qquad V = \frac{dM}{dx} \tag{1.2.18}$$

Other useful expressions for any two cross sections A and B of a beam are

$$V_A - V_B = \int_{x_A}^{x_B} w(x)\,dx = \text{area under } w(x)$$
$$M_B - M_A = \int_{x_A}^{x_B} V\,dx = \text{area under shear force diagram} \tag{1.2.19}$$

Example 7 (Figure 1.2.26)

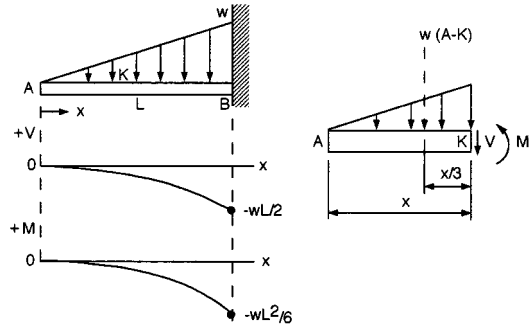

FIGURE 1.2.26 Shear force and bending moment diagrams for a cantilever beam.

Distributed Loads on Flexible Cables

The basic assumptions of simple analyses of cables are that there is no resistance to bending and that the internal force at any point is tangent to the cable at that point. The loading is denoted by $w(x)$, a

continuous but possibly variable load, in terms of force per unit length. The differential equation of a cable is

$$\frac{d^2y}{dx^2} = \frac{w(x)}{T_o} \tag{1.2.20}$$

where T_o = constant = horizontal component of the tension T in the cable.

Two special cases are common.

Parabolic Cables. The cable supports a load w which is uniformly distributed horizontally. The shape of the cable is a parabola given by

$$y = \frac{wx^2}{2T_o} \quad (x = 0 \text{ at lowest point}) \tag{1.2.21}$$

In a symmetric cable the tension is $T = \sqrt{T_o^2 + w^2x^2}$.

Catenary Cables. When the load w is uniformly distributed along the cable, the cable's shape is given by

$$y = \frac{T_o}{w}\left(\cosh\frac{wx}{T_o} - 1\right) \tag{1.2.22}$$

The tension in the cable is $T = T_o + wy$.

Friction

A friction force F (or $\mathcal{F}$, in typical other notation) acts between contacting bodies when they slide relative to one another, or when sliding tends to occur. This force is tangential to each body at the point of contact, and its magnitude depends on the normal force N pressing the bodies together and on the material and condition of the contacting surfaces. The material and surface properties are lumped together and represented by the coefficient of friction μ. The friction force opposes the force that tends to cause motion, as illustrated for two simple cases in Figure 1.2.27.

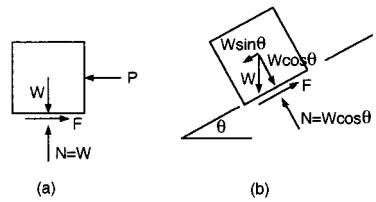

FIGURE 1.2.27 Models showing friction forces.

The friction forces F may vary from zero to a maximum value,

$$F_{\max} = \mu N \quad (0 \le F \le F_{\max}) \tag{1.2.23}$$

depending on the applied force that tends to cause relative motion of the bodies. The coefficient of kinetic friction μ_k (during sliding) is lower than the coefficient of static friction μ or μ_s; μ_k depends on the speed of sliding and is not easily quantified.

Angle of Repose

The critical angle θ_c at which motion is impending is the angle of repose, where the friction force is at its maximum for a given block on an incline.

$$\tan\theta_c = \frac{F}{N} = \mu_s \tag{1.2.24}$$

So θ_c is measured to obtain μ_s. Note that, even in the case of static, dry friction, μ_s depends on temperature, humidity, dust and other contaminants, oxide films, surface finish, and chemical reactions. The contact area and the normal force affect μ_s only when significant deformations of one or both bodies occur.

Classifications and Procedures for Solving Friction Problems

The directions of unknown friction forces are often, but not always, determined by inspection. The magnitude of the friction force is obtained from $F_{max} = \mu_s N$ when it is known that motion is impending. Note that F may be less than F_{max}. The major steps in solving problems of dry friction are organized in three categories as follows.

A. Given: Bodies, forces, or coefficients of friction are known. Impending motion is not assured: $F \neq \mu_s N$.

Procedure: To determine if equilibrium is possible:

1. Construct the free-body diagram.
2. Assume that the system is in equilibrium.
3. Determine the friction and normal forces necessary for equilibrium.
4. Results: (a) $F < \mu_s N$, the body is at rest.
   (b) $F > \mu_s N$, motion is occurring, static equilibrium is not possible. Since there is motion, $F = \mu_k N$. Complete solution requires principles of dynamics.

B. Given: Bodies, forces, or coefficients of friction are given. Impending motion is specified. $F = \mu_s N$ is valid.

Procedure: To determine the unknowns:

1. Construct the free-body diagram.
2. Write $F = \mu_s N$ for all surfaces where motion is impending.
3. Determine μ_s or the required forces from the equation of equilibrium.

C. Given: Bodies, forces, coefficients of friction are known. Impending motion is specified, but the exact motion is not given. The possible motions may be sliding, tipping or rolling, or relative motion if two or more bodies are involved. Alternatively, the forces or coefficients of friction may have to be determined to produce a particular motion from several possible motions.

Procedure: To determine the exact motion that may occur, or unknown quantities required:

1. Construct the free-body diagram.
2. Assume that motion is impending in one of the two or more possible ways. Repeat this for each possible motion and write the equation of equilibrium.
3. Compare the results for the possible motions and select the likely event. Determine the required unknowns for any preferred motion.

Wedges and Screws

A wedge may be used to raise or lower a body. Thus, two directions of motion must be considered in each situation, with the friction forces always opposing the impending or actual motion. The self-locking

aspect of a wedge may be of interest. The analysis is straightforward using interrelated free-body diagrams and equilibrium equations.

Screw threads are special applications of the concept of wedges. Square threads are the easiest to model and analyze. The magnitude M of the moment of a couple required to move a square-threaded screw against an axial load P is

$$M = Pr\tan(\alpha + \phi) \tag{1.2.25}$$

where r = radius of the screw
α = $\tan^{-1}(L/2\pi r) = \tan^{-1}(np/2\pi r)$
L = lead = advancement per revolution
n = multiplicity of threads
p = pitch = distance between similar points on adjacent threads
ϕ = $\tan^{-1}\mu$

The relative values of α and ϕ control whether a screw is self-locking; $\phi > \alpha$ is required for a screw to support an axial load without unwinding.

Disk Friction

Flat surfaces in relative rotary motion generate a friction moment M opposing the motion. For a hollow member with radii R_o and R_i, under an axial force P,

$$M = \frac{2}{3}\mu P\frac{R_o^3 - R_i^3}{R_o^2 - R_i^2} \tag{1.2.26}$$

The friction moment tends to decrease (down to about 75% of its original value) as the surfaces wear. Use the appropriate μ_s or μ_k value.

Axle Friction

The friction moment M of a rotating axle in a journal bearing (sliding bearing) is approximated (if μ is low) as

$$M = Pr\mu \tag{1.2.27}$$

where P = transverse load on the axle
r = radius of the axle

Use the appropriate μ_s or μ_k value.

Rolling Resistance

Rolling wheels and balls have relatively low resistance to motion compared to sliding. This resistance is caused by internal friction of the materials in contact, and it may be difficult to predict or measure.

A coefficient of rolling resistance a is defined with units of length,

$$a \cong \frac{Fr}{P} \tag{1.2.28}$$

where r = radius of a wheel rolling on a flat surface
F = minimum horizontal force to maintain constant speed of rolling
P = load on wheel

Values of a range upward from a low of about 0.005 mm for hardened steel elements.

Belt Friction

The tensions T_1 and T_2 of a belt, rope, or wire on a pulley or drum are related as

$$T_2 = T_1 e^{\mu\beta} \qquad (T_2 > T_1) \tag{1.2.29}$$

where β = total angle of belt contact, radians ($\beta = 2\pi n$ for a member wrapped around a drum n times). Use μ_s for impending slipping and μ_k for slipping.

For a V belt of belt angle 2ϕ,

$$T_2 = T_1 e^{\mu\beta/\sin\phi}$$

Work and Potential Energy

Work is a scalar quantity. It is the product of a force and the corresponding displacement. Potential energy is the capacity of a system to do work on another system. These concepts are advantageous in the analysis of equilibrium of complex systems, in dynamics, and in mechanics of materials.

Work of a Force

The work U of a constant force **F** is

$$U = Fs \tag{1.2.30}$$

where s = displacement of a body in the direction of the vector **F**.

For a displacement along an arbitrary path from point 1 to 2, with $d\mathbf{r}$ tangent to the path,

$$U = \int_1^2 \mathbf{F} \cdot d\mathbf{r} = \int_1^2 \left(F_x\, dx + F_y\, dy + F_z\, dz\right)$$

In theory, there is no work when:

1. A force is acting on a fixed, rigid body ($dr = 0$, $dU = 0$).
2. A force acts perpendicular to the displacement ($\mathbf{F} \cdot d\mathbf{r} = 0$).

Work of a Couple

A couple of magnitude M does work

$$U = M\theta \tag{1.2.31}$$

where θ = angular displacement (radians) in the same plane in which the couple is acting.

In a rotation from angular position α to β,

$$U = \int_\alpha^\beta \mathbf{M} \cdot d\theta = \int_\alpha^\beta \left(M_x\, d\theta_x + M_y\, d\theta_y + M_z\, d\theta_z\right)$$

Virtual Work

The concept of virtual work (through imaginary, infinitesimal displacements within the constraints of a system) is useful to analyze the equilibrium of complex systems. The virtual work of a force **F** or moment **M** is expressed as

$$\delta U = \mathbf{F} \cdot \delta \mathbf{r}$$

$$\delta U = \mathbf{M} \cdot \delta \theta$$

There is equilibrium if

$$\delta U = \sum_{i=1}^{m} \mathbf{F}_i \cdot \delta \mathbf{r}_i + \sum_{j=1}^{n} \mathbf{M}_i \cdot \delta \theta_j = 0 \tag{1.2.32}$$

where the subscripts refer to individual forces or couples and the corresponding displacements, ignoring frictional effects.

Mechanical Efficiency of Real Systems

Real mechanical systems operate with frictional losses, so

$$\underset{\text{(output work)}}{\text{input work = useful work}} + \text{work of friction}$$

The mechanical efficiency η of a machine is

$$\eta = \frac{\text{output work}}{\text{input work}} = \frac{\text{useful work}}{\text{total work required}}$$

$$0 < \eta < 1$$

Gravitational Work and Potential Energy

The potential of a body of weight W to do work because of its relative height h with respect to an arbitrary level is defined as its potential energy. If h is the vertical (y) distance between level 1 and a lower level 2, the work of weight W in descending is

$$U_{12} = \int_1^2 W\, dy = Wh = \text{potential energy of the body at level 1 with respect to level 2}$$

The work of weight W in rising from level 2 to level 1 is

$$U_{21} = \int_2^1 -W\, dy = -Wh = \text{potential energy of the body at level 2 with respect to level 1}$$

Elastic Potential Energy

The potential energy of elastic members is another common form of potential energy in engineering mechanics. For a linearly deforming helical spring, the axial force F and displacement x are related by the spring constant k,

$$F = kx \qquad (\text{similarly, } M = k\theta \text{ for a torsion spring})$$

The work U of a force F on an initially undeformed spring is

$$U = \frac{1}{2} kx^2 \tag{1.2.33}$$

In the general case, deforming the spring from position x_1 to x_2,

$$U = \frac{1}{2}k\left(x_2^2 - x_1^2\right)$$

Notation for Potential Energy

The change in the potential energy V of a system is

$$U = -\Delta V$$

Note that negative work is done by a system while its own potential energy is increased by the action of an external force or moment. The external agent does positive work at the same time since it acts in the same direction as the resulting displacement.

Potential Energy at Equilibrium

For equilibrium of a system,

$$\frac{dV}{dq} = 0$$

where q = an independent coordinate along which there is possibility of displacement.

For a system with n degrees of freedom,

$$\frac{\partial V}{\partial q_i} = 0, \qquad i = 1, 2, \ldots, n$$

Equilibrium is stable if $(d^2V/dq^2) > 0$.
Equilibrium is unstable if $(d^2V/dq^2) < 0$.

Equilibrium is neutral only if all derivatives of V are zero. In cases of complex configurations, evaluate derivatives of higher order as well.

Moments of Inertia

The topics of inertia are related to the methods of first moments. They are traditionally presented in statics in preparation for application in dynamics or mechanics of materials.

Moments of Inertia of a Mass

The moment of inertia dI_x of an elemental mass dM about the x axis (Figure 1.2.28) is defined as

$$dI_x = r^2\ dM = \left(y^2 + z^2\right) dM$$

where r is the nearest distance from dM to the x axis. The moments of inertia of a body about the three coordinate axes are

$$I_x = \int r^2\, dM = \int \left(y^2 + z^2\right) dM$$

$$I_y = \int \left(x^2 + z^2\right) dM \qquad (1.2.34)$$

$$I_z = \int \left(x^2 + y^2\right) dM$$

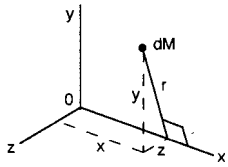

FIGURE 1.2.28 Mass element *dM* in *xyz* coordinates.

Radius of Gyration. The radius of gyration r_g is defined by $r_g = \sqrt{I_x / M}$, and similarly for any other axis. It is based on the concept of the body of mass *M* being replaced by a point mass *M* (same mass) at a distance r_g from a given axis. A thin strip or shell with all mass essentially at a constant distance r_g from the axis of reference is equivalent to a point mass for some analyses.

Moment of Inertia of an Area

The moment of inertia of an elemental area *dA* about the *x* axis (Figure 1.2.29) is defined as

$$dI_x = y^2\, dA$$

where *y* is the nearest distance from *dA* to the *x* axis. The moments of inertia (second moments) of the area *A* about the *x* and *y* axes (because *A* is in the *xy* plane) are

$$I_x = \int y^2\, dA \qquad I_y = \int x^2\, dA \qquad (1.2.35)$$

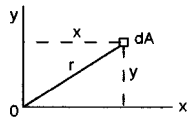

FIGURE 1.2.29 Area *A* in the *xy* plane.

The radius of gyration of an area is defined the same way as it is for a mass: $r_g = \sqrt{I_x / A}$, etc.

Polar Moment of Inertia of an Area

The polar moment of inertia is defined with respect to an axis perpendicular to the area considered. In Figure 1.2.29 this may be the *z* axis. The polar moment of inertia in this case is

$$J_O = \int r^2\, dA = \int \left(x^2 + y^2\right) dA = I_x + I_y \qquad (1.2.36)$$

Parallel-Axis Transformations of Moments of Inertia

It is often convenient to first calculate the moment of inertia about a centroidal axis and then transform this with respect to a parallel axis. The formulas for the transformations are

$$I = I_C + Md^2 \qquad \text{for a mass } M$$
$$I = I_C + Ad^2 \qquad \text{for an area } A \tag{1.2.37}$$
$$J_O = J_C + Ad^2 \qquad \text{for an area } A$$

where I or J_O = moment of inertia of M or A about any line ℓ
I_C or J_C = moment of inertia of M or A about a line through the mass center or centroid and parallel to ℓ
d = nearest distance between the parallel lines
Note that one of the two axes in each equation must be a centroidal axis.

Products of Inertia

The products of inertia for areas and masses and the corresponding parallel-axis formulas are defined in similar patterns. Using notations in accordance with the preceding formulas, products of inertia are

$$I_{xy} = \int xy\, dA \quad \text{for area,} \qquad \text{or} \quad \int xy\, dM \quad \text{for mass}$$
$$I_{yz} = \int yz\, dA \qquad \text{or} \quad \int yz\, dM \tag{1.2.38}$$
$$I_{xz} = \int xz\, dA \qquad \text{or} \quad \int xz\, dM$$

Parallel-axis formulas are

$$I_{xy} = I_{x'y'} + A\, d_x d_y \quad \text{for area,} \qquad \text{or} \quad I_{x'y'} + M\, d_x d_y \quad \text{for mass}$$
$$I_{yz} = I_{y'z'} + A\, d_y d_z \qquad \text{or} \quad I_{y'z'} + M\, d_y d_z \tag{1.2.39}$$
$$I_{xz} = I_{x'z'} + A\, d_x d_z \qquad \text{or} \quad I_{x'z'} + M\, d_x d_z$$

Notes: The moment of inertia is always positive. The product of inertia may be positive, negative, or zero; it is zero if x or y (or both) is an axis of symmetry of the area. Transformations of known moments and product of inertia to axes that are inclined to the original set of axes are possible but not covered here. These transformations are useful for determining the principal (maximum and minimum) moments of inertia and the principal axes when the area or body has no symmetry. The principal moments of inertia for objects of simple shape are available in many texts.

1.3 Dynamics

Stephen M. Birn and Bela I. Sandor

There are two major categories in dynamics, kinematics and kinetics. **Kinematics** involves the time- and geometry-dependent motion of a particle, rigid body, deformable body, or a fluid without considering the forces that cause the motion. It relates position, velocity, acceleration, and time. **Kinetics** combines the concepts of kinematics and the forces that cause the motion.

Kinematics of Particles

Scalar Method

The scalar method of particle kinematics is adequate for one-dimensional analysis. A particle is a body whose dimensions can be neglected (in some analyses, very large bodies are considered particles). The equations described here are easily adapted and applied to two and three dimensions.

Average and Instantaneous Velocity

The average velocity of a particle is the change in distance divided by the change in time. The instantaneous velocity is the particle's velocity at a particular instant.

$$v_{ave} = \frac{\Delta x}{\Delta t} \qquad v_{inst} = \lim_{\Delta t \to 0} \frac{\Delta x}{\Delta t} = \frac{dx}{dt} = \dot{x} \tag{1.3.1}$$

Average and Instantaneous Acceleration

The average acceleration is the change in velocity divided by the change in time. The instantaneous acceleration is the particle's acceleration at a particular instant.

$$a_{ave} = \frac{\Delta v}{\Delta t} \qquad a_{inst} = \lim_{\Delta t \to 0} \frac{\Delta v}{\Delta t} = \frac{dv}{dt} = \dot{v} = \ddot{x} \tag{1.3.2}$$

Displacement, velocity, acceleration, and time are related to one another. For example, if velocity is given as a function of time, the displacement and acceleration can be determined through integration and differentiation, respectively. The following example illustrates this concept.

Example 8

A particle moves with a velocity $v(t) = 3t^2 - 8t$. Determine $x(t)$ and $a(t)$, if $x(0) = 5$.

Solution.

1. Determine $x(t)$ by integration

$$v = \frac{dx}{dt}$$

$$v\,dt = dx$$

$$\int 3t^2 - 8t\,dt = \int dx$$

$$t^3 - 4t^2 + C = x$$

$$\text{from } x(0) = 5 \qquad C = 5$$

$$x(t) = t^3 - 4t^2 + 5$$

2. Determine $a(t)$ by differentiation

$$a = \frac{dv}{dt} = \frac{d}{dt}\left(3t^2 - 8t\right)$$

$$a(t) = 6t - 8$$

There are four key points to be seen from these graphs (Figure 1.3.1).

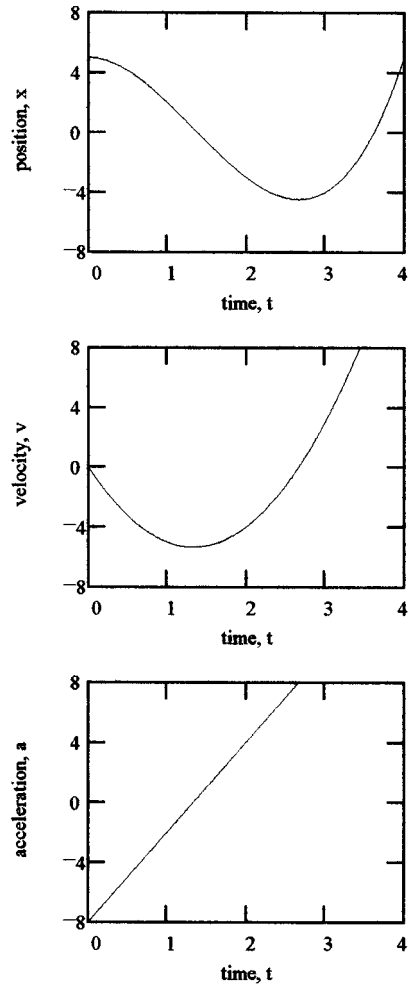

FIGURE 1.3.1 Plots of a particle's kinematics.

1. $v = 0$ at the local maximum or minimum of the x-t curve.
2. $a = 0$ at the local maximum or minimum of the v-t curve.
3. The area under the v-t curve in a specific time interval is equal to the net displacement change in that interval.
4. The area under the a-t curve in a specific time interval is equal to the net velocity change in that interval.

Useful Expressions Based on Acceleration

Equations for nonconstant acceleration:

$$a = \frac{dv}{dt} \Rightarrow \int_{v_0}^{v} dv = \int_{0}^{t} a\, dt \tag{1.3.3}$$

$$v\, dv = a\, dx \Rightarrow \int_{v_0}^{v} v\, dv = \int_{x_0}^{x} a\, dx \tag{1.3.4}$$

Equations for constant acceleration (projectile motion; free fall):

$$\begin{aligned} v &= at + v_0 \\ v^2 &= 2a\left(x - x_0\right) + v_0^2 \\ x &= \frac{1}{2}at^2 + v_0 t + x_0 \end{aligned} \tag{1.3.5}$$

These equations are only to be used when the acceleration is known to be a constant. There are other expressions available depending on how a variable acceleration is given as a function of time, velocity, or displacement.

Scalar Relative Motion Equations

The concept of relative motion can be used to determine the displacement, velocity, and acceleration between two particles that travel along the same line. Equation 1.3.6 provides the mathematical basis for this method. These equations can also be used when analyzing two points on the same body that are not attached rigidly to each other (Figure 1.3.2).

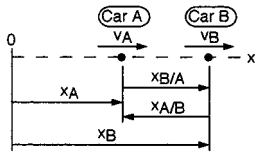

FIGURE 1.3.2 Relative motion of two particles along a straight line.

$$\begin{aligned} x_{B/A} &= x_B - x_A \\ v_{B/A} &= v_B - v_A \\ a_{B/A} &= a_B - a_A \end{aligned} \tag{1.3.6}$$

The notation B/A represents the displacement, velocity, or acceleration of particle B as seen from particle A. Relative motion can be used to analyze many different degrees-of-freedom systems. A degree of freedom of a mechanical system is the number of independent coordinate systems needed to define the position of a particle.

Vector Method

The vector method facilitates the analysis of two- and three-dimensional problems. In general, curvilinear motion occurs and is analyzed using a convenient coordinate system.

Vector Notation in Rectangular (Cartesian) Coordinates

Figure 1.3.3 illustrates the vector method.

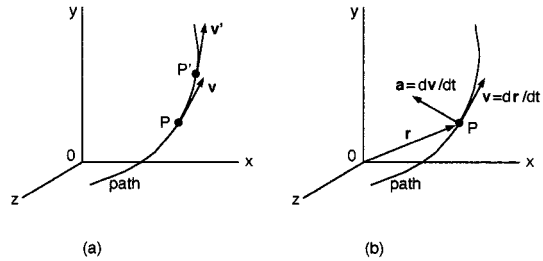

FIGURE 1.3.3 Vector method for a particle.

The mathematical method is based on determining **v** and **a** as functions of the position vector **r**. Note that the time derivatives of unit vectors are zero when the xyz coordinate system is fixed. The scalar components $(\dot{x}, \dot{y}, \ddot{x}, \ldots)$ can be determined from the appropriate scalar equations previously presented that only include the quantities relevant to the coordinate direction considered.

$$\mathbf{r} = x\mathbf{i} + y\mathbf{j} + z\mathbf{k}$$

$$\mathbf{v} = \frac{d\mathbf{r}}{dt} = \frac{dx}{dt}\mathbf{i} + \frac{dy}{dt}\mathbf{j} + \frac{dz}{dt}\mathbf{k} = \dot{x}\mathbf{i} + \dot{y}\mathbf{j} + \dot{z}\mathbf{k} \tag{1.3.7}$$

$$\mathbf{a} = \frac{d\mathbf{v}}{dt} = \frac{d^2x}{dt^2}\mathbf{i} + \frac{d^2y}{dt^2}\mathbf{j} + \frac{d^2z}{dt^2}\mathbf{k} = \ddot{x}\mathbf{i} + \ddot{y}\mathbf{j} + \ddot{z}\mathbf{k}$$

There are a few key points to remember when considering curvilinear motion. First, the instantaneous velocity vector is *always* tangent to the path of the particle. Second, the speed of the particle is the magnitude of the velocity vector. Third, the acceleration vector is *not* tangent to the path of the particle and not collinear with **v** in curvilinear motion.

Tangential and Normal Components

Tangential and normal components are useful in analyzing velocity and acceleration. Figure 1.3.4 illustrates the method and Equation 1.3.8 is the governing equations for it.

$$\mathbf{v} = v\mathbf{n}_t$$

$$\mathbf{a} = a_t\mathbf{n}_t + a_n\mathbf{n}_n$$

$$a_t = \frac{dv}{dt} \qquad a_n = \frac{v^2}{\rho} \tag{1.3.8}$$

$$\rho = \frac{\left[1 + (dy/dx)^2\right]^{3/2}}{d^2y/dx^2}$$

$\rho = r$ = constant for a circular path

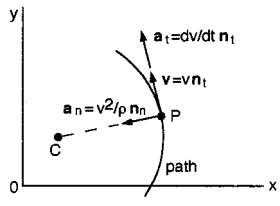

FIGURE 1.3.4 Tangential and normal components. *C* is the center of curvature.

The *osculating plane* contains the unit vectors $\mathbf{n}_t$ and $\mathbf{n}_n$, thus defining a plane. When using normal and tangential components, it is common to forget to include the component of normal acceleration, especially if the particle travels at a constant speed along a curved path.

For a particle that moves in circular motion,

$$v = r\dot{\theta} = r\omega$$
$$a_t = \frac{dv}{dt} = r\ddot{\theta} = r\alpha \tag{1.3.9}$$
$$a_n = \frac{v^2}{r} = r\dot{\theta}^2 = r\omega^2$$

Motion of a Particle in Polar Coordinates

Sometimes it may be best to analyze particle motion by using polar coordinates as follows (Figure 1.3.5):

$$\mathbf{v} = \dot{r}\mathbf{n}_r + r\dot{\theta}\mathbf{n}_\theta \qquad (\text{always tangent to the path})$$
$$\frac{d\theta}{dt} = \dot{\theta} = \omega, \ \text{rad/s} \tag{1.3.10}$$
$$\mathbf{a} = \left(\ddot{r} - r\dot{\theta}^2\right)\mathbf{n}_r + \left(r\ddot{\theta} + 2\dot{r}\dot{\theta}\right)\mathbf{n}_\theta$$

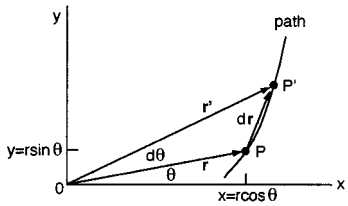

FIGURE 1.3.5 Motion of a particle in polar coordinates.

For a particle that moves in circular motion the equations simplify to

$$\frac{d\dot{\theta}}{dt} = \ddot{\theta} = \dot{\omega} = \alpha, \ \text{rad/s}^2$$
$$\mathbf{v} = r\dot{\theta}\mathbf{n}_\theta \tag{1.3.11}$$
$$\mathbf{a} = -r\dot{\theta}^2\mathbf{n}_r + r\ddot{\theta}\mathbf{n}_\theta$$

Motion of a Particle in Cylindrical Coordinates

Cylindrical coordinates provide a means of describing three-dimensional motion as illustrated in Figure 1.3.6.

$$\mathbf{v} = \dot{r}\mathbf{n}_r + r\dot{\theta}\mathbf{n}_\theta + \dot{z}\mathbf{k}$$
$$\mathbf{a} = \left(\ddot{r} - r\dot{\theta}^2\right)\mathbf{n}_r + \left(r\ddot{\theta} + 2\dot{r}\dot{\theta}\right)\mathbf{n}_\theta + \ddot{z}\mathbf{k} \tag{1.3.12}$$

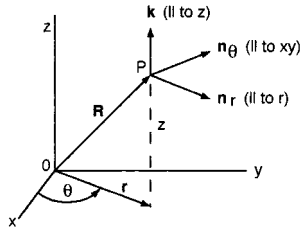

FIGURE 1.3.6 Motion of a particle in cylindrical coordinates.

Motion of a Particle in Spherical Coordinates

Spherical coordinates are useful in a few special cases but are difficult to apply to practical problems. The governing equations for them are available in many texts.

Relative Motion of Particles in Two and Three Dimensions

Figure 1.3.7 shows relative motion in two and three dimensions. This can be used in analyzing the translation of coordinate axes. Note that the unit vectors of the coordinate systems are the same. Subscripts are arbitrary but must be used consistently since $\mathbf{r}_{B/A} = -\mathbf{r}_{A/B}$ etc.

$$\begin{aligned} \mathbf{r}_B &= \mathbf{r}_A + \mathbf{r}_{B/A} \\ \mathbf{v}_B &= \mathbf{v}_A + \mathbf{v}_{B/A} \\ \mathbf{a}_B &= \mathbf{a}_A + \mathbf{a}_{B/A} \end{aligned} \tag{1.3.13}$$

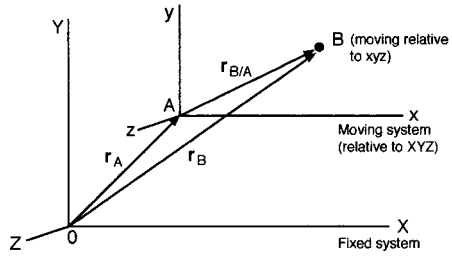

FIGURE 1.3.7 Relative motion using translating coordinates.

Kinetics of Particles

Kinetics combines the methods of kinematics and the forces that cause the motion. There are several useful methods of analysis based on Newton's second law.

Newton's Second Law

The magnitude of the acceleration of a particle is directly proportional to the magnitude of the resultant force acting on it, and inversely proportional to its mass. The direction of the acceleration is the same as the direction of the resultant force.

$$\mathbf{F} = m\mathbf{a} \tag{1.3.14}$$

where m is the particle's mass. There are three key points to remember when applying this equation.

1. **F** is the resultant force.
2. **a** is the acceleration of a single particle (use $\mathbf{a}_C$ for the center of mass for a system of particles).
3. The motion is in a nonaccelerating reference frame.

Equations of Motion

The **equations of motion** for vector and scalar notations in rectangular coordinates are

$$\sum \mathbf{F} = m\mathbf{a}$$
$$\sum F_x = ma_x \qquad \sum F_y = ma_y \qquad \sum F_z = ma_z \tag{1.3.15}$$

The equations of motion for tangential and normal components are

$$\sum F_n = ma_n = m\frac{v^2}{\rho}$$
$$\sum F_t = ma_t = m\dot{v} = mv\frac{dv}{ds} \tag{1.3.16}$$

The equations of motion in a polar coordinate system (radial and transverse components) are

$$\sum F_r = ma_r = m\left(\ddot{r} - r\dot{\theta}^2\right)$$
$$\sum F_\theta = ma_\theta = m\left(r\ddot{\theta} - 2\dot{r}\dot{\theta}\right) \tag{1.3.17}$$

Procedure for Solving Problems

1. Draw a free-body diagram of the particle showing all forces. (The free-body diagram will look unbalanced since the particle is not in static equilibrium.)
2. Choose a convenient nonaccelerating reference frame.
3. Apply the appropriate equations of motion for the reference frame chosen to calculate the forces or accelerations applied to the particle.
4. Use kinematics equations to determine velocities and/or displacements if needed.

Work and Energy Methods

Newton's second law is not always the most convenient method for solving a problem. Work and energy methods are useful in problems involving changes in displacement and velocity, if there is no need to calculate accelerations.

Work of a Force

The total work of a force **F** in displacing a particle *P* from position 1 to position 2 along any path is

$$U_{12} = \int_1^2 \mathbf{F} \cdot d\mathbf{r} = \int_1^2 \left(F_x\, dx + F_y\, dy + F_z\, dz\right) \tag{1.3.18}$$

Potential and Kinetic Energies

Gravitational potential energy: $U_{12} = \int_1^2 W\, dy = Wh = V_g$, where W = weight and h = vertical elevation difference.

Elastic potential energy: $U = \int_{x_1}^{x_2} kx\, dx = \frac{1}{2}k(x_2^2 - x_1^2) = V_e$, where k = spring constant.

Kinetic energy of a particle: $T = 1/2mv^2$, where m = mass and v = magnitude of velocity.

Kinetic energy can be related to work by the *principle of work and energy*,

$$U_{12} = T_2 - T_1 \tag{1.3.19}$$

where U_{12} is the work of a force on the particle moving it from position 1 to position 2, T_1 is the kinetic energy of the particle at position 1 (initial kinetic energy), and T_2 is the kinetic energy of the particle at position 2 (final kinetic energy).

Power

Power is defined as work done in a given time.

$$\text{power} = \frac{dU}{dt} = \frac{\mathbf{F} \cdot d\mathbf{r}}{dt} = \mathbf{F} \cdot \mathbf{v} \tag{1.3.20}$$

where $\mathbf{v}$ is velocity.

Important units and conversions of power are

$$1 \text{ W} = 1 \text{ J/s} = 1 \text{ N} \cdot \text{m/s}$$

$$1 \text{ hp} = 550 \text{ ft} \cdot \text{lb/s} = 33{,}000 \text{ ft} \cdot \text{lb/min} = 746 \text{ W}$$

$$1 \text{ ft} \cdot \text{lb/s} = 1.356 \text{ J/s} = 1.356 \text{ W}$$

Advantages and Disadvantages of the Energy Method

There are four advantages to using the energy method in engineering problems:

1. Accelerations do not need to be determined.
2. Modifications of problems are easy to make in the analysis.
3. Scalar quantities are summed, even if the path of motion is complex.
4. Forces that do not do work are ignored.

The main disadvantage of the energy method is that quantities of work or energy cannot be used to determine accelerations or forces that do no work. In these instances, Newton's second law has to be used.

Conservative Systems and Potential Functions

Sometimes it is useful to assume a conservative system where friction does not oppose the motion of the particle. The work in a conservative system is independent of the path of the particle, and potential energy is defined as

$$\underbrace{U_{12}}_{\substack{\text{work of } \mathbf{F} \\ \text{from 1 to 2}}} = \underbrace{-\Delta V}_{\substack{\text{difference of potential} \\ \text{energies at 1 and 2}}}$$

A special case is where the particle moves in a closed path. One trip around the path is called a *cycle*.

$$U = \oint dU = \oint \mathbf{F} \cdot d\mathbf{r} = \oint \left(F_x \, dx + F_y \, dy + F_z \, dz \right) = 0 \tag{1.3.21}$$

In advanced analysis differential changes in the potential energy function (V) are calculated by the use of partial derivatives,

$$\mathbf{F} = F_x \mathbf{i} + F_y \mathbf{j} + F_z \mathbf{k} = -\left(\frac{\partial V}{\partial x} \mathbf{i} + \frac{\partial V}{\partial y} \mathbf{j} + \frac{\partial V}{\partial z} \mathbf{k} \right)$$

Conservation of Mechanical Energy

Conservation of mechanical energy is assumed if kinetic energy (T) and potential energy (V) change back and forth in a conservative system (the dissipation of energy is considered negligible). Equation 1.3.22 formalizes such a situation, where position 1 is the initial state and position 2 is the final state. The reference (datum) should be chosen to reduce the number of terms in the equation.

$$T_1 + V_1 = T_2 + V_2 \tag{1.3.22}$$

Linear and Angular Momentum Methods

The concept of linear momentum is useful in engineering when the accelerations of particles are not known but the velocities are. The linear momentum is derived from Newton's second law,

$$\mathbf{G} = m\mathbf{v} \tag{1.3.23}$$

The time rate of change of linear momentum is equal to force. When $m\mathbf{v}$ is constant, the conservation of momentum equation results,

$$\sum \mathbf{F} = \dot{\mathbf{G}} = \frac{d}{dt}(m\mathbf{v})$$
$$\sum \mathbf{F} = 0 \qquad m\mathbf{v} = \text{constant} \qquad (\text{conservation of momentum}) \tag{1.3.24}$$

The method of angular momentum is based on the momentum of a particle about a fixed point, using the vector product in the general case (Figure 1.3.8).

$$\mathbf{H}_O = \mathbf{r} \times m\mathbf{v} \tag{1.3.25}$$

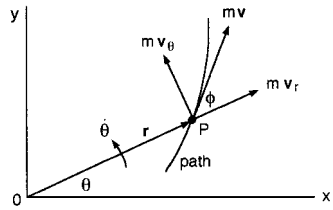

FIGURE 1.3.8 Definition of angular momentum for a particle.

The angular momentum equation can be solved using a scalar method if the motion of the particle remains in a plane,

$$\mathbf{H}_O = mrv\sin\phi = mrv_\theta = mr^2\dot{\theta}$$

If the particle does not remain in a plane, then the general space motion equations apply. They are derived from the cross-product $\mathbf{r} \times m\mathbf{v}$,

$$\mathbf{H}_O = H_x\mathbf{i} + H_y\mathbf{j} + H_z\mathbf{k}$$

$$H_x = m\left(yv_z - zv_y\right)$$

$$H_y = m\left(zv_x - xv_z\right) \tag{1.3.25a}$$

$$H_z = m\left(xv_y - yv_x\right)$$

Time Rate of Change of Angular Momentum

In general, a force acting on a particle changes its angular momentum: *the time rate of change of angular momentum of a particle is equal to the sum of the moments of the forces acting on the particle.*

Vectors: $$\dot{\mathbf{H}}_O = \frac{d}{dt}(\mathbf{r} \times m\mathbf{v}) = \mathbf{r} \times \sum \mathbf{F} = \sum \mathbf{H}_O \tag{1.3.26}$$

Scalars: $$\sum M_x = \dot{H}_x \qquad \sum M_y = \dot{H}_y \qquad \sum M_z = \dot{H}_z$$

$$\sum \mathbf{M}_O = 0 \qquad \mathbf{H}_O = \mathbf{r} \times m\mathbf{v} = \text{constant}$$

$$\left(\text{conservation of angular momentum}\right) \tag{1.3.27}$$

A special case is when the sum of the moments about point *O* is zero. This is the conservation of angular momentum. In this case (motion under a central force), if the distance *r* increases, the velocity must decrease, and vice versa.

Impulse and Momentum

Impulse and momentum are important in considering the motion of particles in impact. The linear impulse and momentum equation is

$$\underbrace{\int_{t_1}^{t_2} \mathbf{F}\, dt}_{\text{impulse}} = \underbrace{m\mathbf{v}_2}_{\substack{\text{final}\\ \text{momentum}}} - \underbrace{m\mathbf{v}_1}_{\substack{\text{initial}\\ \text{momentum}}} \tag{1.3.28}$$

Conservation of Total Momentum of Particles

Conservation of total momentum occurs when *the initial momentum of n particles is equal to the final momentum of those same n particles,*

$$\underbrace{\sum_i^n \left(m_i\mathbf{v}_i\right)_1}_{\substack{\text{total initial}\\ \text{momentum at time } t_1}} = \underbrace{\sum_i^n \left(m_i\mathbf{v}_i\right)_2}_{\substack{\text{total final}\\ \text{momentum at time } t_2}} \tag{1.3.29}$$

When considering the response of two deformable bodies to direct central impact, the coefficient of restitution is used. This coefficient *e* relates the initial velocities of the particles to the final velocities,

$$e = \frac{v_{Bf} - v_{Af}}{v_A - v_B} = \frac{\left|\text{relative velocity of separation}\right|}{\left|\text{relative velocity of approach}\right|} \tag{1.3.30}$$

For real materials, $0 < e < 1$. If both bodies are *perfectly elastic*, $e = 1$, and if either body is *perfectly plastic*, $e = 0$.

Kinetics of Systems of Particles

There are three distinct types of systems of particles: discrete particles, continuous particles in fluids, and continuous particles in rigid or deformable bodies. This section considers methods for discrete particles that have relevance to the mechanics of solids. Methods involving particles in rigid bodies will be discussed in later sections.

Newton's Second Law Applied to a System of Particles

Newton's second law can be extended to systems of particles,

$$\sum_{i=1}^{n} \mathbf{F}_i = \sum_{i=1}^{n} m_i \mathbf{a}_i \tag{1.3.31}$$

Motion of the Center of Mass

The center of mass of a system of particles moves under the action of internal and external forces as if the total mass of the system and all the external forces were at the center of mass. Equation 1.3.32 defines the position, velocity, and acceleration of the center of mass of a system of particles.

$$m\mathbf{r}_C = \sum_{i=1}^{n} m_i \mathbf{r}_i \qquad m\mathbf{v}_C = \sum_{i=1}^{n} m_i \mathbf{v}_i \qquad m\mathbf{a}_C = \sum_{i=1}^{n} m_i \mathbf{a}_i \qquad \sum \mathbf{F} = m\mathbf{a}_C \tag{1.3.32}$$

Work and Energy Methods for a System of Particles

Gravitational Potential Energy. The gravitational potential energy of a system of particles is the sum of the potential energies of the individual particles of the system.

$$V_g = g\sum_{i=1}^{n} m_i y_i = \sum_{i=1}^{n} W_i y_i = mgy_C = Wy_C \tag{1.3.33}$$

where g = acceleration of gravity
y_C = vertical position of center of mass with respect to a reference level

Kinetic Energy. The kinetic energy of a system of particles is the sum of the kinetic energies of the individual particles of the system with respect to a fixed reference frame,

$$T = \frac{1}{2}\sum_{i=1}^{n} m_i v_i^2 \tag{1.3.34}$$

A translating reference frame located at the mass center C of a system of particles can be used advantageously, with

$$T = \underbrace{\frac{1}{2} m v_C^2}_{\substack{\text{motion of total} \\ \text{mass imagined to} \\ \text{be concentrated at C}}} + \underbrace{\frac{1}{2}\sum_{i=1}^{n} m_i v_i'^2}_{\substack{\text{motion of all} \\ \text{particles relative to } C}} \qquad (v' \text{ are with respect to a translating frame}) \tag{1.3.35}$$

Work and Energy

The work and energy equation for a system of particles is similar to the equation stated for a single particle.

$$\sum_{i=1}^{n} U_i' = \sum_{i=1}^{n} V_i + \sum_{i=1}^{n} T_i$$
$$U' = \Delta V + \Delta T \tag{1.3.36}$$

Momentum Methods for a System of Particles

Moments of Forces on a System of Particles. The moments of external forces on a system of particles about a point *O* are given by

$$\sum_{i=1}^{n} \left(\mathbf{r}_i \times \mathbf{F}_i\right) = \sum_{i=1}^{n} \mathbf{M}_{i_O} + \sum_{i=1}^{n} \left(\mathbf{r}_i \times m_i \mathbf{a}_i\right) \tag{1.3.37}$$

Linear and Angular Momenta of a System of Particles. The resultant of the external forces on a system of particles equals the time rate of change of linear momentum of that system.

$$\mathbf{G} = \sum_{i=1}^{n} m_i \mathbf{v}_i \qquad \sum \mathbf{F} = \dot{\mathbf{G}} \tag{1.3.38}$$

The angular momentum equation for a system of particles about a fixed point *O* is

$$\mathbf{H}_O = \sum_{i=1}^{n} \left(\mathbf{r}_i \times m_i \mathbf{a}_i\right)$$
$$\sum \mathbf{M}_O = \dot{\mathbf{H}}_O = \sum_{i=1}^{n} \left(\mathbf{r}_i \times m_i \mathbf{a}_i\right) \tag{1.3.39}$$

The last equation means that *the resultant of the moments of the external forces on a system of particles equals the time rate of change of angular momentum of that system.*

Angular Momentum about the Center of Mass

The above equations work well for reference frames that are stationary, but sometimes a special approach may be useful, noting that *the angular momentum of a system of particles about its center of mass C is the same whether it is observed from a fixed frame at point O or from the centroidal frame which may be translating but not rotating*. In this case

$$\mathbf{H}_O = \mathbf{H}_C + \mathbf{r}_C \times m\mathbf{v}_C$$
$$\sum \mathbf{M}_O = \dot{\mathbf{H}}_C + \mathbf{r}_C \times m\mathbf{a}_C \tag{1.3.40}$$

Conservation of Momentum

The conservation of momentum equations for a system of particles is analogous to that for a single particle.

$$\left.\begin{aligned}\mathbf{G} &= \text{constant}\\ \mathbf{H}_O &= \text{constant}\\ \mathbf{H}_C &= \text{constant}\end{aligned}\right\} \quad \text{not the same constants in general}$$

Impulse and Momentum of a System of Particles

The linear impulse momentum for a system of particles is

$$\sum_{i=1}^{n}\int_{t_1}^{t_2}\mathbf{F}_i\,dt = \mathbf{G}_2 - \mathbf{G}_1 = m\mathbf{v}_{C_2} - m\mathbf{v}_{C_1} \tag{1.3.41}$$

The angular impulse momentum for a system of particles is

$$\sum_{i=1}^{n}\int_{t_1}^{t_2}\mathbf{M}_{i_O}\,dt = \mathbf{H}_{O_2} - \mathbf{H}_{O_1} \tag{1.3.42}$$

Kinematics of Rigid Bodies

Rigid body kinematics is used when the methods of particle kinematics are inadequate to solve a problem. A rigid body is defined as one in which the particles are rigidly connected. This assumption allows for some similarities to particle kinematics. There are two kinds of rigid body motion, translation and rotation. These motions may occur separately or in combination.

Translation

Figure 1.3.9 models the translational motion of a rigid body.

$$\begin{aligned}\mathbf{r}_B &= \mathbf{r}_A + \mathbf{r}_{B/A} \qquad \left(\mathbf{r}_{B/A} = \text{constant}\right)\\ \mathbf{v}_B &= \dot{\mathbf{r}}_B = \dot{\mathbf{r}}_A = \mathbf{v}_A\\ \mathbf{a}_B &= \dot{\mathbf{v}}_B = \dot{\mathbf{v}}_A = \mathbf{a}_A\end{aligned} \tag{1.3.43}$$

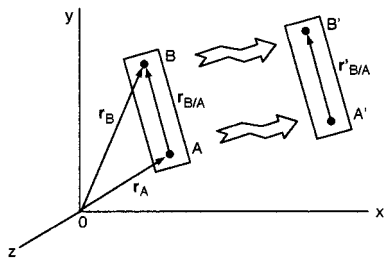

FIGURE 1.3.9 Translational motion of a rigid body.

These equations represent an important fact: *when a rigid body is in translation, the motion of a single point completely specifies the motion of the whole body.*

Rotation about a Fixed Axis

Figure 1.3.10 models a point P in a rigid body rotating about a fixed axis with an angular velocity ω.

The velocity $\mathbf{v}$ of point P is determined assuming that the magnitude of $\mathbf{r}$ is constant,

$$\mathbf{v} = \omega \times \mathbf{r} \tag{1.3.44}$$

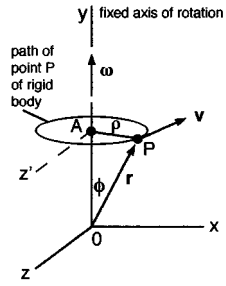

FIGURE 1.3.10 Rigid body rotating about a fixed axis.

The acceleration **a** of point *P* is determined conveniently by using normal and tangential components,

$$\mathbf{a}_P = \underbrace{\alpha \times \mathbf{r}}_{\mathbf{a}_t} + \underbrace{\omega \times (\omega \times \mathbf{r})}_{\mathbf{a}_n} \qquad a_t = \rho\alpha \qquad a_n = \rho\omega^2 \tag{1.3.45}$$

Note that *the angular acceleration α and angular velocity ω are valid for any line perpendicular to the axis of rotation of the rigid body at a given instant.*

Kinematics Equations for Rigid Bodies Rotating in a Plane

For rotational motion with or without a fixed axis, if displacement is measured by an angle θ,

Angular speed: $$\omega = \frac{d\theta}{dt}$$

Angular acceleration: $$\alpha = \frac{d\omega}{dt} = \omega\frac{d\omega}{d\theta}$$

For a constant angular speed ω,

Angular displacement: $\theta = \theta_o + \omega t \quad (\theta = \theta_o \text{ at } t = 0)$

For a constant angular acceleration α,

$$\omega = \omega_o + \alpha t \qquad (\omega = \omega_o \text{ at } t = 0)$$

$$\theta = \theta_o + \omega_o t + \frac{1}{2}\alpha t^2$$

$$\omega^2 = \omega_o^2 + 2\alpha(\theta - \theta_o)$$

Velocities in General Plane Motion

General plane motion of a rigid body is defined by simultaneous translation and rotation in a plane. Figure 1.3.11 illustrates how the velocity of a point A can be determined using Equation 1.3.46, which is based on relative motion of particles.

$$\mathbf{v}_A = \underbrace{\mathbf{v}_B}_{\text{translation}} + \underbrace{\omega \times \mathbf{r}_{A/B}}_{\text{rotation}} \tag{1.3.46}$$

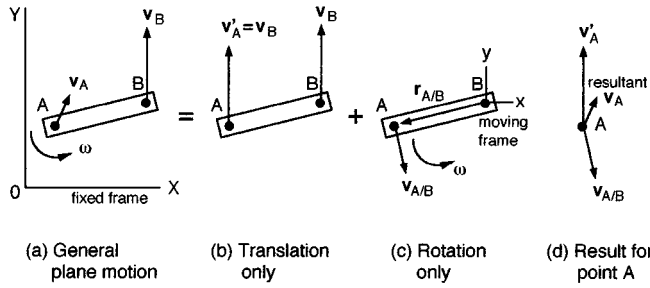

FIGURE 1.3.11 Analysis of velocities in general plane motion.

There are five important points to remember when solving general plane motion problems, including those of interconnected rigid bodies.

1. The angular velocity of a rigid body in plane motion is independent of the reference point.
2. The common point of two or more pin-jointed members must have the same absolute velocity even though the individual members may have different angular velocities.
3. The points of contact in members that are in temporary contact may or may not have the same absolute velocity. If there is sliding between the members, the points in contact have different absolute velocities. The absolute velocities of the contacting particles are always the same if there is no sliding.
4. If the angular velocity of a member is not known, but some points of the member move along defined paths (i.e., the end points of a piston rod), these paths define the directions of the velocity vectors and are useful in the solution.
5. The geometric center of a wheel rolling on a flat surface moves in rectilinear motion. If there is no slipping at the point of contact, the linear distance the center point travels is equal to that portion of the rim circumference that has rolled along the flat surface.

Instantaneous Center of Rotation

The method of *instantaneous center of rotation* is a geometric method of determining the angular velocity when two velocity vectors are known for a given rigid body. Figure 1.3.12 illustrates the method. This procedure can also be used to determine velocities that are parallel to one of the given velocities, by similar triangles.

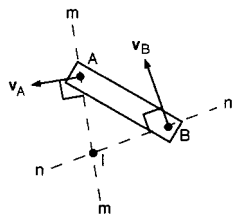

FIGURE 1.3.12 Schematic for instantaneous center of rotation.

Velocities $\mathbf{v}_A$ and $\mathbf{v}_B$ are given; thus the body is rotating about point I at that instant. Point I has zero velocity at that instant, but generally has an acceleration. This method does *not* work for the determination of angular accelerations.

Acceleration in General Plane Motion

Figure 1.3.13 illustrates a method of determining accelerations of points of a rigid body. This is similar to (but more difficult than) the procedure of determining velocities.

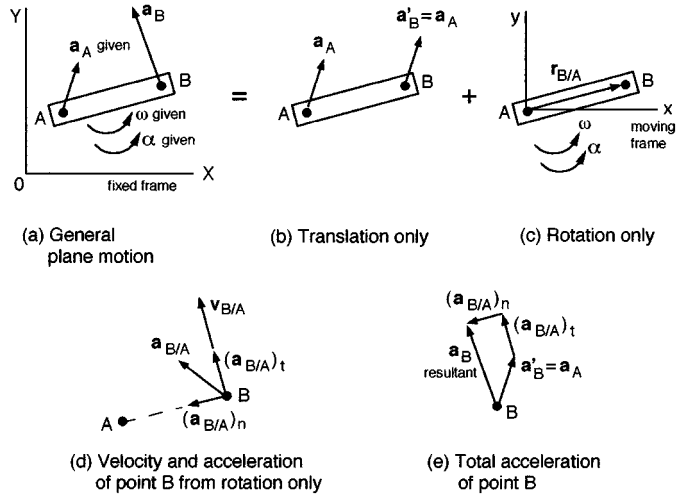

FIGURE 1.3.13 Accelerations in general plane motion.

$$\mathbf{a}_B = \mathbf{a}_A + \alpha \times \mathbf{r}_{B/A} + \omega \times \left(\omega \times \mathbf{r}_{B/A}\right)$$

$$\mathbf{a}_B = \underbrace{\mathbf{a}_A}_{\text{translation}} + \underbrace{\left(\mathbf{a}_{B/A}\right)_t + \left(\mathbf{a}_{B/A}\right)_n}_{\text{rotation}} \tag{1.3.47}$$

There are six key points to consider when solving this kind of a problem.

1. The angular velocity and acceleration of a rigid body in plane motion are independent of the reference point.
2. The common points of pin-jointed members must have the same absolute acceleration even though the individual members may have different angular velocities and angular accelerations.
3. The points of contact in members that are in temporary contact may or may not have the same absolute acceleration. Even when there is no sliding between the members, only the tangential accelerations of the points in contact are the same, while the normal accelerations are frequently different in magnitude and direction.
4. The instantaneous center of zero velocity in general has an acceleration and should *not* be used as a reference point for accelerations unless its acceleration is known and included in the analysis.
5. If the angular acceleration of a member is not known, but some points of the member move along defined paths, the geometric constraints of motion define the directions of normal and tangential acceleration vectors and are useful in the solution.
6. The geometric center of a wheel rolling on a flat surface moves in rectilinear motion. If there is no slipping at the point of contact, the linear acceleration of the center point is parallel to the flat surface and equal to $r\alpha$ for a wheel of radius r and angular acceleration α.

General Motion of a Rigid Body

Figure 1.3.14 illustrates the complex general motion (three-dimensional) of a rigid body. It is important to note that here the angular velocity and angular acceleration vectors are not necessarily in the same direction as they are in general plane motion.

Equations 1.3.48 give the velocity and acceleration of a point on the rigid body. These equations are the same as those presented for plane motion.

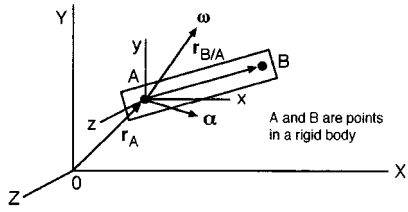

FIGURE 1.3.14 General motion of a rigid body.

$$\mathbf{v}_B = \mathbf{v}_A + \omega \times \mathbf{r}_{B/A}$$

$$\mathbf{a}_B = \mathbf{a}_A + \alpha \times \mathbf{r}_{B/A} + \omega \times \left(\omega \times \mathbf{r}_{B/A}\right) \tag{1.3.48}$$

$$\mathbf{a}_B = \mathbf{a}_A + \left(\mathbf{a}_{B/A}\right)_t + \left(\mathbf{a}_{B/A}\right)_n$$

The most difficult part of solving a general motion problem is determining the angular acceleration vector. There are three cases for the determination of the angular acceleration.

1. The direction of ω is constant. This is plane motion and $\alpha = \dot{\omega}$ can be used in scalar solutions of problems.
2. The magnitude of ω is constant but its direction changes. An example of this is a wheel which travels at a constant speed on a curved path.
3. Both the magnitude and direction of ω change. This is *space motion* since all or some points of the rigid body have three-dimensional paths. An example of this is a wheel which accelerates on a curved path.

A useful expression can be obtained from item 2 and Figure 1.3.15. The rigid body is fixed at point *O* and ω has a constant magnitude. Let ω rotate about the Y axis with angular velocity Ω. The angular acceleration is determined from Equation 1.3.49.

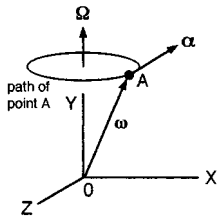

FIGURE 1.3.15 Rigid body fixed at point *O*.

$$\alpha = \frac{d\omega}{dt} = \Omega \times \omega \tag{1.3.49}$$

For *space motion* it is essential to combine the results of items 1 and 2, which provide components of α for the change in magnitude and the change in direction. The following example illustrates the procedure.

Example 9

The rotor shaft of an alternator in a car is in the horizontal plane. It rotates at a constant angular speed of 1500 rpm while the car travels at v = 60 ft/sec on a horizontal road of 400 ft radius (Figure 1.3.16). Determine the angular acceleration of the rotor shaft if v increases at the rate of 8 ft/sec^2.

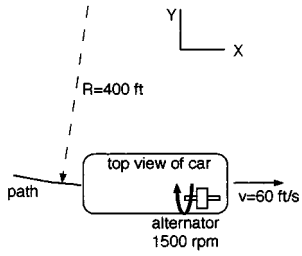

FIGURE 1.3.16 Schematic of shaft's motion.

Solution. There are two components of α. One is the change in the direction of the rotor shaft's ω_x, and the other is the change in magnitude from the acceleration of the car.

1. Component from the change in direction. Determine ω_c of the car.

$$v = r\omega_c$$

$$\omega_c = 0.15 \text{ rad/sec } \mathbf{k}$$

Use Equation 1.3.49:

$$\alpha = \omega_c \times \omega = \begin{vmatrix} \mathbf{i} & \mathbf{j} & \mathbf{k} \\ 0 & 0 & 0.15 \\ 157.1 & 0 & 0 \end{vmatrix} = 23.6\mathbf{j} \text{ rad/sec}^2$$

2. Component from the acceleration of the car. Use Equation 1.3.9:

$$\alpha_C r = a_t$$

$$\alpha_C = 0.02\mathbf{k} \text{ rad/sec}^2$$

The angular acceleration of the rotor shaft is

$$\alpha = (23.6\mathbf{j} + 0.02\mathbf{k}) \text{ rad/sec}^2$$

This problem could also be solved using the method in the next section.

Time Derivative of a Vector Using a Rotating Frame

The basis of determining time derivatives of a vector using a rotating frame is illustrated in Figure 1.3.17.

$$(\mathbf{Q})_{XYZ} = \left(\dot{\mathbf{Q}}\right)_{xyz} + \Omega \times \mathbf{Q}$$

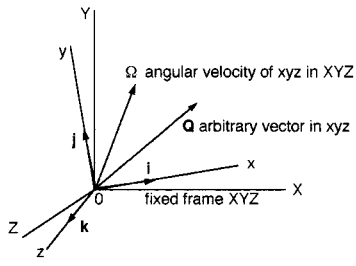

FIGURE 1.3.17 Time derivative of a vector using a rotating reference frame.

Analysis of Velocities and Accelerations Using Rotating and Translating Frames

With the concept of general motion understood, an advantageous method of determining velocities and accelerations is available by the method of rotating reference frames. There are two cases in which this method can be used.

For a common origin of *XYZ* and *xyz*, with **r** being a position vector to a point *P*,

$$\begin{aligned}\mathbf{v}_P &= \mathbf{v}_{xyz} + \Omega \times \mathbf{r} \\ \mathbf{a}_P &= \mathbf{a}_{xyz} + \dot{\Omega} \times \mathbf{r} + \Omega \times (\Omega \times \mathbf{r}) + 2\Omega \times \mathbf{v}_{xyz}\end{aligned} \tag{1.3.50}$$

For the origin *A* of *xyz* translating with respect *XYZ*:

$$\begin{aligned}\mathbf{v}_P &= \mathbf{v}_A + \left(\dot{\mathbf{r}}_{P/A}\right)_{xyz} + \Omega \times \mathbf{r}_{P/A} \\ \mathbf{a}_P &= \mathbf{a}_A + \mathbf{a}_{xyz} + \dot{\Omega} \times \mathbf{r}_{P/A} + \Omega \times \left(\Omega \times \mathbf{r}_{P/A}\right) + 2\Omega \times \mathbf{v}_{xyz}\end{aligned} \tag{1.3.51}$$

where Ω is the angular velocity of the *xyz* frame with respect to *XYZ*. $2\Omega \times \mathbf{v}_{xyz}$ is the Coriolis acceleration.

Kinetics of Rigid Bodies in Plane Motion

Equation of Translational Motion

The fundamental equation for rigid body translation is based on Newton's second law. In Equation 1.3.52, **a** is the acceleration of the center of mass of the rigid body, no matter where the resultant force acts on the body. *The sum of the external forces is equal to the mass of the rigid body times the acceleration of the mass center of the rigid body*, independent of any rotation of the body.

$$\sum \mathbf{F} = m\mathbf{a}_C \tag{1.3.52}$$

Equation of Rotational Motion

Equation 1.3.53 states that *the sum of the external moments on the rigid body is equal to the moment of inertia about an axis times the angular acceleration of the body about that axis*. The angular acceleration α is for the rigid body rotating about an axis. This equation is independent of rigid body translation.

$$\sum \mathbf{M}_C = I_C \alpha \tag{1.3.53}$$

where $\Sigma \mathbf{M}_C = \dot{\mathbf{H}}_C$, $\mathbf{H}_C = I_C \omega$. An application is illustrated in Color Plate 2.

Applications of Equations of Motion

It is important to use the equations of motion properly. For plane motion, three scalar equations are used to define the motion in a plane.

$$\sum F_x = ma_{C_x} \qquad \sum F_y = ma_{C_y} \qquad \sum M_C = I_C \alpha \tag{1.3.54}$$

If a rigid body undergoes only translation,

$$\sum F_x = ma_{C_x} \qquad \sum F_y = ma_{C_y} \qquad \sum M_C = 0 \tag{1.3.55}$$

If the rigid body undergoes pure rotation about the center of mass,

$$\sum F_x = 0 \qquad \sum F_y = 0 \qquad \sum M_C = I_C\alpha \tag{1.3.56}$$

Rigid body motions are categorized according to the constraints of the motion:

1. *Unconstrained Motion*: Equations 1.3.54 are directly applied with all three equations independent of one another.
2. *Constrained Motion*: Equations 1.3.54 are not independent of one another. Generally, a kinematics analysis has to be made to determine how the motion is constrained in the plane. There are two special cases:
   a. Point constraint: the body has a fixed axis.
   b. Line constraint: the body moves along a fixed line or plane.

When considering systems of rigid bodies, it is important to remember that at most only three equations of motion are available from each free-body diagram for plane motion to solve for three unknowns. The motion of interconnected bodies must be analyzed using related free-body diagrams.

Rotation about a Fixed Axis Not Through the Center of Mass

The methods presented above are essential in analyzing rigid bodies that rotate about a fixed axis, which is common in machines (shafts, wheels, gears, linkages). The mass of the rotating body may be nonuniformly distributed as modeled in Figure 1.3.18.

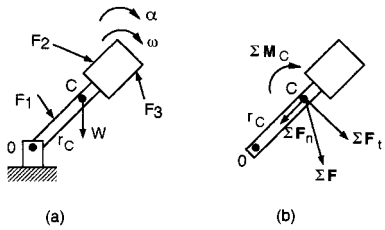

FIGURE 1.3.18 Rotation of a rigid body about a fixed axis.

Note that r_C is the nearest distance between the fixed axis O and the mass center C. The figure also defines the normal and tangential coordinate system used in Equations 1.3.57, which are the scalar equations of motion using normal and tangential components. The sum of the forces must include all reaction forces on the rigid body at the axis of rotation.

$$\sum F_n = mr_C\omega^2 \qquad \sum F_t = mr_C\alpha \qquad \sum M_O = I_O\alpha \tag{1.3.57}$$

General Plane Motion

A body that is translating and rotating is in general plane motion. The scalar equations of motion are given by Equation 1.3.54. If an arbitrary axis A is used to find the resultant moment,

$$\sum \mathbf{M}_A = I_A\alpha + \mathbf{r} \times m\mathbf{a}_C \tag{1.3.58}$$

where *C* is the center of mass. It is a common error to forget to include the cross-product term in the analysis.

There are two special cases in general plane motion, *rolling* and *sliding*.

Figure 1.3.19 shows pure rolling of a wheel without slipping with the center of mass *C* at the geometric center of the wheel. This is called pure rolling of a balanced wheel.

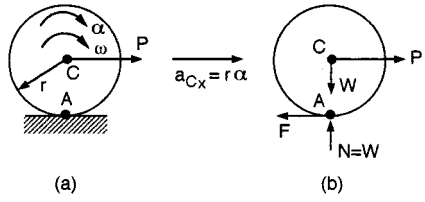

FIGURE 1.3.19 Pure rolling of a wheel.

From this figure the scalar equation of motion results,

$$a_{C_x} = r\alpha \qquad \sum \mathbf{M}_A = I_A \alpha \tag{1.3.59}$$

For balanced wheels either sliding or not sliding, the following schematic is helpful.

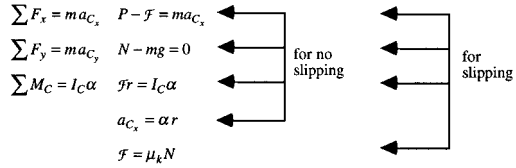

If slipping is not certain, assume there is no slipping and check whether $\mathcal{F} \le \mu_s N$. If $\mathcal{F} > \mu_s N$ (not possible; there is sliding), start the solution over using $\mathcal{F} = \mu_k N$ but not using $a_{C_x} = r\alpha$, which is not valid here.

For the problem involving unbalanced wheels (the mass center and geometric center do not coincide), Equations 1.3.60 result.

$$a_{C_x} \neq r\alpha \qquad a_G = r\alpha$$
$$\mathbf{a}_C = \mathbf{a}_G + \mathbf{a}_{C/G} = \mathbf{a}_G + \left(\mathbf{a}_{C/G}\right)_n + \left(\mathbf{a}_{C/G}\right)_t \tag{1.3.60}$$

Energy and Momentum Methods for Rigid Bodies in Plane Motion

Newton's second law in determining kinetics relationships is not always the most efficient, although it always works. As for particles, energy and momentum methods are often useful to analyze rigid bodies in plane motion.

Work of a Force on a Rigid Body

The work of a force acting on a rigid body moving from position 1 to 2 is

$$U_{12} = \int_1^2 \mathbf{F} \cdot d\mathbf{r} = \int_1^2 \mathbf{F} \cdot \mathbf{v}\, dt \tag{1.3.61}$$

Work of a Moment

The work of a moment has a similar form, for angular positions θ,

$$U_{12} = \int_{\theta_1}^{\theta_2} \mathbf{M} \cdot d\theta \tag{1.3.62}$$

In the common case where the moment vector **M** is perpendicular to the plane of motion, $\mathbf{M} \cdot d\theta = M\, d\theta$.

It is important to note those forces that do no work:

1. Forces that act at fixed points on the body do not do work. For example, the reaction at a fixed, frictionless pin does no work on the body that rotates about that pin.
2. A force which is always perpendicular to the direction of the motion does no work.
3. The weight of a body does no work when the body's center of gravity moves in a horizontal plane.
4. The friction force $\mathcal{F}$ at a point of contact on a body that rolls without slipping does no work. This is because the point of contact is the instantaneous center of zero velocity.

Kinetic Energy of a Rigid Body

The kinetic energy of a particle only consists of the energy associated with its translational motion. The kinetic energy of a rigid body also includes a term for the rotational energy of the body,

$$T = T_{trans} + T_{rot} = \frac{1}{2} m v_C^2 + \frac{1}{2} I_C \omega^2 \tag{1.3.63}$$

where C is the center of mass of the rigid body.

The kinetic energy of a rigid body rotating about an arbitrary axis at point O is

$$T = \frac{1}{2} I_O \omega^2$$

Principle of Work and Energy

The principle of work and energy for a rigid body is the same as used for particles with the addition of the rotational energy terms.

$$T_2 = T_1 + U_{12} \tag{1.3.64}$$

where T_1 = initial kinetic energy of the body
T_2 = final kinetic energy of the body
U_{12} = work of all external forces and moments acting on the body moving from position 1 to 2

This method is advantageous when displacements and velocities are the desired quantities.

Conservation of Energy

The conservation of energy in a conservative rigid body system is

$$T_1 + V_1 = T_2 + V_2 \tag{1.3.65}$$

where T = kinetic energy
V = total potential energy (gravitational and elastic)

Power

The net power supplied to or required of the system is

$$\text{power} = \dot{T}_{trans} + \dot{T}_{rot} + \dot{V}_g + \dot{V}_e \tag{1.3.66}$$

This can be calculated by taking time derivatives of the kinetic and potential energy terms. Each term is considered positive when it represents the power supplied to the system and negative when power is taken from the system.

Impulse and Momentum of a Rigid Body

Impulse and momentum methods are particularly useful when time and velocities are of interest. Figure 1.3.20 shows how rigid bodies are to be considered for this kind of analysis. Notice that rotational motion of the rigid body must be included in the modeling.

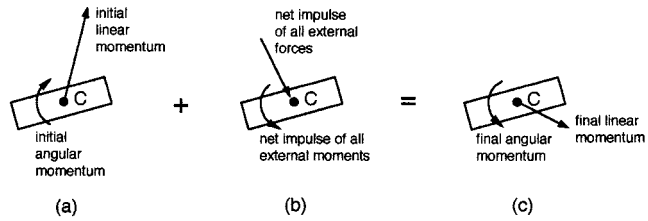

FIGURE 1.3.20 Impulse and momentum for rigid bodies.

The impulse of the external forces in the given interval is

$$\int_{t_1}^{t_2} \sum \mathbf{F}\, dt = m_{C_2}\left(\mathbf{v}_{C_2} - \mathbf{v}_{C_1}\right) \tag{1.3.67}$$

where t is time, C is the center of mass, and $\sum\mathbf{F}$ includes all external forces.

The impulse of the external moments in the given interval is

$$\int_{t_1}^{t_2} \sum \mathbf{M}_C\, dt = \mathbf{H}_{C_2} - \mathbf{H}_{C_1} \tag{1.3.68}$$

For plane motion, if $\sum\mathbf{M}$ is parallel to ω, the scalar expressions are

$$\begin{aligned} &\int_{t_1}^{t_2} \sum M_C\, dt = I_C\left(\omega_2 - \omega_1\right) \\ &\int_{t_1}^{t_2} \sum M_O\, dt = I_O\left(\omega_2 - \omega_1\right) \quad \text{for rotation about a fixed point } O \end{aligned} \tag{1.3.69}$$

Impulse and Momentum of a System of Rigid Bodies

A system of rigid bodies can be analyzed using one of the two following procedures, illustrated in Figure 1.3.21.

1. Apply the principle of impulse and momentum to each rigid member separately. The mutual forces acting between members must be included in the formulation of the solution.
2. Apply the principle of impulse and momentum to the entire system of bodies, ignoring the mutual forces between members.

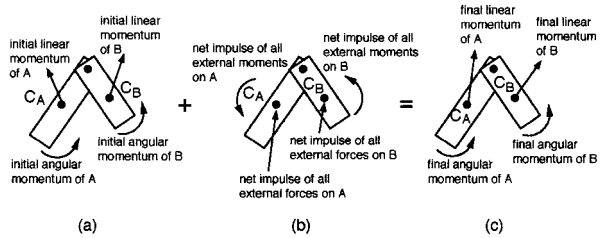

FIGURE 1.3.21 System of rigid bodies.

Conservation of Momentum

The principle of conservation of linear and angular momentum of particles can be extended to rigid bodies that have no external forces or moments acting on them. The conservation of linear momentum means that the center of mass C moves at a constant speed in a constant direction,

$$\sum \mathbf{F} = 0 \Rightarrow \Delta \mathbf{G} = 0$$
$$\mathbf{v}_{C_1} = \mathbf{v}_{C_2} \tag{1.3.70}$$

Likewise, for conservation of angular momentum of rigid bodies,

$$\sum \mathbf{M} = 0 \Rightarrow \Delta \mathbf{H}_C = 0$$
$$I_C \omega_1 = I_C \omega_2 \tag{1.3.71}$$

For a system of rigid bodies, use the same fixed reference point O for all parts of the system. Thus, for plane motion,

$$\Delta \mathbf{H}_O = 0 \qquad I_O \omega_1 = I_O \omega_2 \tag{1.3.72}$$

There are two important points to remember when using these equations. First, $\Delta \mathbf{H}_C = 0$ does not imply that $\Delta \mathbf{H}_O = 0$, or vice versa. Second, conservation of momentum does not require the simultaneous conservation of both angular and linear momenta (for example, there may be an angular impulse while linear momentum is conserved).

Kinetics of Rigid Bodies in Three Dimensions

The concepts of plane rigid body motion can be extended to the more complicated problems in three dimensions, such as of gyroscopes and jet engines. This section briefly covers some fundamental topics. There are many additional topics and useful methods that are included in the technical literature.

Angular Momentum in Three Dimensions

For analyzing three-dimensional angular momentum, three special definitions are used. These can be visualized by considering a spinning top (Figure 1.3.22).

Precession — rotation of the angular velocity vector about the y axis.
Space Cone — locus of the absolute positions of the instantaneous axis of rotation.
Body Cone — locus of the positions of the instantaneous axis relative to the body. The body cone appears to roll on the space cone (not shown here).

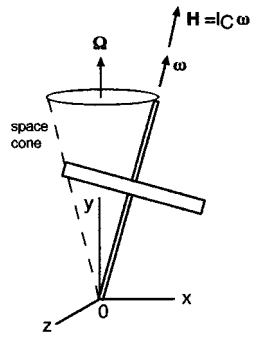

FIGURE 1.3.22 Motion of an inclined, spinning top.

Equations 1.3.73 provide the scalar components of the total angular momentum.

$$\begin{aligned} H_x &= I_x\omega_x - I_{xy}\omega_y - I_{xz}\omega_z \\ H_y &= -I_{xy}\omega_x + I_y\omega_y - I_{yz}\omega_z \\ H_z &= -I_{zx}\omega_x - I_{zy}\omega_y + I_z\omega_z \end{aligned} \tag{1.3.73}$$

Impulse and Momentum of a Rigid Body in Three-Dimensional Motion

The extension of the planar motion equations of impulse and momentum to three dimensions is straightforward.

$$\text{System momenta} = \begin{cases} \text{linear momentum of mass center } (\mathbf{G}) \\ \text{angular momentum about mass center } (\mathbf{H}_C) \end{cases} \tag{1.3.74}$$

where **G** and **H** have different units. The principle of impulse and momentum is applied for the period of time t_1 to t_2,

$$\begin{aligned} \mathbf{G}_2 &= \mathbf{G}_1 + \left(\text{external linear impulses}\right)\Big|_1^2 \\ \mathbf{H}_{C_2} &= \mathbf{H}_{C_1} + \left(\text{external angular impulses}\right)\Big|_1^2 \end{aligned} \tag{1.3.75}$$

Kinetic Energy of a Rigid Body in Three-Dimensional Motion

The total kinetic energy of a rigid body in three dimensions is

$$T = \underbrace{\frac{1}{2}mv_C^2}_{\substack{\text{translation} \\ \text{of mass center}}} + \underbrace{\frac{1}{2}\boldsymbol{\omega}\cdot\mathbf{H}_C}_{\substack{\text{rotation about} \\ \text{mass center}}} \tag{1.3.76}$$

For a rigid body that has a fixed point *O*,

$$T = \frac{1}{2}\boldsymbol{\omega}\cdot\mathbf{H}_O \tag{1.3.77}$$

Equations of Motion in Three Dimensions

The equations of motion for a rigid body in three dimensions are extensions of the equations previously stated.

$$\sum \mathbf{F} = m\mathbf{a}_C$$
$$\sum \mathbf{M}_C = \dot{\mathbf{H}}_C = \left(\dot{\mathbf{H}}_C\right)_{xyz} + \Omega \times \mathbf{H}_C \tag{1.3.78}$$

where $\mathbf{a}_C$ = acceleration of mass center
$\mathbf{H}_C$ = angular momentum of the body about its mass center
xyz = frame fixed in the body with origin at the mass center
Ω = angular velocity of the xyz frame with respect to a fixed XYZ frame

Note that an arbitrary fixed point O may be used for reference if done consistently.

Euler's Equations of Motion

Euler's equations of motion result from the simplification of allowing the xyz axes to coincide with the principal axes of inertia of the body.

$$\sum M_x = I_x\dot{\omega}_x - \left(I_y - I_z\right)\omega_y\omega_z$$
$$\sum M_y = I_y\dot{\omega}_y - \left(I_z - I_x\right)\omega_z\omega_x \tag{1.3.79}$$
$$\sum M_z = I_z\dot{\omega}_z - \left(I_x - I_y\right)\omega_x\omega_y$$

where all quantities must be evaluated with respect to the appropriate principal axes.

Solution of Problems in Three-Dimensional Motion

In order to solve a three-dimensional problem it is necessary to apply the six independent scalar equations.

$$\sum F_x = ma_{C_x} \qquad \sum F_y = ma_{C_y} \qquad \sum F_z = ma_{C_z}$$

$$\sum M_x = \dot{H}_x + \omega_y H_z - \omega_z H_y$$
$$\sum M_y = \dot{H}_y + \omega_z H_x - \omega_x H_z \tag{1.3.80}$$
$$\sum M_z = \dot{H}_z + \omega_x H_y - \omega_y H_x$$

These equations are valid in general. Some common cases are briefly stated.

Unconstrained motion. The six governing equations should be used with xyz axes attached at the center of mass of the body.

Motion of a body about a fixed point. The governing equations are valid for a body rotating about a noncentroidal fixed point O. The reference axes xyz must pass through the fixed point to allow using a set of moment equations that do not involve the unknown reactions at O.

Motion of a body about a fixed axis. This is the generalized form of plane motion of an arbitrary rigid body. The analysis of unbalanced wheels and shafts and corresponding bearing reactions falls in this category.

1.4 Vibrations

Bela I. Sandor with assistance by Stephen M. Birn

Vibrations in machines and structures should be analyzed and controlled if they have undesirable effects such as noise, unpleasant motions, or fatigue damage with potentially catastrophic consequences. Conversely, vibrations are sometimes employed to useful purposes, such as for compacting materials.

Undamped Free and Forced Vibrations

The simplest vibrating system has motion of one degree of freedom (DOF) described by the coordinate x in Figure 1.4.1. (An analogous approach is used for torsional vibrations, with similar results.)

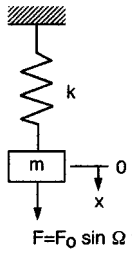

FIGURE 1.4.1 Model of a simple vibrating system.

Assuming that the spring has no mass and that there is no damping in the system, the equation of motion for **free vibration** (motion under internal forces only; $F = 0$) is

$$m\ddot{x} + kx = 0 \qquad \text{or} \qquad \ddot{x} + \omega^2 x = 0 \tag{1.4.1}$$

where $\omega = \sqrt{k/m}$ = natural circular frequency in rad/sec.

The displacement x as a function of time t is

$$x = C_1 \sin \omega t + C_2 \cos \omega t \tag{1.4.2}$$

where C_1 and C_2 are constants depending on the initial conditions of the motion. Alternatively,

$$x = A\sin(\omega t + \phi)$$

where $C_1 = A\cos\phi$, $C_2 = A\sin\phi$, and ϕ is the phase angle, another constant. A complete cycle of the motion occurs in time τ, the *period of simple harmonic motion*,

$$\tau = \frac{2\pi}{\omega} = 2\pi\sqrt{\frac{m}{k}} \ (\text{seconds per cycle})$$

The *frequency* in units of cycles per second (cps) or hertz (Hz) is $f = 1/\tau$.

The simplest case of **forced vibration** is modeled in Figure 1.4.1, with the force F included. Using typical simplifying assumptions as above, the equation of motion for a harmonic force of forcing frequency Ω,

$$m\ddot{x} + kx = F_o \sin \Omega t \tag{1.4.3}$$

The vibrations of a mass m may also be induced by the displacement $d = d_o \sin \Omega t$ of a foundation or another mass M to which m is attached by a spring k. Using the same reference point and axis for both x and d, the equation of motion for m is

$$\begin{aligned} m\ddot{x} + k\left(x - d_o \sin \Omega t\right) &= 0 \\ m\ddot{x} + kx &= kd_o \sin \Omega t \end{aligned} \tag{1.4.4}$$

where d_o is the amplitude of vibration of the moving support M, and Ω is its frequency of motion.

The general solution of the forced vibration in the *steady state* (after the initial, transient behavior) is

$$\begin{aligned} x &= A \sin \Omega t \\ A &= \frac{F_o}{k - m\Omega^2} = \frac{F_o/k}{1 - \left(\Omega/\omega\right)^2} \end{aligned} \tag{1.4.5}$$

where Ω is the forcing frequency and ω is the natural circular frequency of the system of m and k.

Resonance. The amplitude of the oscillations in forced vibrations depends on the frequency ratio Ω/ω. Without damping or physical constraints, the amplitude would become infinite at $\Omega = \omega$, the condition of **resonance**. Dangerously large amplitudes may occur at resonance and at other frequency ratios near the resonant frequency. A *magnification factor* is defined as

$$MF = \frac{F}{F_o/k} = \frac{A}{d_o} = \frac{1}{1 - \left(\Omega/\omega\right)^2} \tag{1.4.6}$$

Several special cases of this are noted:

1. Static loading: $\Omega = 0$, or $\Omega \ll \omega$; MF $\simeq$ 1.
2. Resonance: $\Omega = \omega$; $MF = \infty$.
3. High-frequency excitation: $\Omega \gg \omega$; MF $\simeq$ 0.
4. Phase relationships: The vibration is *in phase* for $\Omega < \omega$, and it is 180° *out of phase* for $\Omega > \omega$.

Damped Free and Forced Vibrations

A vibrating system of one degree of freedom and damping is modeled in Figure 1.4.2. The equation of motion for *damped free vibrations* ($F = 0$) is

$$m\ddot{x} + c\dot{x} + kx = 0 \tag{1.4.7}$$

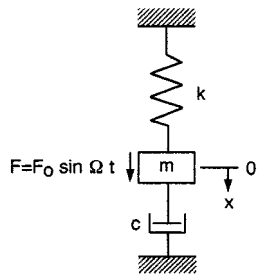

FIGURE 1.4.2 Model of a damped vibrating system.

The displacement x as a function of time t is

$$x = e^{\lambda t} \tag{1.4.8}$$

$$\lambda_{1,2} = \frac{-c}{2m} \pm \sqrt{\left(\frac{c}{2m}\right)^2 - \frac{k}{m}}$$

The value of the coefficient of viscous damping c that makes the radical zero is the *critical damping coefficient* $c_c = 2m\sqrt{k/m} = 2m\omega$. Three special cases of damped free vibrations are noted:

1. Overdamped system: $c > c_c$; the motion is *nonvibratory* or *aperiodic.*
2. Critically damped system: $c = c_c$; this motion is also nonvibratory; x decreases at the fastest rate possible without oscillation of the mass.
3. Underdamped system: $c < c_c$; the roots $\lambda_{1,2}$ are complex numbers; the displacement is

$$x = Ae^{-(c/2m)t}\sin\left(\omega_d t + \phi\right)$$

where A and ϕ are constants depending on the initial conditions, and the *damped natural frequency* is

$$\omega_d = \omega\sqrt{1 - \left(\frac{c}{c_c}\right)^2}$$

The ratio c/c_c is the *damping factor* ζ. The damping in a system is determined by measuring the rate of decay of free oscillations. This is expressed by the *logarithmic decrement* δ, involving any two successive amplitudes x_i and x_{i+1},

$$\delta = \ln\frac{x_i}{x_{i+1}} = \frac{2\pi\zeta}{\sqrt{1-\zeta^2}} \simeq 2\pi\zeta$$

The simplifying approximation for δ is valid for up to about 20% damping ($\zeta \simeq 0.2$).

The *period of the damped vibration* is $\tau_d = 2\pi/\omega_d$. It is a constant, but always larger than the period of the same system without damping. In many real systems the damping is relatively small ($\zeta < 0.2$), where $\tau_d \simeq \tau$ and $\omega_d \simeq \omega$ can be used.

The equation of motion for *damped forced vibrations* (Figure 1.4.2; $F \neq 0$) is

$$m\ddot{x} + c\dot{x} + kx = F_o \sin\Omega t \tag{1.4.9}$$

The solution for steady-state vibration of the system is

$$x = A\sin\left(\Omega t - \phi\right) \tag{1.4.10}$$

where the amplitude and phase angle are from

$$A = \frac{F_o}{\sqrt{\left(c\Omega\right)^2 + \left(k - m\Omega^2\right)^2}}$$

$$\tan\phi = \frac{c\Omega}{k - m\Omega^2}$$

The *magnification factor* for the amplitude of the oscillations is

$$MF = \frac{A}{F_o/k} = \frac{A}{d_o} = \frac{1}{\sqrt{\left[2\zeta(\Omega/\omega)\right]^2 + \left[1-(\Omega/\omega)^2\right]^2}} \tag{1.4.11}$$

This quantity is sketched as a function of the frequency ratio Ω/ω for several damping factors in Figure 1.4.3. Note that the amplitude of vibration is reduced at all values of Ω/ω if the coefficient of damping c is increased in a particular system.

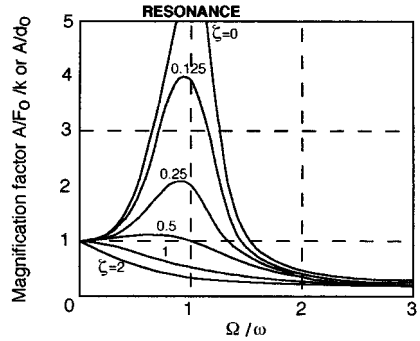

FIGURE 1.4.3 Magnification factor in damped forced vibration.

Vibration Control

Vibration Isolation

It is often desirable to reduce the forces transmitted, or the noise and motions inside or in the neighborhood of vibrating machines and structures. This can be done to some extent within the constraints of space and additional weight and cost by the use of isolators, such as rubber engine mounts and wheel suspension systems in cars. Many kinds of isolating materials and systems are available commercially.

The effectiveness of vibration isolation is expressed by the *transmissibility TR*, the ratio of the force transmitted F_T to the disturbing force F_o. A simple isolation system is modeled as a spring and a dashpot in parallel, for which the transmissibility is given by Equation 1.4.12 and sketched in Figure 1.4.4.

$$TR = \frac{F_T}{F_o} = \frac{\sqrt{1+4\zeta^2(\Omega/\omega)^2}}{\sqrt{\left[1-(\Omega/\omega)^2\right]^2 + 4\zeta^2(\Omega/\omega)^2}} \tag{1.4.12}$$

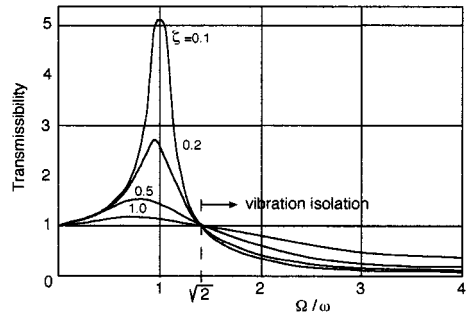

FIGURE 1.4.4 Transmissibility patterns of a vibration isolator.

When damping is negligible,

$$TR \simeq \frac{1}{(\Omega/\omega)^2 - 1}$$

Note from the figure that

1. Vibration isolation occurs at $\Omega/\omega > \sqrt{2}$.
2. Isolation efficiency increases with decreasing stiffness of the isolation mounts.
3. Damping reduces isolation efficiency. However, some damping is normally required if resonance may occur in a system even for short periods.
4. The response curves are essentially independent of damping when Ω/ω is large $(\gtrsim 3)$ and damping is low $(\zeta \lesssim 0.2)$. Here $TR \simeq 1/[(\Omega/\omega)^2 - 1]$.
5. For a system with more than one excitation frequency, the lowest excitation frequency is of primary importance.

The efficiency of an isolating system is defined by the reduction R in transmissibility,

$$R = 1 - TR$$

If a certain reduction R in transmissibility is desired, the appropriate stiffness k of an isolation system is obtained from $\omega = \sqrt{k/m}$ and

$$\frac{\Omega}{\omega} = \sqrt{\frac{2 - R}{1 - R}}$$

A small magnitude of stiffness k makes the reduction R in transmissibility large. It is difficult to achieve isolation for very low excitation frequencies because of the required large static deflections. To obtain highly efficient isolation at low excitation frequencies, a large supporting mass M may be utilized, with the value of $\omega = \sqrt{k/(m + M)}$.

Vibration Absorption

In some cases a vibratory force is purposely generated in a system by a secondary spring-mass system to oppose a primary disturbing force and thereby reduce or eliminate the undesirable net effect. An interesting example of this is the "tuned-mass damper" in a few skyscrapers, designed to counter the oscillatory motions caused by wind. The secondary spring-mass system has disadvantages of its own, such as extra weight, complexity, and effectiveness limited to a single frequency.

Balancing of Rotating Components

The conditions of static or dynamic unbalance of rotating bodies have long been recognized. These can be analyzed by the methods of elementary mechanics, simple tests can be performed in many cases, and adequate corrections can be made routinely to achieve balance, such as for the wheels of automotive vehicles. Three categories of increasing complexity are distinguished.

1. *Static unbalance*. The distributed or lumped masses causing unbalance are in a single axial plane and all on the same side of the axis of rotation (Figure 1.4.5). Thin disks are also in this category. Static unbalance is detected in a static test since the center of gravity of the body is not on the axis, and correction is made by adding or removing mass at a convenient radial distance from the axis.
2. *Static balance with dynamic unbalance*. This may be the case when the masses causing unbalance are in a single axial plane but on opposite sides of the axis of rotation (Figure 1.4.6a). Static balance is achieved if the center of gravity of the body is on the axis, but dynamic unbalance

results from the couple of the unbalance forces ($m\omega^2 r$) during rotation, causing a shaking of the axle.

3. *Static and dynamic unbalance*. This is the general case of unbalance, which can be visualized by letting m_1 and m_2 and the axis of rotation not all lie in the same plane (Figure 1.4.6b).

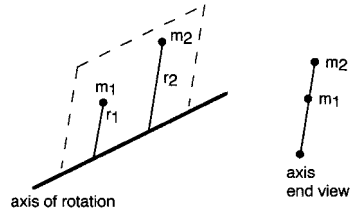

FIGURE 1.4.5 Schematic of static unbalance.

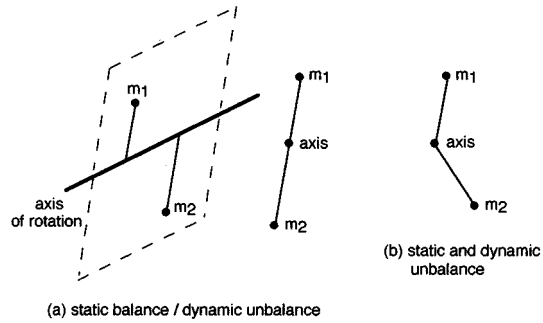

FIGURE 1.4.6 Schematic of two cases of dynamic unbalance.

The magnitude and angular position of a body's unbalance can be determined using a dynamic balancing machine. Here the shaking forces are measured by electronically sensing the small oscillations of the bearings that can be correlated with the position of the body.

Critical Speed of Rotating Shafts

A rotating shaft may become dangerously unstable and whirl with large lateral amplitudes of displacement at a critical speed of rotation. The critical speed, in revolutions per second, corresponds with the natural frequency of lateral vibration of the system. Thus, it can be analytically predicted fairly well and can be safely measured in a real but nonrotating machine with high precision.

If unavoidable, as at startup, the critical speed should be passed over rapidly. Other ways of minimizing the problems of whirling shafts include the proper balancing of rotors and the replacing of bent shafts and worn bearings.

Random Vibrations. Shock Excitation

Many structures are subjected to nonharmonic excitations and respond with transient vibrations rather than steady-state motions. Random vibration is often caused by *shock* excitation, which implies that the loading occurs suddenly, in a short time with respect to the natural period of vibration of the system. Such a loading, typically caused by impact conditions, may be highly irregular in terms of amplitude, waveform, and repetition (Figure 1.4.7), but normally it is possible to extract practically uniform critical events from the loading history for purposes of future design and life prediction.

For most practical purposes, this plot represents aperiodic motion, where the important quantities are the maximum and average large amplitudes and the projected total repetitions (in this case, at the rate of about 1000 per day) over the design life of the structure. The small-amplitude transient vibrations

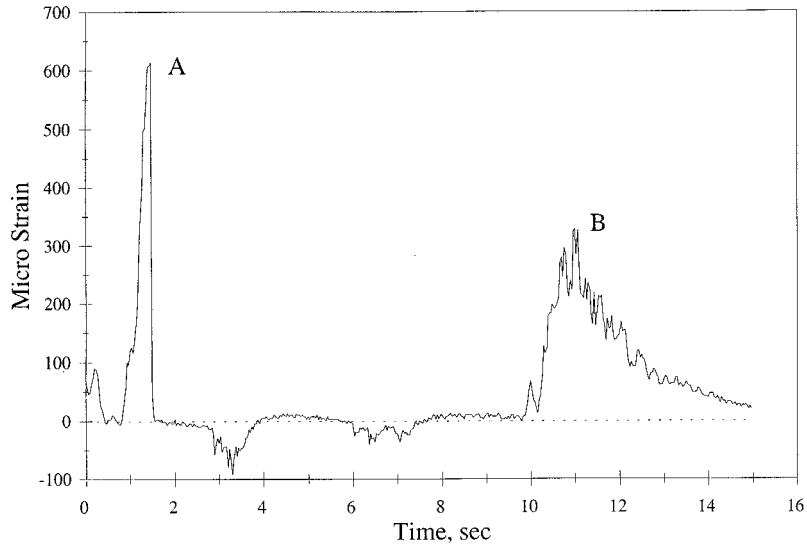

FIGURE 1.4.7 Strain-time history at one strain-gage location on a steel bridge caused by two trucks moving in opposite directions. (A) Garbage truck in the near lane; (B) tractor trailer in the far lane. Weights unknown. (Data courtesy Mark J. Fleming, University of Wisconsin-Madison.)

associated with the large events are likely to be negligible here in terms of both dynamic behavior and fatigue damage, although the relatively large number of small oscillations may cause one to be concerned in some cases.

Random vibrations are difficult to deal with analytically. Numerical methods involving computers are advantageous to obtain response (or shock) spectrums of a system, assuming key parameters and simple models of nonharmonic excitations such as impulsive forces and force step functions. Since the maximum transient response is relatively insensitive to damping, an undamped system is useful in modeling response spectrums. Experimental techniques are needed to verify the analytical predictions, especially when the behavior of a multiple-degree-of-freedom system is determined from the response spectrum of a single-degree-of-freedom system.

Multiple-Degree-of-Freedom Systems. Modal Analysis

The analysis of a system with more than one degree of freedom requires an independent coordinate for each degree of freedom to describe the configurations. Thus, an *n*-degree-of-freedom system has *n* natural frequencies and *n* normal *modes* of vibration. Complex systems can be classified as (1) discrete and lumped-parameter systems with finite numbers of degrees of freedom or (2) continuous elastic bodies of distributed mass with infinite number of degrees of freedom (in theory). A common example of the latter is a vibrating beam, with the first two modes of vibration shown in Figure 1.4.8. Each *nodal point* is a point of zero deflection. Usually the *fundamental natural frequency* (the lowest) is the most important, and only the lowest few frequencies are considered in practice.

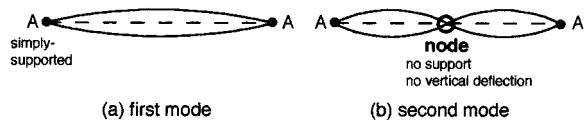

FIGURE 1.4.8 Simply supported beam in two modes of vibration.

A system's harmonic vibrations are its *principal modes*. There are also many ways in which the system can vibrate nonharmonically. Periodic motion of complex wave form can be analyzed as a combination of principal-mode vibrations.

The classical method of mathematical solution and the experimental techniques become increasingly cumbersome and sometimes inaccurate for a system of more than a few degrees of freedom. The recent emergence of sophisticated numerical (finite element; Figure 1.4.9) and experimental (electro-optics) techniques has resulted in significant progress in this area. The synergistic aspects of several new methods are especially remarkable. For example, damage caused by vibrations can significantly affect a system's own modal behavior and, consequently, the rate of damage evolution. Such nonlinear changes of a system can now be investigated and eventually predicted by the hybrid applications of computerized numerical methods, fatigue and fracture mechanics (Section 1.6), and high-speed, noncontacting, full-field vibration and stress imaging (Sections 1.4, "Vibration-Measuring Instruments," and 1.5, "Experimental Stress Analysis and Mechanical Testing"). These enhance the already powerful modern methods of *modal analysis* for accurately describing the response of multiple-degree-of-freedom systems.

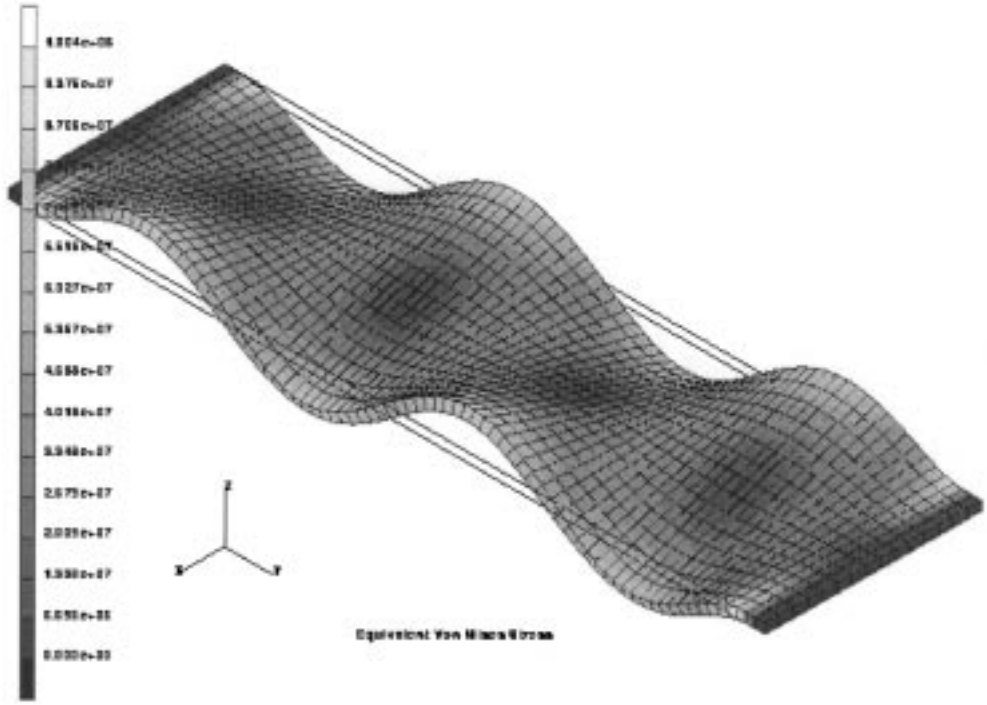

FIGURE 1.4.9 Modal analysis of a vibrating plate. (Photo courtesy David T. Corr, University of Wisconsin-Madison.)

Vibration-Measuring Instruments

There are many kinds of instruments for the experimental investigation of vibrating systems. They range from simple, inexpensive devices to sophisticated electro-optics with lasers or infrared detectors, with the list still expanding in many areas.

The basic quantities of interest regarding a vibrating system are the displacement, velocity, acceleration, and frequency. A typical sensor (or pickup or transducer) for determining these is the piezoelectric accelerometer, which is attached to the vibrating machine or structure to be analyzed. The complete setup normally includes amplifiers, frequency analyzer, oscilloscope, and recorders. An instrumented

impact hammer may be used to provide well-defined impulse excitation to determine the natural frequencies of structures. The frequency analyzer can display the accelerometer output in either the time or the frequency domain.

Other kinds of devices used for vibration sensing include seismic spring-mass systems, electrical-resistance strain gages, and electromagnetic transducers.

Care must be exercised in matching a transducer to the task at hand, since reliable data can be obtained only if the transducer has a "flat-response" frequency region for the measurements of interest. For example, electromagnetic vibrometers (or seismometers) are low-frequency transducers that have low natural frequency compared to the frequency of the motion to be measured. At the other extreme, piezoelectric accelerometers are designed to have higher natural frequency than the frequency to be measured.

It is also important to use transducers of negligible mass compared to the mass of the vibrating system being measured. Very small, light-weight accelerometers are available to satisfy this condition in many cases. There are situations, however, where only noncontacting means of motion measurement provide satisfactory results. Optical techniques are prominent in this area, offering several advantages besides the noncontacting measurement capability. They can be full-field techniques, which means that data may be obtained rapidly from many points on a body using one instrument. They have excellent resolution and precision, and some of them are easy to use. Three kinds of optical instruments are distinguished here for vibratory system analysis, depending on the primary quantity measured:

1. *Displacement measurement*. Holography and speckle pattern imaging have excellent resolution, but they are adversely affected by unstable measuring conditions. They are most useful in laboratory applications.
2. *Velocity measurement*. Laser Doppler systems provide time-resolved, accelerometer-like measurements. They are relatively unaffected by measuring conditions, and are simple and rugged enough to use either in the laboratory or in the field. Several important capabilities of such a vibration pattern imaging system are worth mentioning (Color Plates 3 to 7):
   - Noncontacting; the structure's response is not affected by the instrumentation; applicable in some hazardous environments (hot structures etc.), and short or long range (over 200 m) on natural surfaces
   - Single-point or full-field data acquisition at high resolution from areas of 0.5×0.5 mm to 8×8 m; up to 500 individual points can be programmed
   - Wide frequency range; 0 to 100 kHz (for example, Figure 1.4.10)
   - Sensitivity to a wide range of vibration velocities; 0.005 to 1000 mm/sec
   - Large depth of focus; ±3 m at 10-m working distance
   - Node spacing down to a few millimeters can be resolved
   - Resolution of small displacements, down to the wavelength of the laser source (typically, ≈1 Å)
   - Safe, class II laser system; <1 mW output
   - Conventional signal processing is used to give multipoint modal parameters in familiar format for analytical comparisons
3. *Dynamic stress measurement*. Differential thermography via dynamic thermoelasticity (Figure 1.4.11) has recently become a powerful technique for measuring the modal response of vibrating structures and, uniquely, for directly assessing the structural integrity and durability aspects of the situation. This approach uses high-speed infrared electro-optics and has predictive capability because it can be quantitatively combined with modern fatigue and fracture mechanics methods. For example, it can effectively relate vibration modes to complex fracture modes and damage evolution rates of a real component even under arbitrary and unknown loading with unknown boundary conditions. See Section 1.5, "Experimental Stress Analysis and Mechanical Testing," for more on the dynamic thermoelasticity technique.

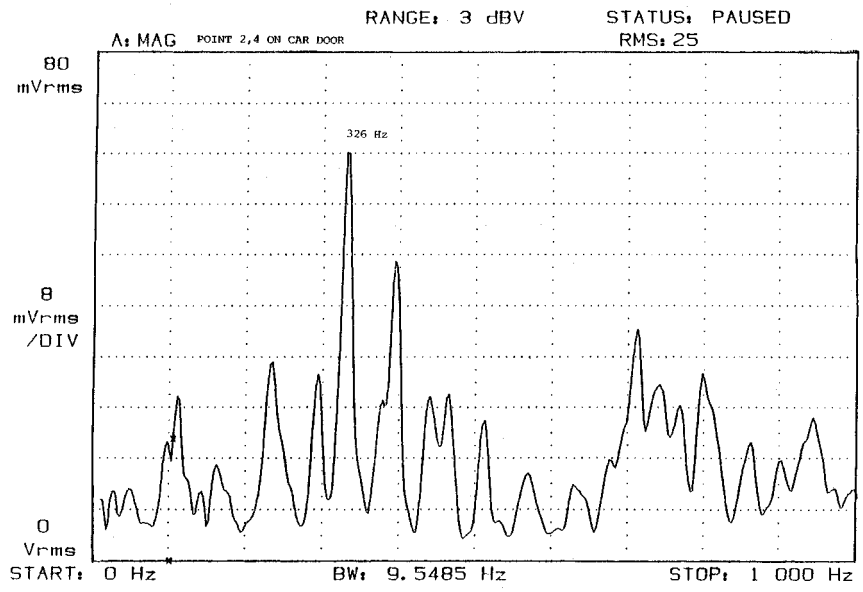

FIGURE 1.4.10 Laser-based, noncontacting vibration analysis of a point on a car door. (Data courtesy of Ometron Inc., Sterling, VA.)

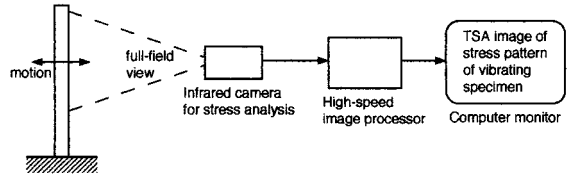

FIGURE 1.4.11 Schematic of modal analysis of a jet engine turbine blade by thermal imaging of the stress field caused by complex vibration. For sample data, see Color Plate 8.

1.5 Mechanics of Materials

Bela I. Sandor

Mechanics of materials, also called strength of materials, provides quantitative methods to determine stresses (the intensity of forces) and strains (the severity of deformations), or overall deformations or load-carrying abilities of components and structures. The stress-strain behavior of materials under a wide range of service conditions must be considered in many designs. It is also crucial to base the analysis on correct modeling of component geometries and external loads. This can be difficult in the case of multiaxial loading, and even more so if time- or temperature-dependent material behaviors must be considered.

Proper modeling involves free-body diagrams and equations of equilibrium. However, it is important to remember that *the equilibrium equations of statics are valid only for forces or for moments of forces*, and not for stresses.

Stress

The intensity of a force is called stress and is defined as the force acting on an infinitesimal area. A normal stress σ is defined as

$$\sigma = \lim_{dA \to 0} \frac{dF}{dA} \tag{1.5.1}$$

where dF is a differential normal force acting on a differential area dA. It is often useful to calculate the average normal stress $\sigma = P/A$, where P is the resultant force on an area A. A shear stress τ caused by a shearing force V is defined likewise,

$$\tau = \lim_{dA \to 0} \frac{dV}{dA} \tag{1.5.2}$$

An average shear stress is obtained from V/A.

It is helpful to consider the general cases of stresses using rectangular elements in two and three dimensions, while ignoring the deformations caused by the stresses.

Plane Stress

There are relatively simple cases where all stress vectors lie in the same plane. This is represented by a two-dimensional element in Figure 1.5.1, where σ_x and/or σ_y may be either tensile (pulling on the element as shown) or compressive (pushing on the element; not shown). Normal stresses are easy to visualize and set up correctly.

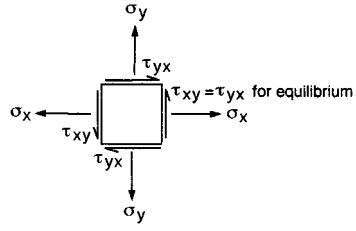

FIGURE 1.5.1 Generalized plane stress.

Shear stresses need to be discussed here in a little detail. The notation means that τ_{xy}, for example, is a shear stress acting in the y direction, on a face that is perpendicular to the x axis. It follows that τ_{yx} is acting in the x direction, on a face that is perpendicular to the y axis. The four shear stress vectors are

pointed as they are because of the requirement that the element be in equilibrium: the net forces and moments of forces on it must be zero. Thus, reversing the direction of all four τ's in Figure 1.5.1 is possible, but reversing less than four is not realistic.

Three-Dimensional State of Stress

The concept of plane stress can be generalized for a three-dimensional element as shown in Figure 1.5.2, working with the three primary faces of the cube and not showing stresses on the hidden faces, for clarity.

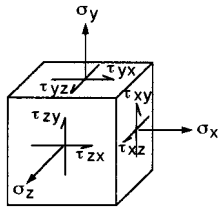

FIGURE 1.5.2 Three-dimensional general state of stress.

Again, the normal stresses are easy to set up, while the shear stresses may require considerable attention. The complex cases of stresses result from multiaxial loading, such as combined axial, bending, and torsional loading. Note that even in complex situations simplifications are possible. For example, if the right face in Figure 1.5.2 is a free surface, $\sigma_x = \tau_{xz} = \tau_{xy} = 0$. This leaves a plane stress state with σ_y, σ_z, and τ_{yz}, at most.

Stress Transformation

A free-body element with known stresses on it allows the calculation of stresses in directions other than the given *xyz* coordinates. This is useful when potentially critical welded or glued joints, or fibers of a composite, are along other axes. The stress transformations are simplest in the case of plane stress and can be done in several ways. In any case, at a given point in a material there is only one state of stress at a particular instant. At the same time, the components of the stresses depend on the orientation of the chosen coordinate system.

The stress transformation equations depend on the chosen coordinate system and the sign convention adopted. A common arrangement is shown in Figure 1.5.3, where (a) is the known set of stresses and (b) is the unknown set, denoted by primes.

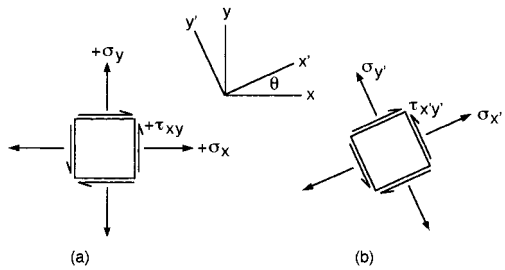

FIGURE 1.5.3 Elements for stress transformation.

In the present sign convention an outward normal stress is positive, and an upward shear stress on the right-hand face of the element is positive. The transformation equations are

$$\sigma_{x'} = \frac{\sigma_x + \sigma_y}{2} + \frac{\sigma_x - \sigma_y}{2}\cos 2\theta + \tau_{xy}\sin 2\theta$$

$$\sigma_{y'} = \frac{\sigma_x + \sigma_y}{2} - \frac{\sigma_x - \sigma_y}{2}\cos 2\theta - \tau_{xy}\sin 2\theta \qquad (1.5.3)$$

$$\tau_{x'y'} = -\frac{\sigma_x - \sigma_y}{2}\sin 2\theta + \tau_{xy}\cos 2\theta$$

If a result is negative, it means that the actual direction of the stress is opposite to the assumed direction.

Principal Stresses

It is often important to determine the maximum and minimum values of the stress at a point and the orientations of the planes of these stresses. For plane stress, the maximum and minimum normal stresses, called **principal stresses**, are obtained from

$$\sigma_{1,2} = \frac{\sigma_x + \sigma_y}{2} \pm \sqrt{\left(\frac{\sigma_x - \sigma_y}{2}\right)^2 + \tau_{xy}^2} \qquad (1.5.4)$$

There is no shear stress acting on the principal planes on which the principal stresses are acting. However, there are shear stresses on other planes. The maximum shear stress is calculated from

$$\tau_{\max} = \sqrt{\left(\frac{\sigma_x - \sigma_y}{2}\right)^2 + \tau_{xy}^2} \qquad (1.5.5)$$

This stress acts on planes oriented 45° from the planes of principal stress. There is a normal stress on these planes of τ_{max}, the average of σ_x and σ_y,

$$\sigma_{ave} = \frac{\sigma_x + \sigma_y}{2} \qquad (1.5.6)$$

Mohr's Circle for Plane Stress

The equations for plane stress transformation have a graphical solution, called Mohr's circle, which is convenient to use in engineering practice, including "back-of-the-envelope" calculations. Mohr's circle is plotted on a $\sigma - \tau$ coordinate system as in Figure 1.5.4, with the center C of the circle always on the σ axis at $\sigma_{ave} = (\sigma_x + \sigma_y)/2$ and its radius $R = \sqrt{[(\sigma_x - \sigma_y)/2]^2 + \tau_{xy}^2}$. The positive τ axis is downward for convenience, to make θ on the element and the corresponding 2θ on the circle agree in sense (both counterclockwise here).

The following aspects of Mohr's circle should be noted:

1. The center C of the circle is always on the σ axis, but it may move left and right in a dynamic loading situation. This should be considered in failure prevention.
2. The radius R of the circle is τ_{max}, and it may change, even pulsate, in dynamic loading. This is also relevant in failure prevention.
3. Working back and forth between the rectangular element and the circle should be done carefully and consistently. An angle θ on the element should be represented by 2θ in the corresponding circle. If τ is positive downward for the circle, the sense of rotation is identical in the element and the circle.

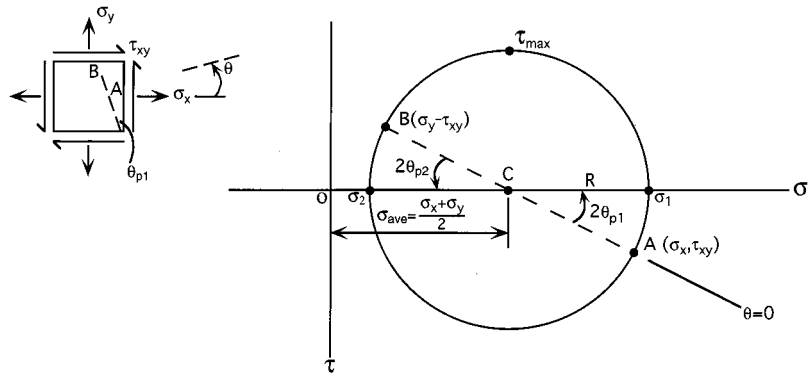

FIGURE 1.5.4 Mohr's circle.

4. The principal stresses σ_1 and σ_2 are on the σ axis ($\tau = 0$).
5. The planes on which σ_1 and σ_2 act are oriented at $2\theta_p$ from the planes of σ_x and σ_y (respectively) in the circle and at θ_p in the element.
6. The stresses on an arbitrary plane can be determined by their σ and τ coordinates from the circle. These coordinates give magnitudes and signs of the stresses. The physical meaning of $+\tau$ vs. $-\tau$ regarding material response is normally not as distinct as $+\sigma$ vs. $-\sigma$ (tension vs. compression).
7. To plot the circle, either use the calculated center *C* coordinate and the radius *R*, or directly plot the stress coordinates for two mutually perpendicular planes and draw the circle through the two points (*A* and *B* in Figure 1.5.4) which must be diametrically opposite on the circle.

Special Cases of Mohr's Circles for Plane Stress

See Figures 1.5.5 to 1.5.9

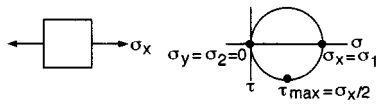

FIGURE 1.5.5 Uniaxial tension.

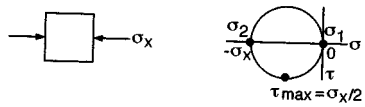

FIGURE 1.5.6 Uniaxial compression.

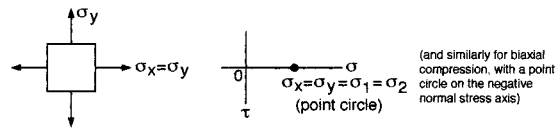

FIGURE 1.5.7 Biaxial tension: $\sigma_x = \sigma_y$ (and similarly for biaxial compression: $-\sigma_x = -\sigma_y$).

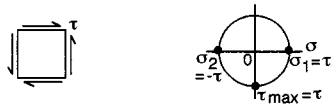

FIGURE 1.5.8 Pure shear.

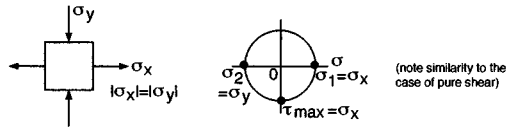

FIGURE 1.5.9 Biaxial tension-compression: $|\sigma_x| = |\sigma_y|$ (similar to the case of pure shear).

Absolute Maximum Shear Stress

In the case of a general three-dimensional state of stress, the transformations to arbitrary planes are complex and beyond the scope of this book. It is useful to note, however, that in general there are three principal stresses at any point in a material. (Plane stress is a special case with one of these stresses being zero.) If the three principal stresses are known, it is easy to determine the absolute maximum shear stress, which is valuable in assessing a material's performance in service. The idea is to view the element as three separate two-dimensional elements, each time from a different principal direction, and plot the Mohr's circles for them in the same diagram. This is illustrated schematically in Figure 1.5.10 for an element with three tensile principal stresses, of a maximum, a minimum, and an intermediate value.

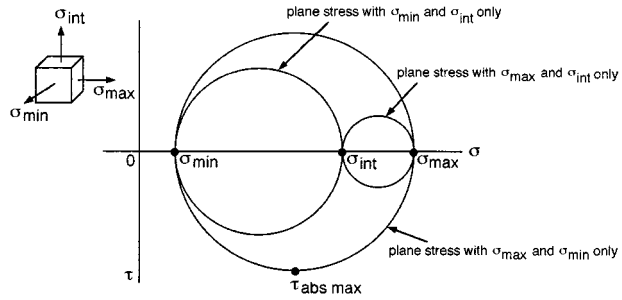

FIGURE 1.5.10 Principal stresses of three-dimensional element.

The Mohr's circles are interrelated since the three views of the element have common principal stresses associated with them. The absolute maximum shear stress is

$$\tau_{\text{abs max}} = \frac{\sigma_{\text{max}} - \sigma_{\text{min}}}{2} \tag{1.5.7}$$

Note that in calculating the absolute maximum shear stress for a state of plane stress, the actual third principal stress of $\sigma_3 = 0$ may be significant if that is the minimum stress, and should be used in Equation 1.5.7 instead of a larger intermediate stress. For example, assume $\sigma_x = 200$ ksi and $\sigma_y = 100$ ksi in a case of plane stress. Using these as σ_{max} and σ_{min}, $\tau_{max} = (200 - 100)/2 = 50$ ksi. However, the fact that $\sigma_z = 0$ is important here. Thus, correctly, $\tau_{abs\ max} = (200 - 0)/2 = 100$ ksi. There is an important lesson here: apparently negligible quantities cannot always be ignored in mechanics of materials.

Strain

Solid materials deform when forces are acting on them. Large deformations are possible in some materials. Extremely small deformations are difficult to measure, but they still may be significant in critical geometry change or gradual damage evolution. Deformations are normally nonuniform even in apparently uniform components of machines and structures. The severity of deformation is called strain, which is separately defined for volumetric change and angular distortion of a body.

Normal Strain

The elongation or shortening of a line segment of unit length is called normal strain or axial strain. To define this quantitatively, consider a uniform bar of length L_o, and call this original length the gage length. Assume the bar elongates by an amount e to a new length L_1 under the action of a force F (Figure 1.5.11) or by thermal expansion. The normal strain ε is defined, with the gage length approaching zero in the limit, as

$$\varepsilon = \frac{e}{L_o} \tag{1.5.8}$$

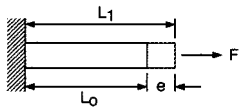

FIGURE 1.5.11 Model for calculating axial or normal strain.

The strain calculated this way is called engineering strain, which is useful and fairly accurate for small deformations. Elongation is considered positive.

Normal strain is a dimensionless quantity, but it is customary to label it in a way that indicates strain, such as in./in., or m/m, or %, or μ in./in., or με (microstrain), depending on the system of units and the numerical representation.

True Strain

A difficulty of proper definition arises if the deformation e is not infinitesimal, because in a sense the gage length itself is increasing. The correct definition in such a case is based on the instantaneous length L and infinitesimal changes dL in that length. Thus, the total true strain in a member axially deforming from length L_o to a final length L_f by an amount e is

$$\varepsilon = \int_{L_o}^{L_f} \frac{dL}{L} = \ell n \frac{L_f}{L_o} = \ell n(1+e) \tag{1.5.9}$$

True strain is practically identical to engineering strain up to a few percent of engineering strain. The approximate final length L_f of an axially deformed, short line segment of original length L_o is sometimes expressed as

$$L_f \approx (1+\varepsilon)L_o \tag{1.5.10}$$

Shear Strain

Angular distortions are called shear strains. More precisely, shear strain γ is the change in angle of two originally perpendicular ($\theta = \pi/2$) line segments. For consistency, assume that a decreasing angle represents positive shear strain, and an increasing angle is from negative shear strain. The angle γ is measured in radians. A useful way to show shear strain is given in Figure 1.5.12.

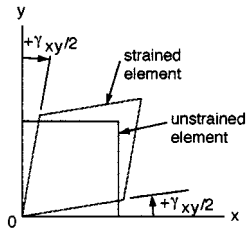

FIGURE 1.5.12 Shear strain in two dimensions.

Strain Transformation

The method of transforming strain at a point is similar to that for stress. In general, there are three components of normal strain, ε_x, ε_y, and ε_z, and three components of shear strain, γ_{xy}, γ_{xz}, and γ_{yz}. Transformations of plane strain components are the simplest.

For a consistent approach, assume that strain transformation is desired from an *xy* coordinate system to an *x′y′* set of axes, where the latter is rotated counterclockwise (+θ) from the *xy* system. The transformation equations for plane strain are

$$\varepsilon_{x'} = \frac{\varepsilon_x + \varepsilon_y}{2} + \frac{\varepsilon_x - \varepsilon_y}{2}\cos 2\theta + \frac{\gamma_{xy}}{2}\sin 2\theta$$

$$\varepsilon_{y'} = \frac{\varepsilon_x + \varepsilon_y}{2} - \frac{\varepsilon_x - \varepsilon_y}{2}\cos 2\theta - \frac{\gamma_{xy}}{2}\sin 2\theta \qquad (1.5.11)$$

$$\frac{\gamma_{x'y'}}{2} = -\frac{\varepsilon_x - \varepsilon_y}{2}\sin 2\theta + \frac{\gamma_{xy}}{2}\cos 2\theta$$

Note the similarity between the strain and stress transformation equations, as well as the differences.

Principal Strains

For isotropic materials only, principal strains (with no shear strain) occur along the principal axes for stress. In plane strain the principal strains ε_1 and ε_2 are expressed as

$$\varepsilon_{1,2} = \frac{\varepsilon_x + \varepsilon_y}{2} +/- \sqrt{\left(\frac{\varepsilon_x - \varepsilon_y}{2}\right)^2 - \left(\frac{\gamma_{xy}}{2}\right)^2} \qquad (1.5.12)$$

The angular position θ_p of the principal axes (measured positive counterclockwise) with respect to the given *xy* system is determined from

$$\tan 2\theta_p = \frac{\gamma_{xy}}{\varepsilon_x - \varepsilon_y} \qquad (1.5.13)$$

Like in the case of stress, the maximum in-plane shear strain is

$$\frac{\gamma_{x'y'\max}}{2} = \sqrt{\left(\frac{\varepsilon_x - \varepsilon_y}{2}\right)^2 + \left(\frac{\gamma_{xy}}{2}\right)^2} \qquad (1.5.14)$$

which occurs along axes at 45° from the principal axes, determined from

$$\tan 2\theta = -\frac{\varepsilon_x - \varepsilon_y}{\gamma_{xy}} \qquad (1.5.15)$$

The corresponding average normal strain is

$$\varepsilon_{ave} = \frac{\varepsilon_x + \varepsilon_y}{2} \qquad (1.5.16)$$

Mohr's Circle for Plane Strain

As in the case of stress, there is a graphical overview by Mohr's circle of the directional dependence of the normal and shear strain components at a point in a material. This circle has a center C at $\varepsilon_{ave} = (\varepsilon_x + \varepsilon_y)/2$ which is always on the ε axis, but is shifting left and right in a dynamic loading situation. The radius R of the circle is

$$R = \sqrt{\left(\frac{\varepsilon_x - \varepsilon_y}{2}\right)^2 + \left(\frac{\gamma_{xy}}{2}\right)^2} \tag{1.5.17}$$

Note the proper labeling (ε vs. $\gamma/2$) and preferred orientation of the strain axes as shown in Figure 1.5.13. This sets up a favorable uniformity of angular displacement between the element ($+\theta$ counterclockwise) and the circle ($+2\theta$ counterclockwise).

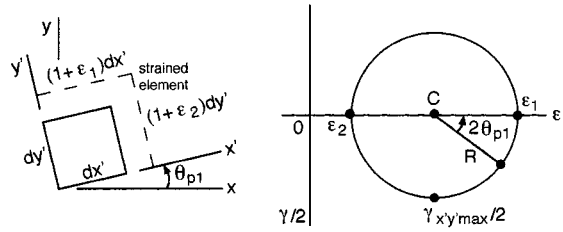

FIGURE 1.5.13 Mohr's circle for plane strain.

Mechanical Behaviors and Properties of Materials

The stress-strain response of a material depends on its chemical composition, microstructure, geometry, the magnitude and rate of change of stress or strain applied, and environmental factors. Numerous quantitative mechanical properties are used in engineering. Some of the basic properties and common variations of them are described here because they are essential in mechanics of materials analyses.

Stress-Strain Diagrams

There are several distinctive shapes of uniaxial tension or compression stress-strain plots, depending on the material, test conditions, and the quantities plotted. The chosen representative schematic diagram here is a true stress vs. true strain curve for a ductile, nonferrous metal tested in tension (Figure 1.5.14). The important mechanical properties listed in Table 1.5.1 are obtained from such a test or a similar one in pure shear (not all are shown in Figure 1.5.14).

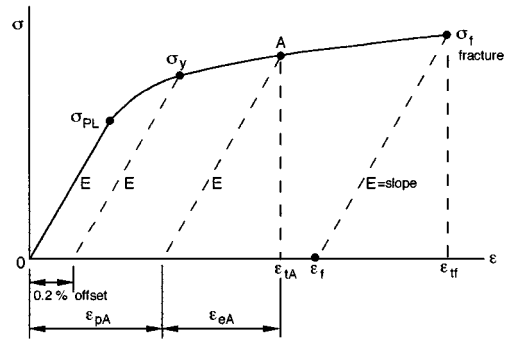

FIGURE 1.5.14 True stress vs. true strain for a ductile, nonferrous metal.

Table 1.5.1 Basic Mechanical Properties

Symbol	Definition	Remarks
E	Modulus of elasticity; Young's modulus; $E = \sigma/\varepsilon_e$	Hooke's law; T and ε_p effects small
G	Shear modulus of elasticity; $G = \dfrac{\tau}{\gamma_e} = E/2(1+\nu)$	T and ε_p effects small
ν	Poisson's ratio; $\nu = \dfrac{\varepsilon_{lateral}}{\varepsilon_{longit.}}$	T and ε_p effects small
σ_{PL}	Proportional limit; at onset of noticeable yielding (or at onset of nonlinear elastic behavior)	Flow property; inaccurate; T and ε_p effects large
σ_y	0.2% offset yield strength (but yielding can occur at $\sigma < \sigma_y$ if $\sigma_{PL} < \sigma_y$)	Flow property; accurate; T and ε_p effects large
σ_f	True fracture strength; $\sigma_f = \dfrac{P_f}{A_f}$	Fracture property; T and ε_p effects medium
ε_f	True fracture ductility; $\varepsilon_f = \ln\dfrac{A_O}{A_f} = \ln\dfrac{100}{100 - \%\text{RA}}$	Max. ε_p; fracture property; T and ε_p effects medium
% RA	Percent reduction of area; $\%\text{RA} = \dfrac{A_O - A_f}{A_O} \times 100$	Fracture property; T and ε_p effects medium
n	Strain hardening exponent; $\sigma = K\varepsilon_p^n$	Flow property; T and ε_p effects small to large
Toughness	Area under σ vs. ε_p curve	True toughness or intrinsic toughness; T and ε_p effects large
σ_u	Ultimate strength; $\dfrac{P_{\max}}{A_O}$	Fracture property; T and ε_p effects medium
M_r	Modulus of resilience; $M_r = \dfrac{\sigma_{PL}^2}{2E}$	Area under original elastic portion of $\sigma - \varepsilon$ curve

Notes: T is temperature; ε_p refers to prior plastic strain, especially cyclic plastic strain (fatigue) (these are qualitative indicators here; exceptions are possible)

$$\underset{\text{total}}{\varepsilon_t} = \underset{\text{elastic}}{\varepsilon_e} + \underset{\text{plastic}}{\varepsilon_p} = \frac{\sigma}{E} + \left(\frac{\sigma}{K}\right)^{1/n} = \frac{\sigma}{E} + \varepsilon_f\left(\frac{\sigma}{\sigma_f}\right)^{1/n}$$

Another useful mechanical property (not measured from the $\sigma - \varepsilon$ plot) is hardness. This is a flow property, with some qualitative correlations to the other properties.

It is important to appreciate that the mechanical properties of a material depend on its chemical composition and its history of thermal treatment and plastic deformations (cold work; cyclic plasticity). For example, consider the wide ranges of monotonic and cyclic stress-strain curves for 1045 steel (a given chemical composition) at room temperature, as functions of its hardness resulting from thermal treatment (Figure 1.5.15). See Section 1.6, "Fatigue," for more on cycle-dependent material behaviors.

Generalized Stress-Strain Expressions. Hooke's Law

An important special case of stress-strain responses is when the material acts entirely elastically ($\varepsilon_p = 0$, $\varepsilon_t = \varepsilon_e$). In this case, for uniaxial loading, the basic **Hooke's law** $\sigma = E\varepsilon$ can be used, and similarly for unidirectional shear, $\tau = G\gamma$. For multiaxial loading (Color Plate 9), the generalized Hooke's law is applicable,

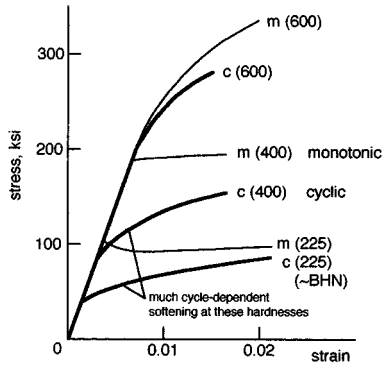

FIGURE 1.5.15 Influence of hardness and deformation history on the stress-strain response of SAE 1045 steel.

$$\varepsilon_x = \frac{1}{E}\left[\sigma_x - \nu\left(\sigma_y + \sigma_z\right)\right]$$

$$\varepsilon_y = \frac{1}{E}\left[\sigma_y - \nu\left(\sigma_x + \sigma_z\right)\right] \tag{1.5.18}$$

$$\varepsilon_z = \frac{1}{E}\left[\sigma_z - \nu\left(\sigma_x + \sigma_y\right)\right]$$

Other useful expressions for ideally elastic behavior are as follows. Relating the axial and shear moduli,

$$G = \frac{E}{2(1+\nu)} \tag{1.5.19}$$

The change in volume per unit volume is the volumetric strain or dilatation,

$$e = \frac{1-2\nu}{E}\left(\sigma_x + \sigma_y + \sigma_z\right) \tag{1.5.20}$$

The bulk modulus k is the ratio of a uniform stress (hydrostatic) to the dilatation,

$$k = \frac{\sigma}{e} = \frac{E}{3(1-2\nu)} \tag{1.5.21}$$

For most metals, $\nu \approx 1/3$ and $k \approx E$.

Uniaxial Elastic Deformations

The total elastic deformation δ of axially loaded bars, columns, and wires is calculated with the aid of basic expressions. Using $\sigma = E\varepsilon$ and $\sigma = P(x)/A(x)$,where $P(x)$ and $A(x)$ are, respectively, the internal force and cross-sectional area of a bar at a distance x from one end,

$$\delta = \int_0^L \frac{P(x)}{A(x)E}\,dx \tag{1.5.22}$$

where L is the total length considered.

In most cases, $A(x)$ is a constant; $P(x)$ may also be a constant, except where several different axial forces are applied, and occasionally for vertical bars and columns, where the member's own weight may cause $P(x)$ to vary significantly along the length. If $A(x)$, $P(x)$, and E are constants,

$$\delta = \frac{PL}{AE} \tag{1.5.23}$$

Thermally Induced Deformations

Thermal expansion or contraction is a linearly dependent, recoverable deformation like purely elastic deformations are. For a homogeneous and isotropic material, the thermally induced deformation from the original length L is calculated from

$$\delta_T = \alpha \Delta T L \tag{1.5.24}$$

where α is the linear coefficient of thermal expansion (strain per degree of temperature, a material property), and ΔT is the change in temperature.

The thermal strain can be prevented or reduced by constraining a member. In that case the stresses and strains can be calculated using the methods pertaining to statically indeterminate members.

Stresses in Beams

To calculate stresses in beams, one must first model the beam correctly in terms of its supports and loading (such as simply supported, with distributed loading), determine the appropriate unknown external reactions, and establish the corresponding shear and moment diagrams using a consistent sign convention. Both normal and shear stresses may have to be calculated, but typically the normal stresses are the most significant.

Flexure Formula

The normal stresses at a particular cross section in a beam are caused by the bending moment that acts at that cross section, and are distributed by magnitude and sign (both tension and compression) so that the beam is in equilibrium. The basic concept for calculating the stresses is that there is a neutral axis n-n of $\varepsilon = \sigma = 0$ in the beam, and that the longitudinal normal strain varies linearly with distance y from the neutral axis.

If the beam is behaving entirely elastically, the stress distribution is also linear, as in Figure 1.5.16. In this case, the stress at a distance y from the neutral axis is calculated from $M = \int \sigma(y) y \, dA$ and results in

$$\sigma(y) = \frac{My}{I} \tag{1.5.25}$$

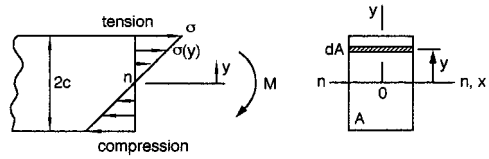

FIGURE 1.5.16 Internal normal stresses in a beam caused by bending.

where I = moment of inertia of the cross-sectional area about the neutral axis.

The maximum stress, with the appropriate sign, is

$$\sigma = \frac{Mc}{I} \tag{1.5.26}$$

There are several special cases of bending that require additional considerations and analysis as outlined below.

Inelastic Bending

A beam may plastically deform under an increasing moment, yielding first in its outer layers and ultimately throughout its depth. Such a beam is analyzed by assuming that the normal strains are still linearly varying from zero at the neutral axis to maximum values at the outer layers. Thus, the stress distributions depend on the stress-strain curve of the material. With the stress distribution established, the neutral axis can be determined from $\int\sigma(y)\,dA = 0$, and the resultant moment from $M = \int y\sigma(y)\,dA$.

A fully plastic beam of rectangular cross section and flat-top yielding supports 50% more bending moment than its maximum elastic moment.

Neutral Axis of Semisymmetric Area

If the cross-sectional area is semisymmetric, such as a T-shape, and the loading is in a centroidal plane of symmetry, the neutral axis for elastic deformations is at the centroid *C* of the area as shown in Figure 1.5.17, and Equation 1.5.25 can be used. Note that the magnitudes of the maximum tensile and compressive stresses are not the same in this case.

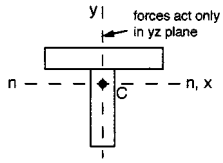

FIGURE 1.5.17 Neutral axis of a semisymmetric area.

Unsymmetric Bending

In the general case, the cross-sectional area has an arbitrary shape and the loading is arbitrarily applied. The problem of an arbitrary area is handled by choosing the centroidal *xy* coordinate system such that the axes are principal axes of inertia for the area. The principal axes can be determined by using inertia transformation equations or Mohr's circle of inertia. Having an axis of symmetry is a simple special case because the principal axes are the axis of symmetry and the axis perpendicular to it.

The **flexure formula** can be applied directly if the principal axes of inertia are known, and the bending moment is applied about one of these centroidal principal axes. A more complex case is if the moment is not about a principal axis as shown in Figure 1.5.18.

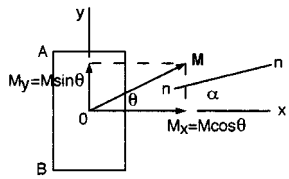

FIGURE 1.5.18 Schematic of arbitrary bending moment.

Different texts may present different formulas for calculating the bending stresses in such situations, depending on the choice of a coordinate system and the sign convention adopted. It is better not to rely on a cookbook formula, but to break down the problem into simple, easily visualized parts, and then reason out an algebraic superposition of the stress components. To illustrate this approach schematically, consider the stresses at points *A* and *B* in Figure 1.5.18. Instead of working directly with the applied moment **M**, resolve **M** into its components M_x and M_y. M_x causes a tensile stress $\sigma_{z_{A_1}}$ at *A* and a compressive stress $-\sigma_{z_{B_1}}$ at *B*. M_y causes tensile stresses at both *A* and *B*, $\sigma_{z_{A_2}}$ and $\sigma_{z_{B_2}}$. The magnitudes of these stress components are readily calculated from the flexure formula with the appropriate dimensions and inertias for each. The resultant stresses are

$$\sigma_A = \sigma_{z_{A_1}} + \sigma_{z_{A_2}}$$

$$\sigma_B = -\sigma_{z_{B_1}} + \sigma_{z_{B_2}}$$

The neutral axis at angle α in the general case is not coincident with the direction of **M** (Figure 1.5.18). In the present case α is defined by

$$\tan\alpha = \frac{I_x}{I_y}\tan\theta \tag{1.5.27}$$

Composite Beams

Nonhomogeneous beams are often designed to take advantage of the properties of two different materials. The approach for analyzing these is to imagine a transformation of the beam's cross section to an equivalent cross section of a different shape but of a single material, so that the flexure formula is usable. This is illustrated for a beam *A* with reinforcing plates *B*, as in Figure 1.5.19.

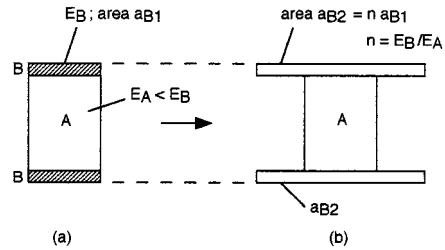

FIGURE 1.5.19 Equivalent area method for a symmetric composite beam.

The transformation factor *n* is obtained from

$$n = \frac{E_B}{E_A} \tag{1.5.28}$$

Note that in a composite beam the strains vary linearly with distance from the neutral axis, but the stresses do not, because of the different elastic moduli of the components. The actual stress σ in the transformed area is determined by first calculating the "pretend" stress σ' for the uniform transformed area and then multiplying it by *n*,

$$\sigma = n\sigma' \tag{1.5.29}$$

Nonsymmetric composite beams (such as having only one reinforcing plate *B* in Figure 1.5.19) are analyzed similarly, but first require the location of the neutral axis.

Reinforced concrete beams are important special cases of composite beams. The stress analysis of these is influenced by the fact that concrete is much weaker in tension than in compression. Empirical approaches are particularly useful in this area.

Curved Beams

The stress analysis of curved beams requires some additional considerations. For example, the flexure formula is about 7% in error (the calculated stresses are too low) when the beam's radius of curvature is five times its depth (hooks, chain links). The curved-beam formula provides realistic values in such cases.

Shear Stresses in Beams

Transverse loads on beams are common, and they cause transverse and complementary longitudinal shear stresses in the beams. Schematically, the transverse shear stresses are distributed on a rectangular cross section as shown in Figure 1.5.20. The shear stress is zero at free surfaces by definition.

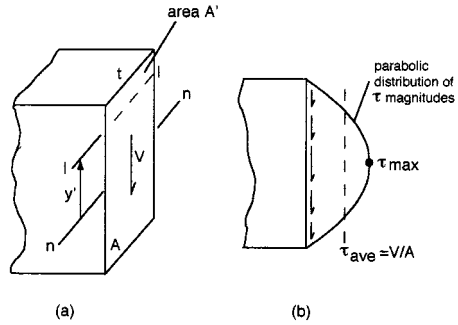

FIGURE 1.5.20 Transverse shear stress distribution.

The internal shear stress is calculated according to Figure 1.5.20 from

$$\tau = \frac{VQ}{It} \tag{1.5.30}$$

where τ = shear stress value at any point on the line $\ell - \ell$ at a distance y' from the neutral axis
V = total shear force on cross-sectional area A
$Q = \bar{y}'A'$; A' = area above line $\ell - \ell$; $\bar{y}'$ = distance from neutral axis to centroid of A'
I = moment of inertia of entire area A about neutral axis
t = width of cross section where τ is to be determined

This shear formula gives $\tau_{max} = 1.5\ V/A$ if t is constant for the whole section (rectangle).

Note that the magnitude of the shear stress distribution changes sharply where there is an abrupt change in width t, such as in an I-beam, Figure 1.5.21.

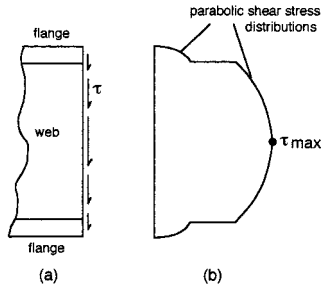

FIGURE 1.5.21 Shear stress distribution for I-beam.

Shear Flow

In the analysis of built-up members, such as welded, bolted, nailed, or glued box beams and channels, a useful quantity is the shear flow q measured in force per unit length along the beam,

$$q = \frac{VQ}{I} \tag{1.5.31}$$

where all quantities are defined as for Equation 1.5.30. Care must be taken to use the appropriate value for Q. For example, consider a channel section of three flat pieces glued together as in Figure 1.5.22. There are two critical joint regions B here, and the area A' is between them. The shear flow is carried by the two joints together, so the actual force per unit length on one joint is $q/2$ here.

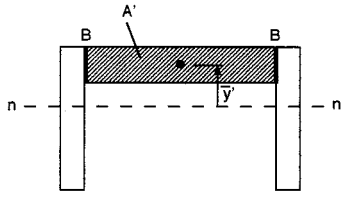

FIGURE 1.5.22 Critical joint regions of a built-up beam.

Shear Flow in Thin-Walled Beams

The shear-flow distribution over the cross section of a thin-walled member is governed by equilibrium requirements. Schematic examples of this are given in Figure 1.5.23. Note the special case of unsymmetrical loading in part (c), which causes a bending and a twisting of the beam. The twisting is prevented if the vertical force V is applied at the shear center C, defined by the quantity e,

$$e = \frac{dH}{V} \tag{1.5.32}$$

where d is the centroidal distance between the two horizontal flanges and H is the shear force in the flanges (q_{ave} times width of flange).

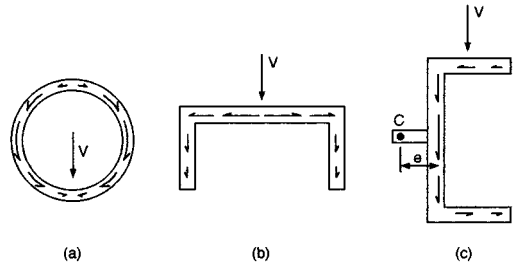

FIGURE 1.5.23 Shear flow distributions.

Deflections of Beams

Small deflections of beams can be determined relatively easily. The first step is to assess a beam's loading and support conditions and sketch an exaggerated elastic deflection curve as in Figure 1.5.24.

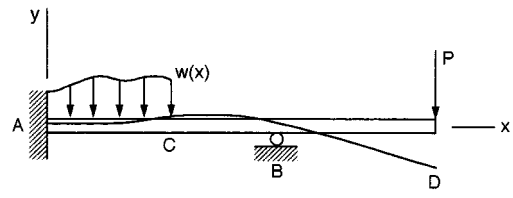

FIGURE 1.5.24 Exaggerated elastic curve of a beam in bending.

The boundary conditions at the supports are useful in the solution for the whole beam. Here at the fixed end *A* there is no vertical displacement and no rotation, while at the roller support *B* there is no vertical displacement but rotation of the continuous beam occurs. The boundary and continuity conditions can be determined by inspection in simple cases.

Moment vs. Curvature

For a homogeneous and elastic beam,

$$\frac{1}{\rho} = \frac{M}{EI} \tag{1.5.33}$$

where ρ = radius of curvature at a specific point on the elastic curve; 1/ρ is the curvature. The product *EI* is called the flexural rigidity; it is often a constant along the whole beam.

Integration Method for Slope and Displacement

For small displacements, $1/\rho = d^2y/dx^2$. In the general case, a distributed external loading $w(x)$ should be included in the modeling of the problem. A set of expressions is available to solve for the deflections in rectangular coordinates:

$$-w(x) = \frac{dV}{dx} = EI\frac{d^4y}{dx^4}$$

$$V(x) = \frac{dM}{dx} = EI\frac{d^3y}{dx^3} \tag{1.5.34}$$

$$M(x) = EI\frac{d^2y}{dx^2}$$

The deflection *y* of the elastic curve is obtained by successive integrations, using appropriate constants of integration to satisfy the boundary and continuity conditions. In general, several functions must be written for the moment $M(x)$, one for each distinct region of the beam, between loading discontinuities. For example, these regions in Figure 1.5.24 are *AC*, *CB*, and *BD*. Considerable care is required to set up a solution with a consistent sign convention and selection of coordinates for simple and efficient forms of $M(x)$.

In practice, even relatively complex problems of beam deflections are solved using the principle of superposition and handbook values of slopes and deflections for subsets of basic loadings and supports. The literature contains a large variety of such subsets. A sampling of these is given in Table 1.5.2.

Deflection Caused by Shear

The transverse shear acting on a beam causes a displacement that tends to be significant compared to bending deflections only in very short beams. The shear deflection over a length *L* is approximated by

$$y = \frac{\tau_{ave} L}{G} \tag{1.5.35}$$

Torsion

The simplest torsion members have circular cross sections. The main assumptions in their analysis are that cross-sectional circles remain plane circles during twisting of a shaft and that radial lines on any cross section remain straight and rotate through the same angle. The length and diameter of the shaft are unchanged in small angular displacements. It is useful in the analysis that shear strain γ varies linearly

TABLE 1.5.2

Beam	Slope: ldy/dxl	Max. deflection
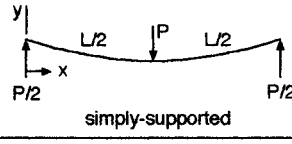 simply-supported	$PL^2 / 16EI$ at x=0, L	$PL^3 / 48EI$ at x=L/2
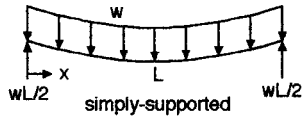 simply-supported	$wL^3 / 24EI$ at x=0, L	$5wL^4 / 384EI$ at x=L/2
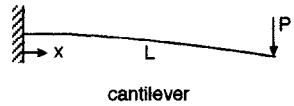 cantilever	$PL^2 / 2EI$ at x=L	$PL^3 / 3EI$ at x=L
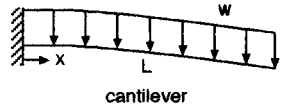 cantilever	$wL^3 / 6EI$ at x=L	$wL^4 / 8EI$ at x=L
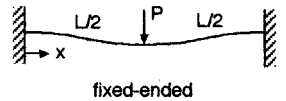 fixed-ended	0 at x=0, L/2, L	$PL^3 / 192EI$ at x=L/2
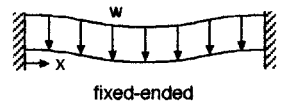 fixed-ended	0 at x=0, L/2, L	$wL^4 / 384EI$ at x=L/2

along any radial line, from zero at the centerline of a solid or tubular shaft to a maximum at the outer surface,

$$\gamma = \frac{\rho}{r}\gamma_{max} \tag{1.5.36}$$

where ρ = radial distance to any element in the shaft
r = radius of the shaft

Using $\tau = G\gamma$ for an elastically deforming material (Figure 1.5.25),

$$\tau = \frac{\rho}{r}\tau_{max} \tag{1.5.37}$$

The torsion formula relating shear stress to the applied torque T is from $T = 2\pi\int\tau\rho^2\, d\rho$,

$$\tau_{max} = \frac{Tr}{J} \quad \text{or} \quad \tau = \frac{T\rho}{J} \tag{1.5.38}$$

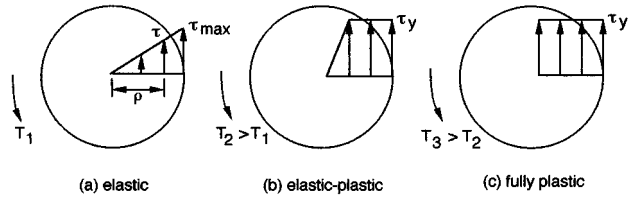

FIGURE 1.5.25 Shear stress distributions in a shaft.

where J = the polar moment of inertia of the cross-sectional area; for a solid circle, $J = \pi r^4/2$; for a tube, $J = (\pi/2)(r_0^4 - r_i^4)$.

Power Transmission

The power P transmitted by a shaft under torque T and rotating at angular velocity ω is

$$P = T\omega \tag{1.5.39}$$

where $\omega = 2\pi f$; f = frequency of rotation or number of revolutions per second.

Angle of Twist

For a homogeneous shaft of constant area and G over a length L, under a torque T, the angular displacement of one end relative to the other is

$$\phi = \frac{TL}{JG} \tag{1.5.40}$$

For a shaft consisting of segments with various material and/or geometric properties, under several different torques in each, the net angular displacement is calculated from the vector sum of the individual twists,

$$\phi = \sum \frac{T_i L_i}{J_i G_i} \tag{1.5.41}$$

The right-hand rule is used for a sign convention for torques and angles: both T and ϕ are positive, with the thumb pointing outward from a shaft and the fingers curling in the direction of torque and/or rotation, as in Figure 1.5.26. Note that regardless of the number of torques applied to a shaft at various places along its length, there is only one torque at a given cross section, and this torque is a constant in that segment of the shaft (until another external torque is encountered, requiring a different free-body diagram).

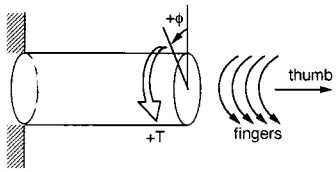

FIGURE 1.5.26 Right-hand rule for positive torque and angle.

Inelastic Torsion

A shaft may plastically deform under an increasing torque, yielding first in its outer layers and ultimately throughout the cross section. Such a shaft is analyzed by assuming that the shear strains are still linearly

varying from zero at the centerline to a maximum at the outer layers. Thus, the shear stress distribution depends on the shear stress-strain curve of the material. For example, an elastic, elastic-plastic, and fully plastic solid circular shaft is modeled in Figure 1.5.25, assuming flat-top yielding at τ_y. The torque T in any case is obtained by integrating the shear stresses over the whole area,

$$T = 2\pi \int_A \tau \rho^2 \, d\rho \tag{1.5.42}$$

The fully plastic torque in this case is 33% greater than the maximum elastic torque.

Noncircular Shafts

The analysis of solid noncircular members, such as rectangles and triangles, is beyond the scope of this book. The reason for the difficulty is that plane sections do not remain plane, but warp. It can be noted here, however, that a circular shaft utilizes material the most efficiently since it has a smaller maximum shear stress and a smaller angle of twist than a noncircular shaft of the same weight per unit length under the same torque.

Noncircular tubes with thin walls can be analyzed using the concept of shear flow that must be continuous and constant on the closed path of the cross-sectional area. The shear stress under a torque T is essentially constant over a uniformly thin wall (from inside to outside), and is given by

$$\tau = \frac{T}{2tA_m} \tag{1.5.43}$$

where t = thickness of the tube
A_m = mean area within the centerline of the wall thickness

The angle of twist for an elastically deforming thin-walled tube of length L and constant thickness t is

$$\phi = \frac{TL}{4A_m^2 Gt} \oint ds \tag{1.5.44}$$

where the line integral represents the total length of the wall's centerline boundary in the cross section (for a circular tube, this becomes $\approx 2\pi r$). For a tube with variable thickness t, the integrand becomes $\oint ds/t$.

Statically Indeterminate Members

Members that have more supports or constraints than the minimum required for static equilibrium are called statically indeterminate. They can be analyzed if a sufficient number of additional relationships are available. These are fundamentally similar to one another in terms of compatibility for displacements, and are described separately for special cases.

Statically Indeterminate Axially Loaded Members

Several subsets of these are common; three are shown schematically in Figure 1.5.27.

1. From a free-body diagram of part (a), assuming upward forces F_A and F_B at ends A and B, respectively, the force equilibrium equation is

$$F_A + F_B - P = 0$$

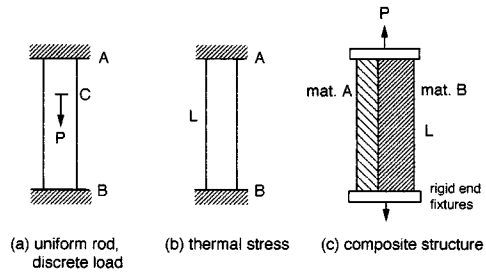

FIGURE 1.5.27 Statically indeterminate axially loaded members.

The displacement compatibility condition is that both ends are fixed, so

$$\delta_{A/B} = 0$$

Then

$$\frac{F_A L_{AC}}{AE} - \frac{F_B L_{BC}}{AE} = 0, \quad F_A = P\frac{L_{BC}}{L_{AB}}, \quad F_B = P\frac{L_{AC}}{L_{AB}}$$

Alternatively, first assume that $F_B = 0$, and calculate the total downward displacement (tensile) of the free end *B*. Then calculate the required force F_B to compressively deform the rod upward so that after the superposition there is no net displacement of end *B*. The results are the same as above for elastically deforming members.

2. Constrained thermal expansion or contraction of part (b) is handled as above, using the expression for thermally induced deformation,

$$\delta_T = \alpha\, \Delta T L \tag{1.5.45}$$

where α = linear coefficient of thermal expansion
ΔT = change in temperature

3. The force equilibrium equation of part (c) is

$$P - F_A - F_B = 0$$

Here the two different component materials are deforming together by the same amount, so

$$\delta_A = \delta_B$$

$$\frac{F_A L}{A_A E_A} = \frac{F_B L}{A_B E_B}$$

providing two equations with two unknowns, F_A and F_B. Note that rigid supports are not necessarily realistic to assume in all cases.

Statically Indeterminate Beams

As for axially loaded members, the redundant reactions of beams are determined from the given conditions of geometry (the displacement compatibility conditions). There are various approaches for solving problems of statically indeterminate beams, using the methods of integration, moment-areas, or

superposition. Handbook formulas for the slopes and deflections of beams are especially useful, noting that the boundary conditions must be well defined in any case. The method of superposition is illustrated in Figure 1.5.28.

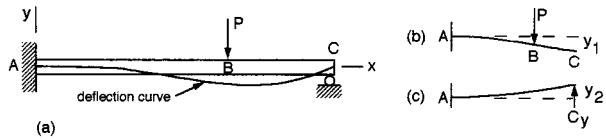

FIGURE 1.5.28 A statically indeterminate beam.

Choosing the reaction at C as the redundant support reaction (otherwise, the moment at A could be taken as redundant), and first removing the unknown reaction C_y, the statically determinate and stable primary beam is obtained in Figure 1.5.28b. Here the slope and deflection at A are both zero. The slopes at B and C are the same because segment BC is straight. Next the external load P is removed, and a cantilever beam fixed at A and with load C_y is considered in Figure 1.5.28c. From the original boundary conditions at C, $-y_1 + y_2 = 0$, and the problem can be solved easily using any appropriate method.

Statically Indeterminate Torsion Members

Torsion members with redundant supports are analyzed essentially the same way as other kinds of statically indeterminate members. The unknown torques, for example, are determined by setting up a solution to satisfy the requirements of equilibrium ($\sum T = 0$), angular displacement compatibility, and torque-displacement (angle = TL/JG) relationships. Again, the boundary conditions must be reasonably well defined.

Buckling

The elastic buckling of relatively long and slender members under axial compressive loading could result in sudden and catastrophic large displacements. The critical buckling load is the smallest for a given ideal column when it is pin-supported at both ends; the critical load is larger than this for other kinds of supports. An ideal column is made of homogeneous material, is perfectly straight prior to loading, and is loaded only axially through the centroid of its cross-sectional area.

Critical Load. Euler's Equation

The buckling equation (Euler's equation) for a pin-supported column gives the critical or maximum axial load P_{cr} as

$$P_{cr} = \frac{\pi^2 EI}{L^2} \tag{1.5.46}$$

where E = modulus of elasticity
I = smallest moment of inertia of the cross-sectional area
L = unsupported length of the pinned column

A useful form of this equation gives the critical average stress prior to any yielding, for arbitrary end conditions,

$$\sigma_{cr} = \frac{\pi^2 E}{(kL/r)^2} \tag{1.5.47}$$

where $r = \sqrt{I/A}$ = radius of gyration of cross-sectional area A
L/r = slenderness ratio
k = effective-length factor; constant, dependent on the end constraints
kL/r = effective-slenderness ratio

The slenderness ratio indicates, for a given material, the tendency for elastic buckling or failure by yielding (where the Euler formula is not applicable). For example, buckling is expected in mild steel if L/r is approximately 90 or larger, and in an aluminum alloy if $L/r > 60$. Yielding would occur first at smaller values of L/r. Ratios of 200 or higher indicate very slender members that cannot support large compressive loads.

Several common end conditions of slender columns are shown schematically in Figure 1.5.29.

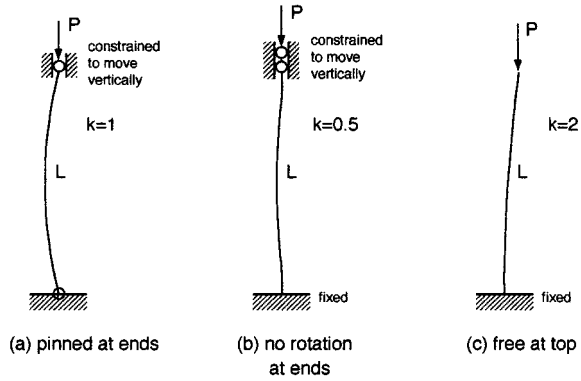

FIGURE 1.5.29 Common end conditions of slender columns.

Secant Formula

Real columns are not perfectly straight and homogeneous and are likely to be loaded eccentrically. Such columns first bend and deflect laterally, rather than buckle suddenly. The maximum elastic compressive stress in this case is caused by the axial and bending loads and is calculated for small deflections from the secant formula,

$$\sigma_{\max} = \frac{P}{A}\left[1 + \frac{ec}{r^2}\sec\left(\frac{L}{2r}\sqrt{\frac{P}{EA}}\right)\right] \tag{1.5.48}$$

where e is the eccentricity of the load P (distance from the neutral axis of area A) and c is measured from the neutral axis to the outer layer of the column where $\sigma_{\max}$ occurs.

The load and stress are nonlinearly related; if there are several loads on a column, the loads should be properly combined first before using the secant formula, rather than linearly superposing several individually determined stresses. Similarly, factors of safety should be applied to the resultant load.

Inelastic Buckling

For columns that may yield before buckling elastically, the generalized Euler equation, also called the Engesser equation, is appropriate. This involves substituting the tangent modulus E_T (tangent to the stress-strain curve) for the elastic modulus E in the Euler equation,

$$\sigma_{cr} = \frac{\pi^2 E_T}{(kL/r)^2} \tag{1.5.49}$$

Note that E_T must be valid for the stress σ_{cr}, but E_T is dependent on stress when the deformations are not entirely elastic. Thermal or plastic-strain events may even alter the stress-strain curve of the material, thereby further changing E_T. Thus, Equation 1.5.49 should be used with caution in a trial-and-error procedure.

Impact Loading

A mass impacting another object causes deformations that depend on the relative velocity between them. The simplest model for such an event is a mass falling on a spring. The maximum dynamic deformation d of a linearly responding spring is related to the static deformation d_{st} (the deformation caused by a weight W applied slowly) by a factor that depends on h, the height of free fall from a static position.

$$d = d_{st}\left(1 + \sqrt{1 + \frac{2h}{d_{st}}}\right) \tag{1.5.50}$$

The dynamic and static stresses are related in a similar way,

$$\sigma = \sigma_{st}\left(1 + \sqrt{1 + \frac{2h}{d_{st}}}\right) \tag{1.5.51}$$

The quantity in parentheses is called the impact factor, which shows the magnification of deflection or stress in impacts involving free fall. Note that the real impact factor is somewhat smaller than what is indicated here, because some energy is always dissipated by friction during the fall and deceleration of the body. This includes internal friction during plastic flow at the points of contact between the bodies. Other small errors may result from neglecting the mass and possible inelasticity of the spring.

A special value of the impact factor is worth remembering. When the load is applied suddenly without a prior free fall, $h = 0$, and

$$d = 2d_{st} \quad \text{and} \quad \sigma = 2\sigma_{st}$$

This means that the minimum impact factor is about two, and it is likely to be larger than two, causing perhaps a “bottoming out” of the spring, or permanent damage somewhere in the structure or the payload supported by the spring.

Combined Stresses

Combinations of different kinds of loads on a member are common. The resultant states of stress at various points of interest can be determined by superposition if the material does not yield. The three-dimensional visualization and correct modeling of such a problem is typically the most difficult part of the solution, followed by routine calculations of the stress components and resultants. No new methods of analysis are needed here.

The approach is to sketch an infinitesimal cube at each critical point in the member and determine the individual stresses (magnitudes and signs) acting on that element, generally caused by axial, shear, bending, torsion, and internal pressure loading. This is illustrated in Figure 1.5.30, for a case of medium complexity.

Consider a solid circular rod of radius R, fixed at $z = 0$ (in the xy plane), and loaded by two forces at point B of a rigid arm. Set up the stress analysis at point A ($–R$, 0, 0), assuming there is no stress concentration at the wall fixture of the rod (Figure 1.5.30a).

First the equivalent loading at the origin 0 is determined (Figure 1.5.30b). This can be done most accurately in vector form. The individual stresses at point A are set up in the subdiagram (c). Check that

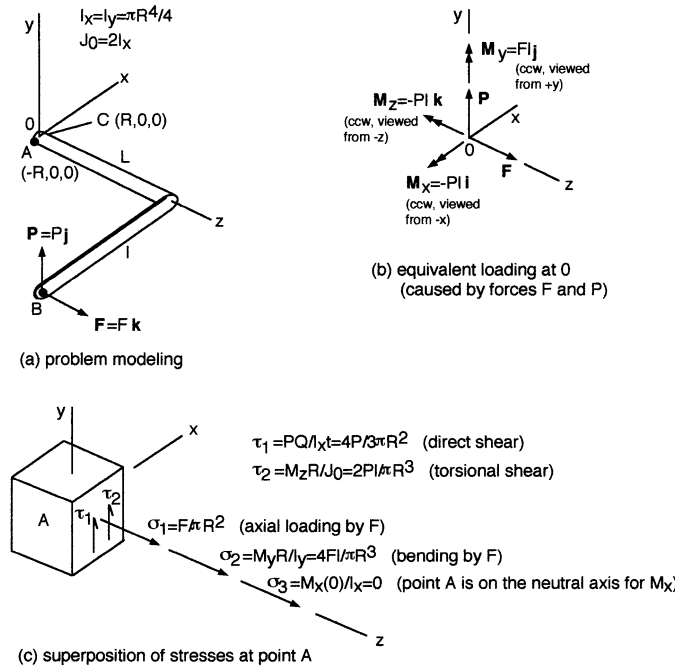

FIGURE 1.5.30 Illustration of stress analysis for combined axial, shear, bending, and torsion loading.

each stress even in symbolic form has the proper units of force per area. The net normal force in this case is $\sigma_1 + \sigma_2$, and the net shear stress is $\tau_1 + \tau_2$.

The state of stress is different at other points in the member. Note that some of the stresses at a point could have different signs, reducing the resultant stress at that location. Such is the case at a point *C* diametrically opposite to point *A* in the present example (*R*, 0, 0), where the axial load **F** and $\mathbf{M}_y$ generate normal stresses of opposite signs. This shows the importance of proper modeling and setting up a problem of combined loads before doing the numerical solution.

Pressure Vessels

Maan H. Jawad and Bela I. Sandor

Pressure vessels are made in different shapes and sizes (Figure 1.5.31 and Color Plate 10) and are used in diverse applications. The applications range from air receivers in gasoline stations to nuclear reactors in submarines to heat exchangers in refineries. The required thicknesses for some commonly encountered pressure vessel components depend on the geometry as follows.

Cylindrical Shells

The force per unit length in the hoop (tangential) direction, N_t, required to contain a given pressure p in a cylindrical shell is obtained by taking a free-body diagram (Figure 1.5.32a) of the cross section. Assuming the thickness t to be much smaller than the radius R and summing forces in the vertical direction gives

$$2N_tL = 2RLp$$

or

$$N_t = pR \tag{1.5.52}$$

(a)

(b)

FIGURE 1.5.31 Various pressure vessels. (Photos courtesy Nooter Corp., St. Louis, MO.)

The corresponding hoop stress is $\sigma_t = pR/t$.

The longitudinal force per unit length, N_x, in the cylinder due to pressure is obtained by summing forces in the axial direction (Figure 1.5.32b),

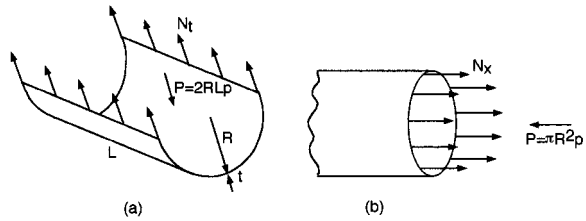

FIGURE 1.5.32 Analysis of cylindrical pressure vessels.

$$2\pi RN_x = \pi R^2 p$$

or

$$N_x = pR/2 \tag{1.5.53}$$

The corresponding axial stress is $\sigma_x = pR/2t$. It is seen that the magnitude of N_t (and σ_t) is twice that of N_x (and σ_x). If S is the allowable stress and t is the required minimum thickness,

$$t = pR/S \tag{1.5.54}$$

Spherical Shells

A free-body diagram of the spherical cross section is shown in Figure 1.5.33. Summation of forces gives

$$t = pR/2S \tag{1.5.55}$$

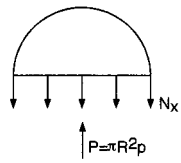

FIGURE 1.5.33 Analysis of spherical pressure vessels.

Example 10

Determine the required thickness of the shell and heads of the air receiver shown in Figure 1.5.34 if p = 100 psi and S = 15,000 psi.

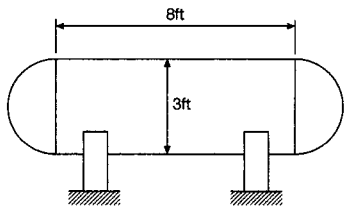

FIGURE 1.5.34 Sketch of a pressure vessel.

Solution. From Equation 1.5.54, the required thickness for the cylindrical shell is

$$t = 100 \times 18/15{,}000 = 0.12 \text{ in.}$$

The required head thickness from Equation 1.5.55 is

$$t = 100 \times 18/2 \times 15{,}000 = 0.06 \text{ in.}$$

Conical Shells

The governing equations for the longitudinal and circumferential forces in a conical shell (Figure 1.5.35a) due to internal pressure are similar to Equations 1.5.52 and 1.5.53 for cylindrical shells, with the radius taken normal to the surface. Thus,

$$N_t = pr/\cos\alpha \tag{1.5.56}$$

$$N_x = pr/2\cos\alpha \tag{1.5.57}$$

where α is half the apex angle of the cone.

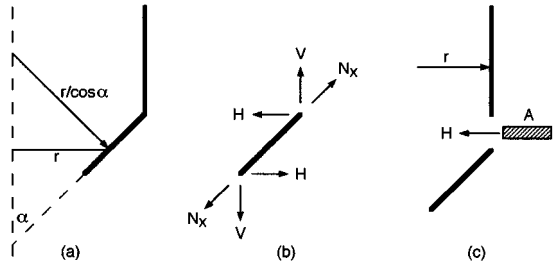

FIGURE 1.5.35 Analysis of conical shells.

The junction between a conical and cylindrical shell, Figure 1.5.35b, is subjected to an additional force, *H*, in the horizontal direction due to internal pressure. The magnitude of this additional force per unit length can be obtained by taking a free-body diagram as shown in Figure 1.5.35b,

$$H = N_x \sin\alpha \tag{1.5.58}$$

A ring is usually provided at the cone-to-cylinder junction to carry the horizontal force H. The required area *A* of the ring is obtained from Figure 1.5.35c as

$$H2r = 2AS$$

or

$$A = Hr/S = \left(N_x \sin\alpha\right)r/S = \left(pr^2 \sin\alpha\right)/\left(2S\cos\alpha\right) \tag{1.5.59}$$

The stress in the ring is compressive at the large end of the cone and tensile at the small end of the cone due to internal pressure. This stress may reverse in direction due to other loading conditions such as weight of contents and end loads on the cone due to wind and earthquake loads.

Example 11

Determine the required thickness of the two cylindrical shells and cone shown in Figure 1.5.36a due to an internal pressure of 200 psi. Calculate the area of the rings required at the junctions. Assume the allowable stress to be 20 ksi in tension and 10 ksi in compression.

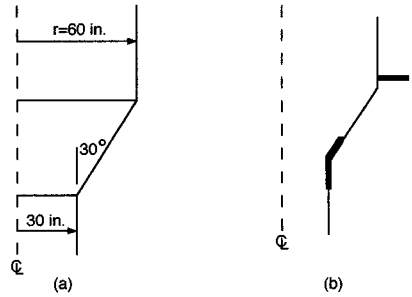

FIGURE 1.5.36 Cylindrical shells with cone connection.

Solution. From Equation 1.5.54, the thickness of the large cylinder is

$$t = 200 \times 60/20{,}000 = 0.60 \text{ in.}$$

The thickness of the small cylinder is

$$t = 200 \times 30/20{,}000 = 0.30 \text{ in.}$$

The thickness of the cone is obtained from Equation 1.5.56 as

$$t = 200 \times 60/(20{,}000 \times \cos 30°) = 0.69 \text{ in.}$$

The required area of the ring at the large end of the cone is obtained from Equation 1.5.59 using the allowable compressive stress of 10 ksi.

$$\text{A} = 200 \times 60^2 \times \sin 30°/(2 \times 10{,}000 \times \cos 30°) = 20.78 \text{ in.}^2$$

The required area of the ring at the small end of the cone is obtained from Equation 1.5.59 using the allowable tensile stress of 20 ksi.

$$\text{A} = 200 \times 30^2 \times \sin 30°/(2 \times 20{,}000 \times \cos 30°) = 2.60 \text{ in.}^2$$

The rings at the junction are incorporated in a number of ways such as those shown in Figure 1.5.36b.

Nozzle Reinforcement

Reinforcements around openings in pressure vessels are needed to minimize the local stress in the area of the opening. The calculation for the needed reinforcement around an opening is based on the concept that pressure in a given area of a vessel is contained by the material in the vessel wall surrounding the pressure. Thus in Figure 1.5.37, if we take an infinitesimal length *dL* along the cylinder, the force caused by the pressure within this length is given by the quantity *pR dL*. The force in the corresponding vessel wall is given by *St dL*. Equating these two quantities results in the expression $t = pR/S$ which is given earlier as Equation 1.5.54. Similarly for the nozzle in Figure 1.5.37, $T = pr/S$. The intersection of the nozzle with the cylinder results in an opening where the pressure in area *ABCD* is not contained by any material. Accordingly, an additional area must be supplied in the vicinity of the opening to prevent overstress of the vessel. The required area *A* is determined from Figure 1.5.37 as

$$A = pRr/S$$

Substituting Equation 1.5.54 into this expression gives

$$A = tr \tag{1.5.60}$$

This equation indicates that the needed additional area is equal to the removed area of the vessel wall.

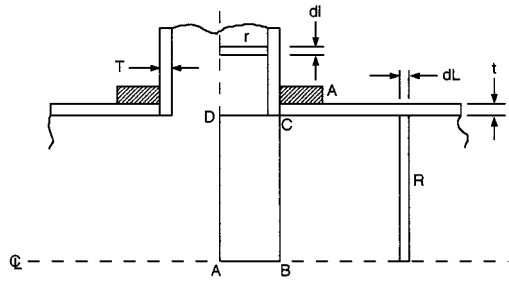

FIGURE 1.5.37 Nozzle reinforcement.

Creep-Fatigue of Boilers and Pressure Vessels

See Figure 1.6.27 in Section 1.6, "Fatigue."

Composite Materials for Pressure Vessels

Ian K. Glasgow

Some pressure vessels can be made of fibrous composite materials with high strength-to-weight ratios. The advantages of using such a material are remarkable in the case of a tubular vessel, where the hoop stress is twice the longitudinal stress, if the fiber quantities and orientations are optimally designed to resist the applied load caused by internal pressure. Simplistically (since a basic element of a composite is strong along the fibers and weak perpendicular to the fibers), this requires twice as many fibers oriented circumferentially as axially. In practice, fibers are commonly laid at ± (a winding angle) at which the hoop and axial stress components are equal, to efficiently create an optimized configuration.

Example 12

Determine the minimum weight of the tube portion of a thin-walled cylindrical pressure vessel of r = 8 in. (20 mm), ℓ = 10 ft (3.05 m), p = 8 ksi (55 MPa); t = ? Assume using a typical graphite/epoxy composite of 60% fibers by volume with allowable tensile stress σ_y = 300 ksi (207 MPa) at 0.058 lb/in.^{3} (1600 kg/m^3). For comparison, consider a steel of σ_y = 200 ksi (138 MPa) at 0.285 lb/in.^{3} (7890 kg/m^3).

Solution.

Composite: $\sigma_y = pr/t$, t = 0.213 in. (5.41 mm) for circumferential plies
$\sigma_y = pr/2t$, t = 0.107 in. (2.72 mm) for axial plies

Total minimum wall thickness: 0.32 in. (8.13 mm)
Total material in tube: 112 lb (50.8 kg)
Steel: $\sigma_y = pr/t$, t = 0.32 in. (8.13 mm)
Total material in tube: 550 lb (249 kg) = 4.9 (composite material)
Note that there are additional considerations in practice, such as cost and potential problems in making adequate connections to the tube.

Experimental Stress Analysis and Mechanical Testing

Michael L. Brown and Bela I. Sandor

Experimental stress analysis is based mostly on the measurement of strains, which may be transformed into stresses. A variety of techniques are available to measure strains. A few of these are described here.

Properties of Strain-Measuring Systems

Strain-measuring systems are based on a variety of sensors, including mechanical, optical, and electrical devices. Each has some special advantages but can usually be adapted for other needs as well. No one system is entirely satisfactory for all practical requirements, so it is necessary to optimize the gage system to each problem according to a set of desirable characteristics. Some of the common characteristics used to evaluate the system's adequacy for a typical application are

1. The calibration constant for the gage should be stable; it should not vary with either time, temperature, or other environmental factors.
2. The gage should be able to measure strains with an accuracy of ±1 με over a strain range of ±10%.
3. The gage size, i.e., the gage length l_0 and width w_0, should be small so that strain at a point is approximated with small error.
4. The response of the gage, largely controlled by its inertia, should be sufficient to permit recording of dynamic strains with frequency components exceeding 100 kHz.
5. The gage system should permit on-location or remote readout.
6. Both the gage and the associated auxiliary equipment should be inexpensive.
7. The gage system should be easy to install and operate.
8. The gage should exhibit a linear response to strain over a wide range.

Three of these basic characteristics deserve further mention here: the gage length l_0, the gage sensitivity, and the range of the strain gage. The gage length is often the most important because in nonlinear strain fields the error will depend on the gage length.

Sensitivity is the smallest value of strain that can be read on the scale associated with the strain gage and should not be mistaken for accuracy or precision. The sensitivity chosen should not be higher than necessary because it needlessly increases the complexity of the measuring method and introduces new problems.

The range of the strain gage refers to the maximum value of strain that can be recorded. Since the range and sensitivity of the gage are interrelated, it is often necessary to compromise between the two for optimal performance of both. Various compromises have resulted in the two main kinds of strain gages, extensometers and electrical strain gages. There are numerous electrical strain gage systems, but only electrical-resistance strain gages will be considered here.

Extensometers

Various extensometers involving mechanical, electrical, magnetic, or optical devices are used in material test systems. A typical extensometer (Figure 1.5.38) is used in the conventional tensile test where the stress-strain diagram is recorded. This kind of extensometer is attached to the specimen by knife edges and spring clips. Electrical-resistance strain gages are attached to the cross-flexural member and provide the strain output. The main advantage of extensometers is that they can be reused and recalibrated after each test. The disadvantages are that they are much larger and more expensive than electrical-resistance strain gages.

Electrical-Resistance Strain Gages

The electrical-resistance strain gage fulfills most of the requirements of an optimum system and is widely used for experimental stress analysis. The electrical-resistance strain gage consists of a metal-foil grid bonded to a polymer backing (Figure 1.5.39). A Wheatstone bridge is often used in this system to enhance the ability to measure changes in resistance. As a specimen is deformed the strain is transmitted

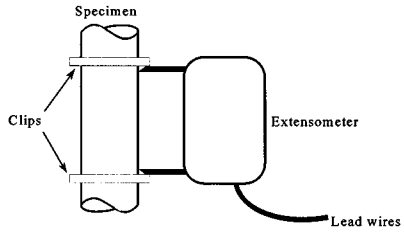

FIGURE 1.5.38 Extensometer attached to a tensile specimen.

to the grid, which has a current applied to it. The change in resistance of the grid is converted to a voltage signal output of the Wheatstone bridge. The basic equation used with this system is

$$\frac{\Delta R}{R} = S_A \varepsilon \tag{1.5.61}$$

where R is the resistance of the gage, ε is the applied strain, and S_A is the sensitivity, or gage factor, of the metallic alloy used in the conductor. The most commonly used alloy is a copper-nickel alloy called Advance, for which the sensitivity is 2.1.

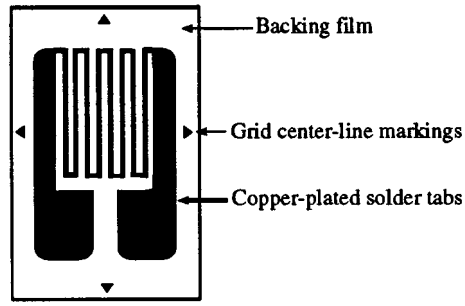

FIGURE 1.5.39 Model of metal-foil strain gages.

Electrical-Resistance Strain Gage Mounting Methods

For precision strain measurements, both the correct adhesive and proper mounting procedures must be employed. The adhesive serves a vital function in the strain-measuring system; it must transmit the strain from the specimen to the sensing element without distortion. Bonding a strain gage to a specimen is one of the most critical steps in the entire process of measuring strain with an electric-resistance strain gage. When mounting a strain gage, it is important to carefully prepare the surface of the component where the gage is to be located. This includes sanding, degreasing, etching, cleaning, and finally neutralizing the surface where the gage is to be mounted. Next, the surface is marked to allow accurate orientation of the strain gage. The gage is then put in place and held with tape while the adhesive is allowed to dry. Several of the adhesive systems commonly used for this are epoxy cements, cyanoacrylate cement, polyester adhesives, and ceramic adhesives. Once the adhesive has been placed, the drying process becomes vitally important, as it can cause residual stresses in the grid work of the gage which could influence the output. After allowing the adhesive to dry, the cure must be tested to ensure complete drying. Failure to do so will affect the stability of the gage and the accuracy of the output. The cure state of the adhesive can be tested by various resistance tests. Also, the bonded surface is inspected to determine if any voids are present between the gage and the specimen due to bubbling of the adhesive.

After the bonding process is complete, the lead wires are attached from the soldering tabs of the gage to an anchor terminal, which is also bonded to the test specimen. This anchoring terminal is used to protect the fragile metal-foil gages. Finally, wires are soldered from this anchor terminal to the instrumentation being used to monitor the resistance changes.

Gage Sensitivities and Gage Factor

The electrical-resistance strain gage has a sensitivity to both axial and transverse strain. The magnitude of the transverse strain transmitted to the grid depends on a number of factors, including the thickness and elastic modulus of the adhesive, the carrier material, the grid material, and the width-to-thickness ratio of the axial segments of the grid. Sometimes it is necessary to calculate the true value of strain that includes all contributions, from

$$\varepsilon_a = \frac{(\Delta R/R)}{S_g}\frac{1-\nu_0 K_t}{1+K_t(\varepsilon_t/\varepsilon_a)} \tag{1.5.62}$$

where ε_a is the normal strain along the axial direction of the gage, ε_t is the normal strain along the transverse direction of the gage, $\nu_0 = 0.285$ is Poisson's ratio for the calibration beam, and K_t is the transverse-sensitivity factor of the gage. The strain gage sensitivity factor, S_g, is a calibration constant provided by the manufacturer. By using Equations 1.5.61 and 1.5.62 the percent error involved in neglecting the transverse sensitivity can be calculated. These errors can be significant for large values of both K_t and $\varepsilon_t/\varepsilon_a$, so it may be necessary to correct for the transverse sensitivity of the gage (Figure 1.5.40).

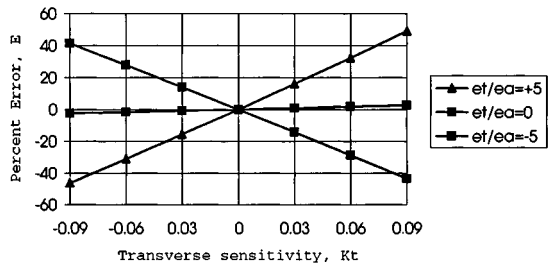

FIGURE 1.5.40 Error as a function of transverse-sensitivity factor with the biaxial strain ratio as a parameter.

Strain Analysis Methods

Electrical-resistance strain gages are normally employed on the free surface of a specimen to establish the stress at a particular point on this surface. In general it is necessary to measure three strains at a point to completely define either the stress or the strain field. For this general case, where nothing is known about the stress field or its directions before experimental analysis, three-element rosettes are required to establish the stress field. This is accomplished by using the three-element gage with orientations at arbitrary angles, as shown in Figure 1.5.41. Using this setup, the strains ε_x, ε_y, and γ_{xy} can be determined. These values can be used to determine the principal strains and principal directions,

$$\varepsilon_1 = \frac{1}{2}(\varepsilon_{xx}+\varepsilon_{yy}) + \frac{1}{2}\sqrt{(\varepsilon_{xx}-\varepsilon_{yy})^2+\gamma_{xy}^2}$$

$$\varepsilon_2 = \frac{1}{2}(\varepsilon_{xx}+\varepsilon_{yy}) - \frac{1}{2}\sqrt{(\varepsilon_{xx}-\varepsilon_{yy})^2+\gamma_{xy}^2} \tag{1.5.63}$$

$$\tan 2\phi = \frac{\gamma_{xy}}{\varepsilon_{xx}-\varepsilon_{yy}}$$

where ϕ is the angle between the principal axis (σ_1) and the *x* axis. The principal stresses can be computed using the principal strains,

$$\sigma_1 = \frac{E}{1-\nu^2}\left(\varepsilon_1 + \nu\varepsilon_2\right)$$
$$\sigma_2 = \frac{E}{1-\nu^2}\left(\varepsilon_2 + \nu\varepsilon_1\right) \tag{1.5.64}$$

These expressions give the complete state of stress since the principal directions are known from Equation 1.5.63.

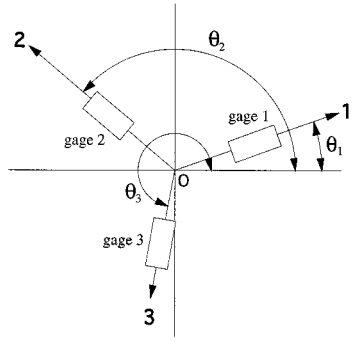

FIGURE 1.5.41 Three gage elements placed at arbitrary angles relative to the *x* and *y* axes.

Optical Methods of Strain Analysis

Moiré Method of Strain Analysis. The moiré technique depends on an optical phenomenon of fringes caused by relative displacement of two sets of arrays of lines. The arrays used to produce the fringes may be a series of straight parallel lines, a series of radial lines emanating from a point, a series of concentric circles, or a pattern of dots. The straight parallel line "grids" are used most often for strain analysis work and consist of equal width lines with opaque spacing of the same width between them. These straight parallel lines are spaced in a "grating" scheme of typically 50 to 1000 lines per inch for moiré work. In the cross-grid system of two perpendicular line arrays, the grid placed on the specimen is referred to as the model grid. The second grid is referred to as the reference grid and is overlaid on top of the model grid. Often a thin layer of oil or some other low-friction substance is placed between the model grid and the reference grid to keep them in contact while attempting to minimize the transmission of strains from the model to the reference grid.

To obtain a moiré fringe pattern the grids are first aligned on the unloaded model so that no pattern is present. The model is loaded and light is transmitted through the two grids. Strain displacement is observed in the model grid while the reference grid remains unchanged. A moiré fringe pattern is formed each time the model grating undergoes a deformation in the primary direction equal to the pitch p of the reference grating. For a unit gage length, $\Delta L = np$, where ΔL is the change in length per unit length, p is the pitch of the reference grating and n is the number of fringes in the unit gage length. In order to calculate ε_x, ε_y, and γ_{xy}, two sets of gratings must be applied in perpendicular directions. Then displacements u and v (displacements in the x and y directions, respectively) can be established and the Cartesian strain components can be calculated from slopes of the displacement surfaces: $\varepsilon_{xx} = \partial u/\partial x$, $\varepsilon_{yy} = \partial v/\partial y$, and $\gamma_{xy} = \partial v/\partial x + \partial u/\partial y$. The displacement gradients in the z direction, $\partial w/\partial x$ and $\partial w/\partial y$, have been neglected here because they are not considered in moiré analysis of in-plane deformation fields.

Photoelasticity. The method of photoelasticity is based on the physical behavior of transparent, noncrystalline, optically isotropic materials that exhibit optically anisotropic characteristics, referred to as temporary double refraction, while they are stressed. To observe and analyze these fringe patterns a device called a polariscope is used. Two kinds of polariscope are common, the plane polariscope and the circular polariscope.

The plane polariscope (Figure 1.5.42) consists of a light source, two polarizing elements, and the model. The axes of the two polarizing elements are oriented at a 90° angle from each other. If the specimen is not stressed, no light passes through the analyzer and a dark field is observed. If the model is stressed, two sets of fringes, isoclinics and isochromatics, will be obtained. Black isoclinic fringe patterns are the loci of points where the principal-stress directions coincide with the axis of the polarizer. These fringe patterns are used to determine the principal stress directions at all points of a photoelastic model. When the principal stress difference is zero ($n = 0$) or sufficient to produce an integral number of wavelengths of retardation ($n = 1, 2, 3, ...$), the intensity of light emerging from the analyzer is zero. This condition for extinction gives a second fringe pattern, called isochromatics, where the fringes are the loci of points exhibiting the same order of extinction ($n = 0, 1, 2, 3, \ldots$).

$$n = N = \frac{h}{f_\sigma}(\sigma_1 - \sigma_2) \tag{1.5.65}$$

where N is the isochromatic fringe order. The order of extinction n depends on the principal stress difference $(\sigma_1 - \sigma_2)$, the thickness h of the model, and the material fringe value f_σ. When monochromatic light is used, the isochromatic fringes appear as dark bands. When white light is used, the isochromatic fringes appear as a series of colored bands. Black fringes appear in this case only where the principal stress difference is zero.

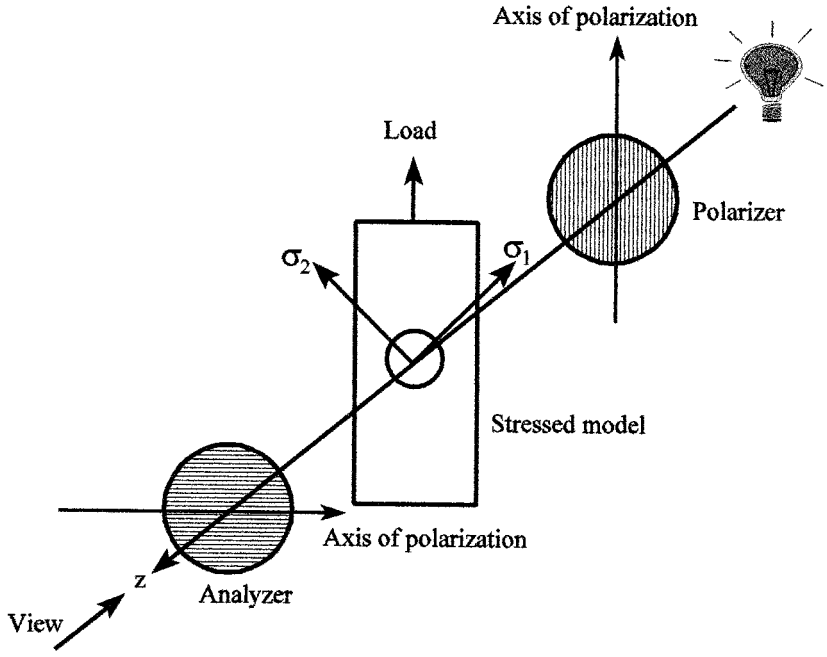

FIGURE 1.5.42 Schematic of a stressed photoelastic model in a plane polariscope.

A circular polariscope is a plane polariscope with two additional polarizing plates, called quarter-wave plates, added between the model and the original polarizing plates (Figure 1.5.43). The two quarter-wave plates are made of a permanently doubly refracting material. The circular polariscope is used to eliminate the isoclinic fringes while maintaining the isochromatic fringes. To accomplish this, monochromatic light must be used since the quarter-wave plates are designed for a specific wavelength of light. For the dark-field arrangement shown, no light is passed through the polariscope when the model is unstressed. A light-field arrangement is achieved by rotating the analyzer 90°. The advantage of using

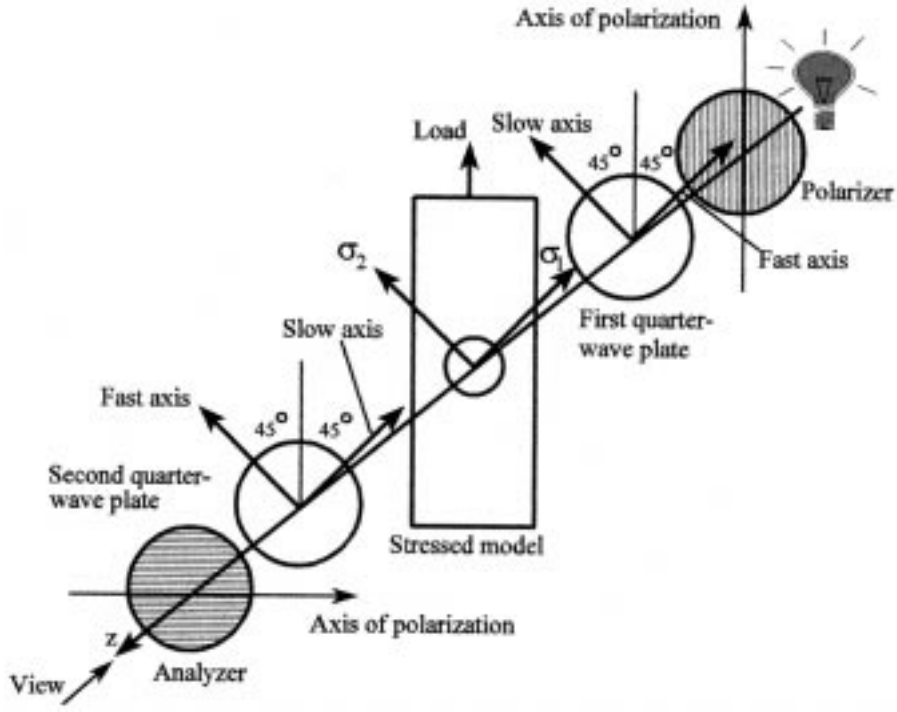

FIGURE 1.5.43 Schematic of a stressed photoelastic model in a circular polariscope.

both light- and dark-field analysis is that twice as much data is obtained for the whole-field determination of $\sigma_1 - \sigma_2$. If a dark-field arrangement is used, n and N still coincide, as in Equation 1.5.65. If a light-field arrangement is used, they are not coincident. In this case Equation 1.5.65 becomes

$$N = \frac{1}{2} + n = \frac{h}{f_\sigma}\left(\sigma_1 - \sigma_2\right) \qquad n = 0,\ 1,\ 2,\ 3,\ \ldots \tag{1.5.66}$$

By determining both the isoclinic fringes and the isochromatic fringes, the principal-stress directions and the principal-stress difference can be obtained. In order to obtain the individual principal stresses, a stress separation technique would need to be employed.

The advantages of the photoelastic method are that it allows a full-field stress analysis and it makes it possible to determine both the magnitude and direction of the principal stresses. The disadvantages are that it requires a plastic model of the actual component and it takes a considerable effort to separate the principal stresses.

Thermoelastic Stress Analysis. Modern thermoelastic stress analysis (TSA) employs advanced differential thermography (or AC thermography) methods based on dynamic thermoelasticity and focal-plane-array infrared equipment capable of rapidly measuring small temperature changes (down to 0.001°C) caused by destructive or nondestructive alternating stresses. Stress resolutions comparable to those of strain gages can be achieved in a large variety of materials. The digitally stored data can be processed in near-real time to determine the gradient stress fields and related important quantities (such as combined-mode stress intensity factors) in complex components and structures, with no upper limit in temperature. The efficient, user-friendly methods can be applied in the laboratory and in the field, in vehicles, and structures such as bicycles, automobiles, aircraft, surgical implants, welded bridges, and microelectronics. Optimum

design, rapid prototyping, failure analysis, life prediction, and rationally accelerated testing can be facilitated with the new TSA methods (Color Plates 8 and 11 to 14).

Brittle Coatings. If a coating is applied to a specimen that is thin in comparison with the thickness of the specimen, then the strains developed at the surface of the specimen are transmitted without significant change to the coating. This is the basis of the brittle coating method of stress analysis. The two kinds of coatings available are resin-based and ceramic-based coatings. The ceramic-based coatings are seldom used due to the high application temperatures (950 to 1100°F) required. The coatings are sprayed on the component until a layer approximately 0.003 to 0.010 in. thick has accumulated. It is also necessary to spray calibration bars with the coating at the same time in order to obtain the threshold strain at which the coating will crack. These calibration bars are tested in a cantilever apparatus and the threshold strain is calculated using the flexure formula and Hooke's law. Once the threshold strain is known and the actual specimen has been tested, the principal stress perpendicular to the crack can be determined by using Hooke's law. The procedure is to load the component, apply the coating, and then quickly release the loading in steps to observe any cracks.

The main advantages of this method are that both the magnitude and direction of the principal strains can be quickly obtained and that the coating is applied directly to the component. This also allows a quick analysis of where the maximum stress regions are located so that a better method can be used to obtain more accurate results. The main disadvantage is that the coatings are very sensitive to ambient temperature and might not have sufficiently uniform thickness.

Mechanical Testing

Standards. Many engineering societies have adopted mechanical testing standards; the most widely accepted are the standards published by the American Society for Testing and Materials. Standards for many engineering materials and mechanical tests (tension, compression, fatigue, plane strain fracture toughness, etc.) are available in the *Annual Book of ASTM Standards*.

Open-Loop Testing Machines. In an open-loop mechanical testing system there is no feedback to the control mechanism that would allow for continuous adjustment of the controlled parameter. Instead, the chosen parameter is "controlled" by the preset factory adjustments of the control mechanism. It is not possible for such a machine to continually adjust its operation to achieve a chosen (constant or not constant) displacement rate or loading rate.

A human operator can be added to the control loop in some systems in an attempt to maintain some parameter, such as a loading rate, at a constant level. This is a poor means of obtaining improved equipment response and is prone to error.

Closed-Loop Testing Machines. In a closed-loop, most commonly electrohydraulic, testing system, a servo controller is used to continuously control the chosen parameter. When there is a small difference between the desired value that has been programmed in and the actual value that is being measured, the servo controller adjusts the flow of hydraulic fluid to the actuator to reduce the difference (the error). This correction occurs at a rate much faster than any human operator could achieve. A standard system makes 10,000 adjustments per second automatically.

A typical closed-loop system (Color Plates 9, 11, 15) allows the operator to control load, strain, or displacement as a function of time and can be adjusted to control other parameters as well. This makes it possible to perform many different kinds of tests, such as tension, compression, torsion, creep, stress relaxation, fatigue, and fracture.

Impact Testing. The most common impact testing machines utilize either a pendulum hammer or a dropped weight. In the pendulum system a hammer is released from a known height and strikes a small notched specimen, causing it to fracture. The hammer proceeds to some final height. The difference between the initial and final heights of the hammer is directly proportional to the energy absorbed by the specimen. For the Charpy test the specimen is mounted horizontally with the ends supported so that

the pendulum will strike the specimen in midspan, opposite the notch. In the Izod test the specimen bottom is mounted in a vertical cantilever support so that the pendulum will strike the specimen at a specific distance above the notch, near the unsupported top end.

A large variety of the drop-weight tests are also available to investigate the behaviors of materials and packages during impact.

Hardness Testing. The major hardness tests are the Brinell, Rockwell, Vickers, and Shore scleroscope tests.

The Brinell hardness test uses a hardened steel ball indenter that is pushed into the material under a specified force. The diameter of the indentation left in the surface of the material is measured and a Brinell hardness number is calculated from this diameter.

The Rockwell hardness test differs from the Brinell test in that it uses a 120° diamond cone with a spherical tip for hard metals and a 1/16-in. steel ball for soft metals. The Rockwell tester gives a direct readout of the hardness number. The Rockwell scale consists of a number of different letter designators (B, C, etc.) based on the depth of penetration into the test material.

The Vickers hardness test uses a small pyramidal diamond indenter and a specified load. The diagonal length of the indentation is measured and used to obtain the Vickers hardness number.

The Shore scleroscope uses a weight that is dropped on the specimen to determine the hardness. This hardness number is determined from the rebound height of the weight.

1.6 Structural Integrity and Durability

Bela I. Sandor

The engineer is often concerned about the long-term behavior and durability of machines and structures. Designs based just on statics, dynamics, and basic mechanics of materials are typically able to satisfy only minimal performance and reliability requirements. For realistic service conditions, there may be numerous degradations to consider. A simple and common approach is to use safety factors based on experience and judgment. The degradations could become severe and require sophisticated analyses if unfavorable interactions occur. For example, fatigue with corrosion or high temperatures is difficult to predict accurately, and much more so when corrosion is occurring at a high temperature.

There are many kinds of degradations and interactions between them, and a large (and still growing) technical literature is available in most of these areas. The present coverage cannot possibly do justice to the magnitude of the most serious problems and the available resources to deal with them. Instead, the material here is to highlight some common problems and provide fundamental concepts to prepare for more serious efforts. The reader is encouraged to study the technical literature (including that by technical societies such as ASM, ASME, ASNT, ASTM, SAE), attend specialized short courses, and seek consulting advice (ASM, ASTM, Teltech) as necessary.

Finite Element Analysis. Stress Concentrations

The most common problem in creating a machine or structure with good strength-to-weight ratio is to identify its critical locations and the corresponding maximum stresses or strains and to adjust the design optimally. This is difficult if a member's geometry, including the geometry and time-dependence of the loading, is complex. The modern analytical tool for addressing such problems is finite element analysis (FEA) or finite element modeling (FEM).

Finite Element Analysis

The finite element (FE) method was developed by engineers using physical insight. In all applications the analyst seeks to calculate a *field quantity*: in stress analysis it is the displacement field or the stress field; in thermal analysis it is the temperature field or the heat flux; and so on. Results of the greatest interest are usually peak values of either the field quantity or its gradients. The FE method is a way of getting a *numerical* solution to a *specific* problem. An FEA does not produce a formula as a solution, nor does it solve a class of problems. Also, the solution is approximate unless the problem is so simple that a convenient exact formula is already available. Furthermore, it is important to validate the numerical solution instead of trusting it blindly.

The power of the FE method is its versatility. The structure analyzed may have arbitrary shape, arbitrary supports, and arbitrary loads. Such generality does not exist in classical analytical methods. For example, temperature-induced stresses are usually difficult to analyze with classical methods, even when the structure geometry and the temperature field are both simple. The FE method treats thermal stresses as readily as stresses induced by mechanical load, and the temperature distribution itself can be calculated by FE. However, it is easy to make mistakes in describing a problem to the computer program. Therefore *it is essential that the user have a good understanding of the problem and the modeling* so that errors in computed results can be detected by judgment.

Stress Concentrations

Geometric discontinuities cause localized stress increases above the average or far-field stress. A stress raiser's effect can be determined quantitatively in several ways, but not always readily. The simplest method, if applicable, is to use a known theoretical **stress concentration factor**, K_t, to calculate the peak stress from the nominal, or average, value,

$$\sigma_{\max} = K_t \sigma_{ave} \tag{1.6.1}$$

This is illustrated in Figure 1.6.1. The area under the true stress distribution always equals the area under the nominal stress level,

$$\int_A \sigma_{true}\, dA = \int_A \sigma_{ave}\, dA = \sigma_{ave} A \tag{1.6.2}$$

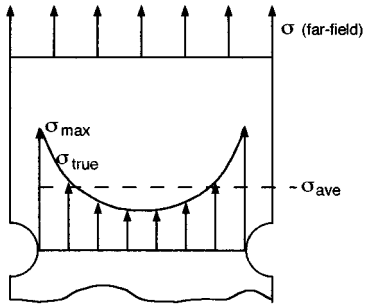

FIGURE 1.6.1 Stress distribution (simplistic) in a notched member under uniaxial load.

The factor K_t depends mainly on the geometry of the notch, not on the material, except when the material deforms severely under load. K_t values are normally obtained from plots such as in Figure 1.6.2 and are strictly valid only for ideally elastic, stiff members. K_t values can also be determined by FEA or by several experimental techniques. There are no K_t values readily available for sharp notches and cracks, but one can always assume that such discontinuities produce the highest stress concentrations, sometimes factors of tens. This is the reason for brittle, high-strength materials being extremely sensitive even to minor scratches. In fatigue, for example, invisible toolmarks may lead to premature, unexpected failures in strong steels.

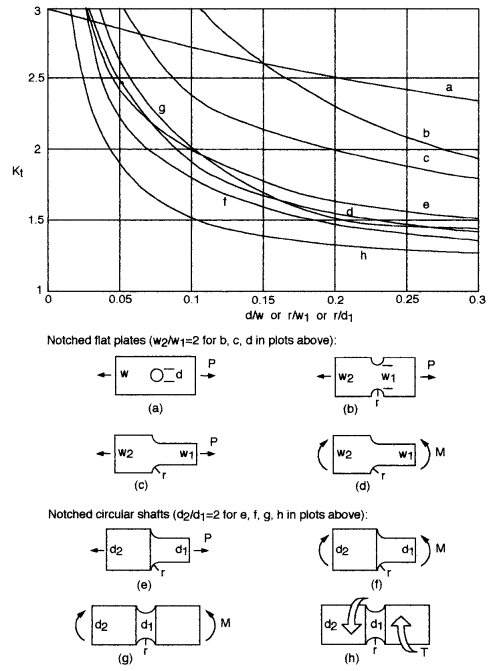

FIGURE 1.6.2 Samples of elastic stress concentration factors. (Condensed from Figures 10.1 and 10.2, Dowling, N. E. 1993. *Mechanical Behavior of Materials*. Prentice-Hall, Englewood Cliffs, NJ. With permission.)

There are many other factors that may seem similar to K_t, but they should be carefully distinguished. The first is the true stress concentration factor K_σ, defined as

$$K_\sigma = \frac{\sigma_{max}}{\sigma_{ave}} \tag{1.6.3}$$

which means that $K_\sigma = K_t$ (by Equation 1.6.1) for ideally elastic materials. K_σ is most useful in the case of ductile materials that yield at the notch tip and lower the stress level from that indicated by K_t.

Similarly, a true strain concentration factor, K_ε, is defined as

$$K_\varepsilon = \frac{\varepsilon_{max}}{\varepsilon_{ave}} \tag{1.6.4}$$

where $\varepsilon_{ave} = \sigma_{ave}/E$.

Furthermore, a large number of **stress intensity factors** are used in fracture mechanics, and these (such as K, K_c, K_I, etc.) are easily confused with K_t and K_σ, but their definitions and uses are different as seen in the next section.

Fracture Mechanics

Notches and other geometric discontinuities are common in solid materials, and they tend to facilitate the formation of cracks, which are in turn more severe stress raisers. Sharp cracks and their further growth are seldom simple to analyze and predict, because the actual stresses and strains at a crack tip are not known with the required accuracy. In fact, this is the reason the classical failure theories (maximum normal stress, or Rankine, theory; maximum shear stress, or Tresca, theory; distortion energy, or von Mises or octahedral shear stress, theory), elegantly simple as they are, are not sufficiently useful in dealing with notched members. A powerful modern methodology in this area is fracture mechanics, which was originated by A. A. Griffith[**] in 1920 and has grown in depth and breadth enormously in recent decades. The space here is not adequate to even list all of the significant references in this still expanding area. The purpose here is to raise the engineer's awareness to a quantitative, practically useful approach in dealing with stress concentrations as they affect structural integrity and durability.

Brittle and Ductile Behaviors. Embrittlements

Brittleness and ductility are often the first aspects of fracture considerations, but they often require some qualifications. Simplistically, a material that fractures in a tension test with 0% reduction of area (RA) is perfectly brittle (and very susceptible to fracture at stress raisers), while one with 100% RA is perfectly ductile (and quite tolerant of discontinuities). Between these extremes fall most engineering materials, with the added complication that embrittlement is often made possible by several mechanisms or environmental conditions. For example, temperature, microstructure, chemical environment, internal gases, and certain geometries are common factors in embrittlement. A few of these will be discussed later.

[**] The Griffith criterion of fracture states that a crack may propagate when the decrease in elastic strain energy is at least equal to the energy required to create the new crack surfaces. The available elastic strain energy must also be adequate to convert into other forms of energy associated with the fracture process (heat from plastic deformation, kinetic energy, etc.). The critical nominal stress for fracture according to the Griffith theory is proportional to $1/\sqrt{\text{crack length}}$. This is significant since crack length, even inside a member, is easier to measure nondestructively than stresses at a crack tip. Modern, practical methods of fracture analysis are sophisticated engineering tools on a common physical and mathematical basis with the Griffith theory.

Linear-Elastic Fracture Mechanics (LEFM)

A major special case of fracture mechanics is when little or no plastic deformations occur at the critical locations of notches and cracks. It is important that even intrinsically ductile materials may satisfy this condition in common circumstances.

Modes of Deformation. Three basic modes of deformation (or crack surface displacement) of cracked members are defined as illustrated schematically in Figure 1.6.3. Each of these modes is very common, but Mode I is the easiest to deal with both analytically and experimentally, so most data available are for Mode I.

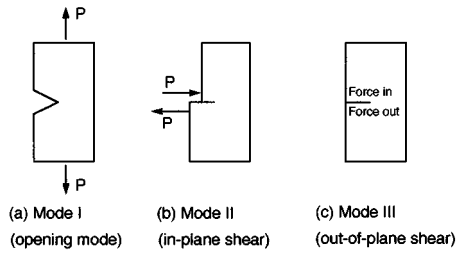

FIGURE 1.6.3 Modes of deformation.

Stress Intensity Factors. The stresses on an infinitesimal element near a crack tip under Mode I loading are obtained from the theory of linear elasticity. Referring to Figure 1.6.4,

$$\sigma_x = \frac{K_I}{\sqrt{2\pi r}} f_1(\theta) + \ldots$$

$$\sigma_y = \frac{K_I}{\sqrt{2\pi r}} f_2(\theta) + \ldots \qquad (1.6.5)$$

$$\tau_{xy} = \frac{K_I}{\sqrt{2\pi r}} f_3(\theta) + \ldots$$

$$\tau_{xz} = \tau_{zx} = 0$$

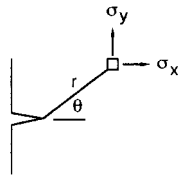

FIGURE 1.6.4 Coordinates for fracture analysis.

There are two special cases of σ_z:

$\sigma_z = 0$ for plane stress (thin members)
$\sigma_z = \nu(\sigma_x + \sigma_y)$ for plane strain, with $\varepsilon_z = 0$ (thick members)

The factor K in these and similar expressions characterizes the intensity or magnitude of the stress field near the crack tip. It is thus called the stress intensity factor, which represents a very useful concept, but different from that of the well-known stress concentration factor. K_I is a measure of the severity of a crack, and most conveniently it is expressed as

$$K_I = \sigma\sqrt{\pi a}\, f(\text{geometry}) \tag{1.6.6}$$

where a is the crack length and f is a function of the geometry of the member and of the loading (typically, $f \cong 1 \pm 0.25$). Sometimes f includes many terms, but all stress intensity factors have the same essential features and units of stress $\sqrt{\text{length}}$. In any case, expressions of K for many common situations are available in the literature, and numerical methods are presented for calculating special K values. Differential thermography via dynamic thermoelasticity is a powerful, efficient modern method for the measurement of actual stress intensity factors under a variety of complex conditions (Section 1.6, "Experimental Stress Analysis and Mechanical Testing"; Figure 1.6.12; Color Plates 8 and 11 to 14).

Fracture Toughness of Notched Members

The stress intensity factor, simply K for now, is analogous to a stress-strain curve, as in Figure 1.6.5. K increases almost linearly from 0 at $\sigma = 0$, to a value K_c at a critical (fracture) event. K_c is called the *fracture toughness* of a particular member tested. It does depend on the material, but it is not a reliable material property because it depends on the size of the member too much. This is illustrated in Figure 1.6.6 for plates of the same material but different thicknesses.

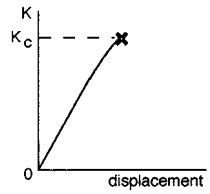

FIGURE 1.6.5 K_c = fracture toughness of a particular member.

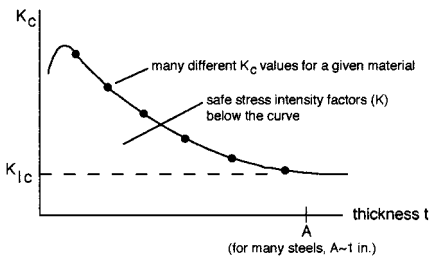

FIGURE 1.6.6 K_{Ic} = plane strain fracture toughness of material.

At very small thickness, K_c tends to drop. More significantly, K_c approaches a lower limiting value at large thickness (>*A*). This worst-case value of K_c is called K_{Ic}, the *plane strain fracture toughness* in Mode I. It may be considered a pseudomaterial property since it is independent of geometry at least over a range of thicknesses. It is important to remember that the thickness effect can be rather severe. An intrinsically ductile metal may fracture in an apparently brittle fashion if it is thick enough and has a notch.

Fracture Toughness Data. Certain criteria about crack sharpness and specimen dimensions must be satisfied in order to obtain reliable basic K_{Ic} data (see *ASTM Standards*). K_{Ic} data for many engineering materials are available in the technical literature. A schematic overview of various materials' K_{Ic} values is given in Figure 1.6.7. Note that particular expected values are not necessarily attained in practice. Poor material production or manufacturing shortcomings and errors could result in severely lowered toughness. On the other hand, special treatments or combinations of different but favorably matched materials (as in composites) could substantially raise the toughness.

Besides the thickness effect, there are a number of major influences on a given material's toughness, and they may occur in favorable or unfavorable combinations. Several of these are described here schematically, showing general trends. Note that some of the actual behavior patterns are not necessarily as simple or well defined as indicated.

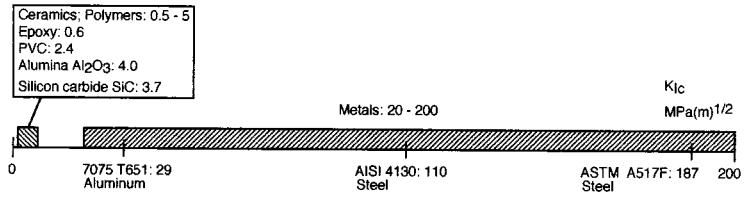

FIGURE 1.6.7 Plane strain fracture toughness ranges (approximate).

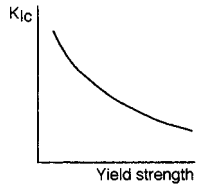

FIGURE 1.6.8 Yield strength effect on toughness.

Yield Strength. High yield strength results in a low fracture toughness (Figure 1.6.8), and therefore it should be chosen carefully, understanding the consequences.

Temperature. Two kinds of temperature effect on toughness should be mentioned here. They both may appear, at least for part of the data, as in Figure 1.6.9, with high temperature causing increased toughness. One temperature effect is by the increased ductility at higher temperature. This tends to lower the yield strength (except in low-carbon steels that strain-age at moderately elevated temperatures, about 100 to 500°C), increase the plastic zone at the notch tip, and effectively blunt the stress concentration. Another effect, the distinct temperature-transition behavior in low-carbon steels (BCC metals, in general; easily shown in Charpy tests), is caused by microstructural changes in the metal and is relatively complex in mechanism.

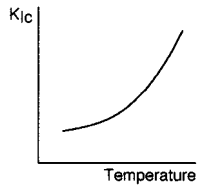

FIGURE 1.6.9 Temperature effect on toughness.

Loading Rate. The higher the rate of loading, the lower the fracture toughness in most cases. Note that toughness results obtained in notch-impact or explosion tests are most relevant to applications where the rate of loading is high.

Microstructural Aspects. In some cases apparently negligible variations in chemical composition or manufacturing processes may have a large effect on a material's fracture toughness. For example, carbon, sulfur, and hydrogen contents may be significant in several embrittling mechanisms. Also, the common mechanical processing of cold or hot working (rolling, extruding, forging) influences the grain structure (grain size and texture) and the corresponding toughness. Neutron radiation also tends to cause microscopic defects, increasing the yield strength and consequently lowering the ductility and toughness of the material.

Overview of Toughness Degradations. There is a multitude of mechanisms and situations that must be considered singly and in realistic combinations, as illustrated schematically in Figure 1.6.10 (review Figure 1.6.6 for relevant toughness definitions).

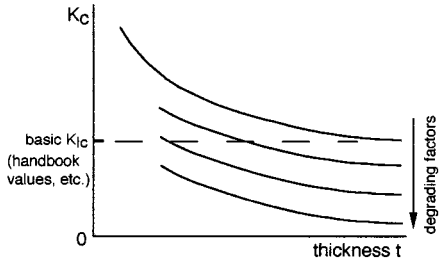

FIGURE 1.6.10 Trends of toughness degradations.

Degrading factors
Some chemical compositions
Sharper notch
Greater thickness
Faster loading
Lower temperature
Higher yield strength
Hostile chemical environment
Liquid metal embrittlement
Tensile residual stress
Neutron irradiation
Microstructural features
Moisture
Gases in solid solution
Surface hardening

Note: The toughness can drop essentially to zero in some cases.

Crack Propagation

Crack growth may be classified as either stable (subcritical) or unstable (critical). Often stable cracks become unstable in time, although the opposite behavior, cracks decelerating and even stopping, is sometimes possible. Unstable cracks under load control are extremely dangerous because they propagate at speeds nearly 40% of the speed of sound in that particular solid. This means, for example in steels, a crack growth speed of about 1 mi/sec. Thus, warnings and even electronically activated, automated countermeasures during the unstable propagation are useless. The only reasonable course is to provide, by design and proper manufacture, preventive measures such as ductile regions in a structure where cracks become stable and slow to grow, allowing for inspection and repair.

There are three kinds of stable crack growth, each important in its own right, with interactions between them possible. Under steady loads, environmentally assisted crack growth (also called stress corrosion cracking) and creep crack growth are commonly found. Under cyclic loading fatigue crack growth is likely to occur. In each case the **rate of crack growth** tends to accelerate in time or with progressive cycles of load if the loads are maintained while the cracks reduce the load-bearing cross-sectional area. This common situation, caused by increasing true stresses, is illustrated schematically in Figure 1.6.11, where a_0 is an initial flaw's size, da/dN and da/dt are the fatigue and creep crack growth rates, respectively, and a_c is the critical crack size. The rate of stable crack growth is controlled by the stress intensity factor. This will be discussed later.

Design and Failure Analysis Using Stress Intensity Concepts

The concept of stress intensity of cracked members is highly useful and practical. Three major possibilities are outlined here with respect to the essential framework of

$$K \propto \text{stress} \sqrt{\text{crack length}} \tag{1.6.7}$$

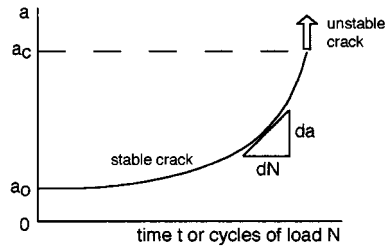

FIGURE 1.6.11 Crack growth rates under constant load.

Here K may be either an operating stress intensity factor or a K_{Ic} value, a material property (the units are the same). In design, the idea is to fix one or two quantities by some initial constraints of the case, then work with the results according to Equation 1.6.7.

1. Operating stress and material (K_{Ic}) are predetermined. This forces one to measure crack length and set the maximum allowable size of cracks.
2. Operating stress and detectable crack size are predetermined. This forces one to choose an appropriate material with the required K_{Ic} value.
3. The material (K_{Ic} value) and the detectable crack size are predetermined. This forces one to limit the operating stress accordingly.

Similar thinking can be used in failure analysis and corresponding design iteration. For example, the critical crack size at the end of the stable propagation (and start of the unstable, high-speed growth) can often be determined by looking at the broken parts. The material property, K_{Ic}, can also be estimated from the parts at hand, and thus the stress that caused the failure can be calculated. It can be determined if the stress was within normal bounds or was an overload from misuse of the equipment. These are powerful, quantitative methods that are useful in improving designs and manufacturing.

Special Methods

There are many other important and useful methods in fracture mechanics that cannot even be listed here. For example, there are several methods in the area of elastic-plastic fracture mechanics. Within this area, mainly applicable to thin members of ductile materials, the J-integral approach alone has been covered in a large number of books and journal articles.

Nondestructive Evaluation

Since all of fracture mechanics is based on knowing the crack size and its location and orientation, nondestructive evaluation (NDE) is a major part of quantitative, predictive work in this area. Many techniques of NDE are available, and some are still rapidly evolving. Two major categories of NDE methods are defined here:

1. *Geometry-based methods.* At best, the size, shape, location, and orientation of a flaw are measured. Considerable additional effort is needed to estimate the effect of the flaw on structural integrity and durability. Common methods involve acoustic, magnetic, microwave, optical (including thermal), or X-ray instruments.
2. *Stress-based methods*. A flaw's effect on the stress-strain field is directly measured, which is often much more important than just finding that flaw (a flaw of a given geometry may be benign or malignant, depending on the stress field of the neighborhood). Only a few optical methods are readily available for stress-based NDE; the most effective one for laboratory and field applications is thermoelastic stress analysis by infrared means (Figure 1.6.12; Color Plates 8, 11 to 14; Section 1.5, "Experimental Stress Analysis and Mechanical Testing").

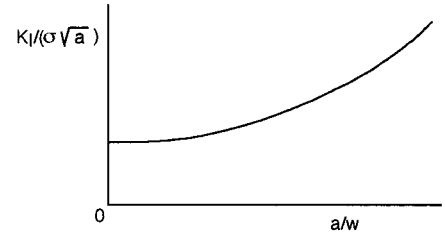

FIGURE 1.6.12 Practical fracture mechanics with NDE: nearly instantaneous measurement of crack size *and* the actual stress intensity factor via advanced thermoelastic stress analysis. The member's loading (including boundary conditions) need not be known to obtain reliable data using this method.

Creep and Stress Relaxation

Creep and stress relaxation are related time- and temperature-dependent phenomena, with creep occurring under load control and stress relaxation under deformation control. In both cases the material's temperature is a governing factor regarding what happens. Specifically, for most metals, the creep and relaxation regimes are defined as high homologous (relative, dimensionless) temperatures, normally those above half the melting point in absolute temperature for each metal. Thus, solder at room temperature creeps significantly under load, while steel and aluminum do not. However, some creep and relaxation may occur even at low homologous temperatures, and they are not always negligible. For polymers, the creep regime is above the glass transition temperature. This is typically not far from room temperature. Figures 1.6.13 and 1.6.14 show trends of creep and stress relaxation in the large-scale phenomenon region.

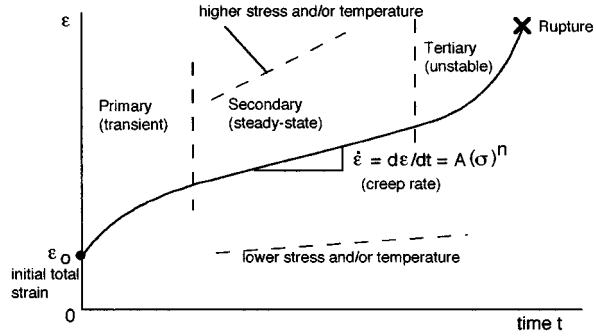

FIGURE 1.6.13 Creep under constant load. $d\varepsilon/dt = A(\sigma)^n$. A and n are material parameters.

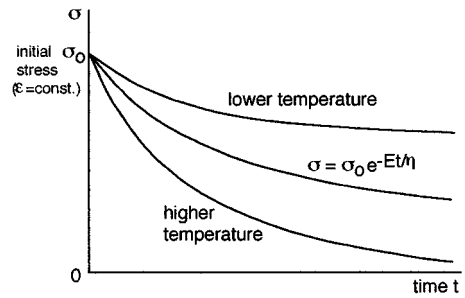

FIGURE 1.6.14 Stress relaxation under constant deformation. $\sigma = \sigma_0 e^{-Et/\eta}$. E and η are material parameters.

Stress vs. rupture life curves for creep may be nearly linear when plotted on log-log coordinates (Figure 1.6.15).

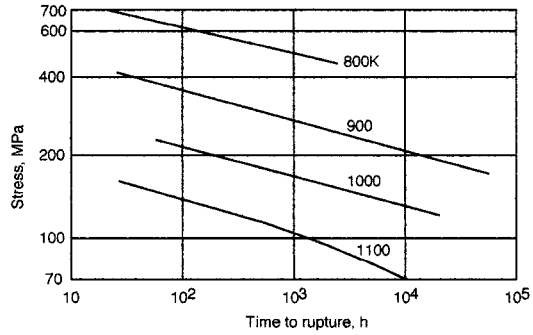

FIGURE 1.6.15 Approximate stress vs. rupture lives of S-590 alloy as functions of temperature. (After Figure 15.8, Dowling, N. E. 1993. *Mechanical Behavior of Materials.* Prentice-Hall, Englewood Cliffs, NJ. With permission.)

Mechanical Models of Viscoelastic Behaviors

Creep and stress relaxation appear to be combinations of behaviors of viscous liquids and elastic solids. The so-called viscoelastic phenomena are commonly modeled by simple mechanical components, springs and dashpots, as in Figure 1.6.16. The Maxwell model and related others are based on such elements.

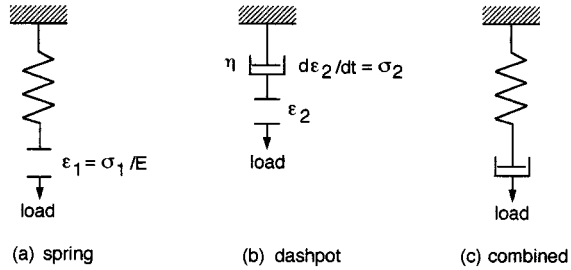

FIGURE 1.6.16 Viscoelastic elements.

The Maxwell model for creep under constant stress σ_0 is

$$\varepsilon = \varepsilon_1 + \varepsilon_2 = \frac{\sigma}{E} + \int_0^t \sigma_0 \, dt = \frac{\sigma_0}{E} + \frac{\sigma_0 t}{\eta} \tag{1.6.8}$$

For relaxation, ε = constant and σ varies, so

$$\frac{d\varepsilon}{dt} = 0 = \frac{1}{E}\frac{d\sigma}{dt} + \frac{\sigma}{\eta} \tag{1.6.9}$$

$$\int_{\sigma_0}^{\sigma} \frac{d\sigma}{\sigma} = -\frac{E}{\eta}\int_0^t dt, \quad \sigma = \sigma_0 e^{-Et/\eta}$$

Time-Temperature Parameters. Life Estimation

It is often necessary to extrapolate from laboratory creep test data, which are limited in time (from days to years), to real service lives, which tend to be from years to several decades. Time-temperature parameters are useful for this purpose. Three common parameters are outlined here. Note that no such parameter is entirely reliable in all cases. They are best if used consistently in direct comparisons of materials.

Sherby-Dorn Parameter (P_{SD})

$$P_{SD} = \log\theta_r = \log t_r - 0.217Q\left(\frac{1}{T}\right) \tag{1.6.10}$$

where, for steady-state creep,

θ_r = temperature-compensated time to rupture
t_r = rupture time, hours
Q = activation energy = constant
T = temperature, K

Stress-life data at high T and low t_r are needed to plot P_{SD} vs. stress, in order to predict a longer t_r at a lower T.

Larson-Miller Parameter (P_{LM})

This approach is analogous to the Sherby-Dorn approach, but is based on different assumptions and equations.

$$P_{LM} = 0.217Q = T\left(\log t_r + C\right) \tag{1.6.11}$$

where $C = -\log\theta_r \cong 20$ for steels. For using temperature in degrees Fahrenheit (as in most of the data),

$$P_{LM}\big|_{\circ F} = 1.8P_{LM}\big|_{K} \tag{1.6.12}$$

Manson-Haferd Parameter (P_{MH})

$$P_{MH} = \frac{T - T_a}{\log t_r - \log t_a} \tag{1.6.13}$$

where T_a and t_a are temperature and time constants representing a point of convergence for a family of data points. As above, for different temperature scales,

$$P_{MH}\big|_{\circ F} = 1.8P_{MH}\big|_{K} \tag{1.6.14}$$

Overview. The greater the extrapolation using any parameter, the greater the likelihood of error. A factor of ten or less extrapolation in life is often reasonable. At very large extrapolations there may be different damage mechanisms from that of the tests, as well as unpredictable service loading and environmental conditions.

Fatigue

Fatigue is a process of damage evolving in a material due to repeated loads, also called cyclic loads. This is a common degradation that affects virtually all solid materials, and thus it is often the main (or a contributing) factor in the failure of vehicles, machinery, structures, appliances, toys, electronic devices, and surgical implants. Many apparently well-designed and -fabricated items that fail inexplicably have problems rooted in the fatigue area.

Nearly two centuries of fatigue studies and engineering efforts have resulted in a huge, and still expanding, technical literature. This brief review can cover only a few major topics, some old but valuable items of wisdom, and practical modern methods. Three important approaches are presented: the stress-based (useful for long lives), strain-based (useful for short lives), and fracture mechanics methods.

Definitions

Constant-amplitude, stress- or strain-controlled cycling is common in testing and some service situations. Figure 1.6.17 shows the stress (σ) quantities in such cycling. Similar notations are used for strains. In completely reversed stress $\sigma_m = 0$ and $R = -1$. Zero-to-tension (a special case of pulsating tension) has $\sigma_{min} = 0$ and $R = 0$.

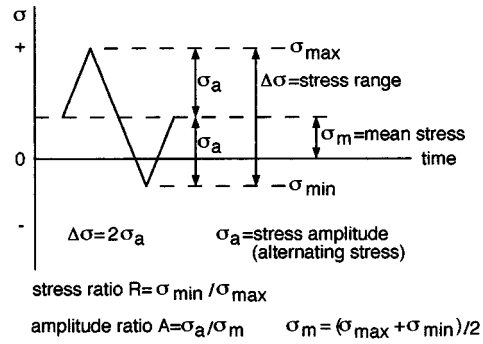

FIGURE 1.6.17 Notation for constant-amplitude stress cycling.

Material Properties in Cyclic Loading

The mechanical properties of some materials are gradually changed by cyclic plastic strains. The changes that occur are largest early in the fatigue life and become negligible beyond about 20 to 50% of the life. The most important material properties that could change significantly this way are the flow properties (yield strength, proportional limit, strain hardening exponent), while the modulus of elasticity is little affected. For metals, three initial conditions can be defined using the strain hardening exponent n as a key parameter. The concept of a cyclic stress-strain curve, as opposed to that in monotonic (static) loading, is also used to distinguish possible material behaviors in fatigue, as follows.

- **Stable**: $0.15 < n < 0.2$ (approx.)

  The monotonic and cyclic stress-strain curves are the same for most practical purposes (though seldom coincident).

  Examples: 7075-T6 Al; 4142 steel (550 BHN)
- **Cycle-Dependent Softening**: $n < 0.15$ (approx.) (means initially hard, cold-worked material)

  The cyclic stress-strain curve falls significantly below the monotonic curve, which means a gradually decreasing deformation resistance as cyclic loading progresses. The cyclic yield strength may be less than half the tensile yield strength in some cases.

  Examples: 4340 steel (350 BHN); 4142 steel (400 BHN)
- **Cycle-Dependent Hardening**: $n > 0.2$ (approx.) (means initially soft, annealed material)

  The cyclic stress-strain curve is significantly above the monotonic curve, which means a gradually increasing deformation resistance as cyclic loading progresses.

  Examples: 2024-T4 Al; 4142 steel (670 BHN)

Note that the hardest steels tend to further harden in cyclic loading. Thus, a given steel (such as 4142) may be stable, softening, or hardening, depending on its initial hardness.

In the technical literature, primes are normally used to denote cyclic material properties. For example, σ'_y is the yield strength obtained from a cyclic stress-strain curve.

Stress vs. Life (S-N) Curves

The most common and historical fatigue life plots present data of stress amplitude (simplistically, S or S_a) on a linear scale vs. cycles to failure (N or N_f) on a logarithmic scale as in Figure 1.6.18.

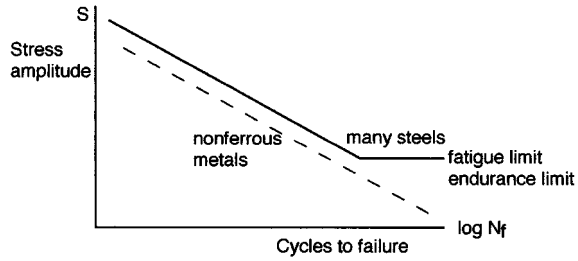

FIGURE 1.6.18 Schematic of S-N curves.

Many steels (plain carbon or low alloy) appear to have a distinct fatigue limit. For other metals that do not have such a limit (aluminum, for example), an arbitrary fatigue limit is defined as a stress amplitude corresponding to a specified life, typically 10^7 or 10^8 cycles.

Trends in S-N Curves

There are many influences on the shape and position of a material's fatigue life curve as briefly discussed below.

Ultimate Strength. It is widely believed that, at least for steels, the fatigue limit σ_e is about one half of the ultimate strength σ_u. In fact, this is a gross oversimplification, with actual values being lower or higher than that in many cases.

Mean Stress, Residual Stress. Several main points are worth remembering: residual stresses (also called self-stresses) are common, and they are to be treated as mean stresses (by sign and magnitude) in fatigue; a tensile mean stress lowers the life while a compressive one increases it. Simplistically, a tensile mean stress lowers the allowable cyclic stress amplitude according to Figure 1.6.19 where

$$\sigma_m + \sigma_a \le \sigma_u \quad \text{or} \quad \sigma_y \qquad (\text{if yielding is to be prevented})$$

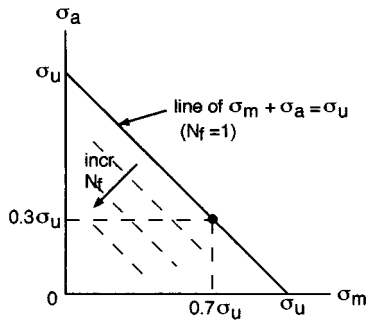

FIGURE 1.6.19 Schematic of tensile mean stress effect.

For example, if $\sigma_m = 0.7\sigma_u$, then the maximum alternating stress for one cycle is $0.3\sigma_u$. This kind of graphical relationship is called a Goodman diagram. There are several special expressions for dealing with the detrimental effects of tensile mean stresses. For example, the modified Goodman equation is

$$\frac{\sigma_a}{\sigma_e} + \frac{\sigma_m}{\sigma_u} = 1 \qquad (1.6.15)$$

where σ_e is the fatigue limit for fully reversed loading.

Sometimes curved lines represent real behavior better than the linear theory shown in Figure 1.6.19. In that case the Gerber parabola may be appropriate, in the form of

$$\frac{\sigma_a}{\sigma_e} + \left(\frac{\sigma_m}{\sigma_u}\right)^2 = 1 \qquad \text{for} \quad \sigma_m \geq 0 \tag{1.6.16}$$

Another approach worth mentioning is the Morrow expression, a mechanistically elegant and sensible one, which will be presented later.

Note that tensile mean stresses are generally detrimental and that many approaches have been proposed to deal with them, yet no single method is capable of good predictions in all cases. In practice it is best to use a particular method that has a good track record for the material and situation at hand. Constant-life diagrams are useful, elaborate derivatives of the Goodman approach, if they include a broad data base (Figure 1.6.20).

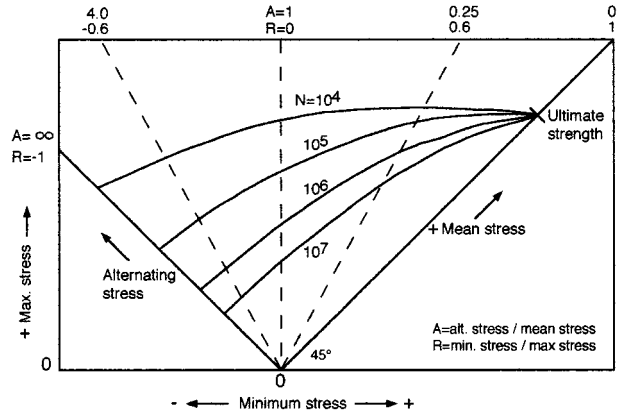

FIGURE 1.6.20 Constant-life diagram.

Notch Effects. Stress raisers can be extremely detrimental in fatigue, except when they help create localized compressive residual stresses in ductile metals, delaying crack formation and growth. These are discussed in connection with the strain-based approach.

Microstructure. Large grain size (annealed metals) lowers the fatigue strength, and small grain size (by cold working) increases it, especially at long lives, under load control.

Surface Effects. The condition of a material's surface may influence the fatigue behavior in many ways, typically in combinations.

Toolmarks are common detrimental features, especially since often they are aligned perpendicular to the principal tensile stress in axial or bending loading. An example is a shaft cut in a lathe. Note that in the case of high-strength, hard materials even invisible scratches from grinding and buffing may be stress raisers. Machining also tends to create tensile or compressive residual stresses in surface layers.

Surface treatments such as carburizing or nitriding of steels affect the fatigue life by changes in chemical composition, microstructure, hardness, or residual stress. Shot peening, surface rolling, or burnishing is done to introduce compressive residual stresses, which delay cracking in long-life service. Plating (chromium, nickel) tends to create layers of poor fatigue resistance and harmful tensile residual stresses. Shot peening after plating is a beneficial step.

Environment. Hostile chemical environments can severely reduce most materials' fatigue resistance. Common causes of problems are salt water, salt in the air, salt on the road, moisture, and even pollutants in the air. For example, sulfur in the air results in aggressive sulfuric acid on machines and structures.

Statistical Scatter. There is always statistical scatter in a material's fatigue life at any given stress level, especially at long lives. The scatter band may cover several orders of magnitude in life at a single stress

level. Because of the scatter, there is no unique fatigue life curve for any material — the curve depends not only on physical factors such as environment, but also on the number of tests done. It is not sufficient to do a handful of tests and draw a curve somewhere through the data points. As a simple rule, to have a high level of confidence (>99%) in a fatigue life curve, at least six identical tests are needed to obtain a mean value at each of several levels of stresses in the general life range of interest. A curve through these mean values is fairly representative of the average life curve (50% probability of failure), but still may not be adequate to deal with scatter. Note that the minimum number of test specimens according to the ASTM Standard E 739 is 6 to 12 for preliminary, exploratory work, or for research and development and component testing, and 12 to 24 for design allowables or reliability assessment.

Ideally, additional analysis is done, using Gaussian (normal) statistical distribution or some other model, such as the Weibull distribution. The latter is particularly informative in determining the probability of fatigue failure. The practical problem is that engineers may require very low probabilities of failure (less than 1%), but neither the necessary mathematical methods nor the data bases are available for that. A family of fatigue life curves for various probabilities of failure and other relevant considerations for one material are shown schematically in Figures 1.6.21 to 1.6.23.

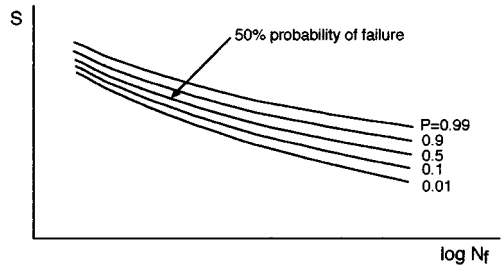

FIGURE 1.6.21 Schematic S-N curves with various probabilities of failure.

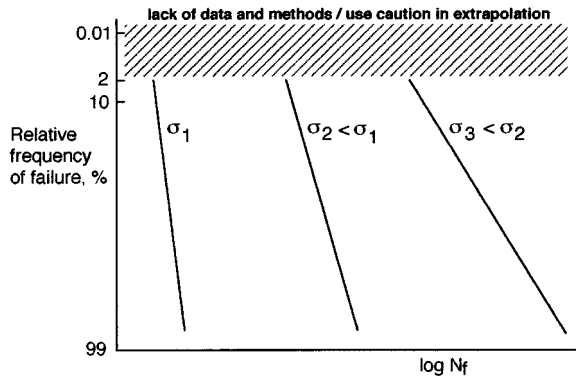

FIGURE 1.6.22 Probability aspects of fatigue depending on stress level.

Variable Amplitude Loading

Many machines, vehicles, and structures experience random or blockwise changing loading. They can be simplistically modeled for life prediction using the Palmgren-Miner rule, illustrated in Figure 1.6.24.

There are two major assumptions for this rule for completely reversed loading:

1. Every cycle at a given level of stress amplitude causes the same amount of damage, whether the cycle is early or late in the life.
2. The percentage of damage caused by a cycle of load at any level of stress is equivalent to the same percentage of damage at any other level of stress.

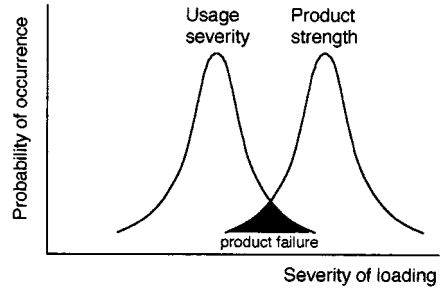

FIGURE 1.6.23 Probability aspects of fatigue depending on applied stress and product strength.

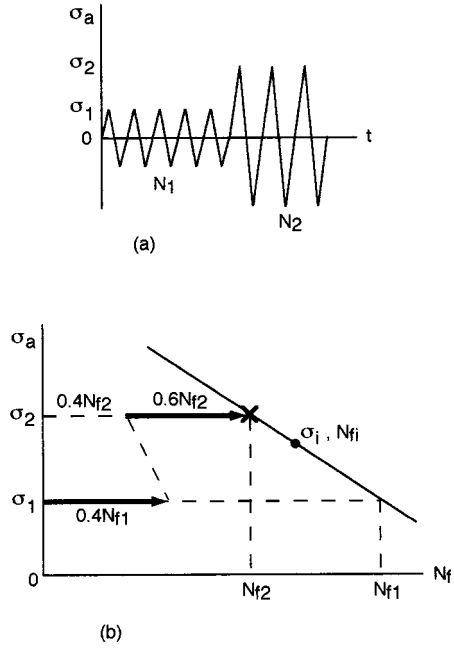

FIGURE 1.6.24 Schematic for Palmgren-Miner rule.

Thus, since 100% of the life N_{fi} is exhausted at failure at any single stress amplitude σ_i, in multilevel loading the life fractions sum to unity, as mathematically formulated here and illustrated in Figure 1.6.24,

$$\frac{N_1}{N_{f1}} + \frac{N_2}{N_{f2}} + \ldots = \sum \frac{N_i}{N_{fi}} = 1 \tag{1.6.17}$$

where N_i is the actual number of cycles at σ_i and N_{fi} is the life at σ_i.

In practice, summations of about 0.8 to 1.2 can be accepted, saying that the Palmgren-Miner rule is valid in that case. Gross deviations from summations of 1 are common, especially when the mean stress is not zero. There are modified versions of the basic rule for such cases, but they should be used with caution.

Cycle Counting. Highly irregular loading requires the use of special cycle counting methods, such as level crossing, range counting, or rainflow cycle counting. The latter is the best modern method, lending itself to efficient field data acquisition and computer work (ASTM Standard E1049; *SAE Fatigue Design Handbook*).

Multiaxial Fatigue

Complex states of stress are common in engineering components, and in fatigue analysis they may cause serious difficulties. There are many methods available, but none of them are adequate for all cases. The simplest situations that might be handled reasonably well involve fully reversed loading by in-phase or 180° out-of-phase proportional stresses at the same frequency. Multiaxial fatigue testing is difficult and expensive, so it is often desired to use uniaxial test data for predicting the multiaxial behavior. A typical approach for this is based on computing an effective stress amplitude σ_e from the amplitudes of the principal stresses σ_{1a}, σ_{2a}, σ_{3a}. With the concept of the octahedral shear yield criterion,

$$\sigma_e = \frac{1}{\sqrt{2}}\sqrt{\left(\sigma_{1a}-\sigma_{2a}\right)^2+\left(\sigma_{2a}-\sigma_{3a}\right)^2+\left(\sigma_{3a}-\sigma_{1a}\right)^2} \tag{1.6.18}$$

where in-phase stresses are positive and 180° out-of-phase stresses are negative.

The life is estimated by entering σ_e on the appropriate S-N curve. Note that mean stresses, localized or general yielding, creep, and random frequencies of loading further complicate the problem and require more sophisticated methods than outlined here.

Strain vs. Life (ε-N) Curves

A strain-based approach is necessary in fatigue when measurable inelastic strains occur. In general, total strain consists of elastic, plastic, and creep strains, with the latter two being in the category of inelastic strains,

$$\varepsilon_t = \varepsilon_e + \varepsilon_p + \varepsilon_c \tag{1.6.19}$$

When ε_p or/and ε_c are dominant, the life is relatively short and the situation is called low-cycle fatigue (LCF), as opposed to high-cycle fatigue (HCF), where ε_e is dominant. The mechanics of LCF can be understood by first considering hysteresis loops of elastic and plastic strains as defined in Figure 1.6.25.

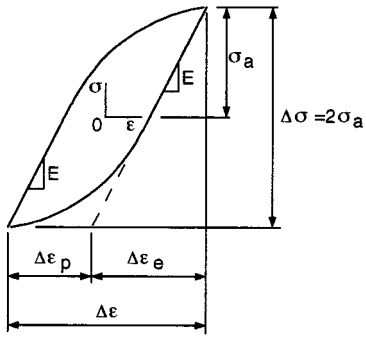

FIGURE 1.6.25 Hysteresis loop.

Simplistically, HCF means a thin loop (a straight line at very long life) and LCF means a fat loop. Strain-life plots are especially useful in the LCF regime where material properties (ε_f, σ_f) obtained in monotonic tension tests are directly useful in fatigue life prediction as shown in Figure 1.6.26. Most commonly the total strain amplitude ε_a is plotted vs. the life $2N_f$, with a corresponding equation (called Coffin-Manson equation) for fully reversed loading,

$$\varepsilon_a = \frac{\sigma_f}{E}\left(2N_f\right)^b + \varepsilon_f\left(2N_f\right)^c \tag{1.6.20}$$

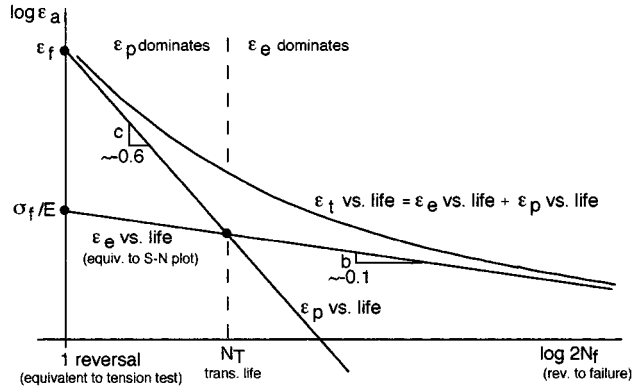

FIGURE 1.6.26 Schematic of strain vs. life curves.

It is remarkable that all metals are similar to one another in their values of the exponents b (≈ -0.1) and c (≈ -0.6), differing only in fracture strength σ_f and fracture ductility ε_f. These allow a simplistic fatigue life prediction if at least σ_f and ε_f are known.

If there is a mean stress, its effect is equivalent to an altered fracture strength. Using the Morrow approach in a simplified version,

$$\varepsilon_a = \frac{\sigma_f}{E}\left(1 - \frac{\sigma_m}{\sigma_f}\right)\left(2N_f\right)^b + \varepsilon_f\left(2N_f\right)^c \tag{1.6.21}$$

where σ_m is positive for tensile and negative for compressive mean stress.

Notch Effects

The localized plastic strains of notched members complicate the fatigue analysis considerably. It should be noted, first of all, that the theoretical stress concentration factor K_t is not entirely relevant to such members, because yielding lowers the actual peak stresses from those predicted. This leads to the definitions of the true stress and strain concentration factors,

$$K_\sigma = \frac{\text{peak stress}}{\text{ave. stress}} \qquad K_\varepsilon = \frac{\text{peak strain}}{\text{ave. strain}} \tag{1.6.22}$$

According to Neuber's rule,

$$K_t = \sqrt{K_\sigma K_\varepsilon} \tag{1.6.23}$$

which is useful for notch analysis in fatigue. This expression is strictly true for ideally elastic behavior and is qualitatively evident for elastic-plastic deformations.

Residual Stresses at Notches. An extremely important, and somewhat surprising, phenomenon can occur in notched members if they yield locally under variable-amplitude loading. If a large load (called an overload) causes yielding at a notch and is followed only by smaller loads, a residual stress of the opposite sign to the overload's sign is generated at the root of the notch. Thus, a tensile overload (such as at one side of a shaft in a straightening operation) creates a compressive residual stress, and vice versa. These stresses may remain in the member for a long time or be relaxed by other plastic strain events or by annealing. Of course, such stresses are effective mean stresses and can alter the life greatly.

Creep-Fatigue Interactions

Inelastic strains (plastic and creep strains) are the basic causes of time- and cycle-dependent damage processes. When both kinds of strains occur during the life of a particular component, complex damage interactions may arise. The simplest and most elegant approach in such a case is to sum both of the different damages linearly (as in the Palmgren-Miner summation for pure fatigue), assuming that they are equivalent to one another. In other words, assume that X percentage of creep life exhausted is equivalent to the same X percentage of fatigue life exhausted. Thus, a linear expression involving time and cycle fractions can be stated,

$$\underset{\text{pure creep}}{\sum \frac{t_i}{t_{ri}}} + \underset{\text{pure fatigue}}{\sum \frac{n_j}{N_{fj}}} = \underset{\text{at failure}}{1} \tag{1.6.24}$$

where t_i = actual time spent at stress level i in creep, t_{ri} = total time to rupture at stress level i, n_j = actual number of cycles at stress level j, and N_{fj} = cycles to failure at stress level j.

This idealized linear expression is plotted as a dashed line in Figure 1.6.27; in contrast, a more realistic ASME code and possible severe degradations are also plotted.

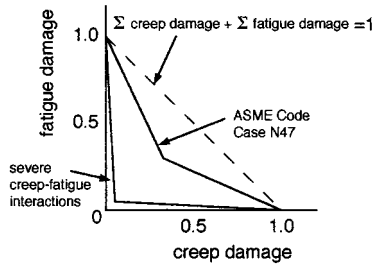

FIGURE 1.6.27 Schematic of creep-fatigue interactions. The bilinear damage rule is recommended in the ASME Boiler and Pressure Vessel Code, Section III, Code Case N47.

There are many other methods (such as damage rate equations; strain-range partitioning) to deal with creep-fatigue problems, but none of them are adequate for all situations. The difficulty is mainly because of the need to account for important, complex details of the loading cycle (frequency, hold times, temperature, and deformation wave shape).

Fracture Mechanics Method in Fatigue

Cyclic loading can cause crack growth with or without the presence of a hostile chemical environment. The rate of crack growth depends on the stress intensity factor $K \propto \sigma\sqrt{a}$. Investigations of this dependence have led to the development of powerful techniques in design and failure analysis. The fatigue crack growth behavior is quantified by the Paris equation,

$$\frac{da}{dN} = C(\Delta K)^m \tag{1.6.25}$$

where da/dN = crack growth rate
C, m = material constants
$\Delta K = K_{max} - K_{min}$ = stress intensity factor range
$K_{max} \propto \sigma_{max}$
$K_{min} \propto \sigma_{min}$

Typical data for a wide range of crack growth rates have patterns as in Figure 1.6.28, where ΔK_{th} is a threshold value akin to a fatigue limit. The linear part of the curve is useful for life prediction and failure analysis.

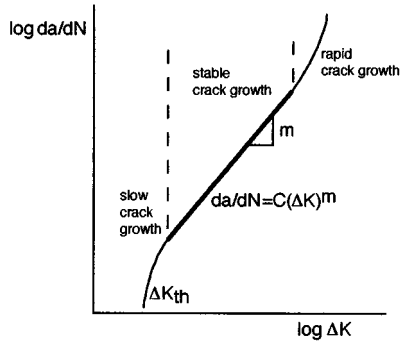

FIGURE 1.6.28 Schematic of fatigue crack propagation data.

Abridged Example of a Modern Fatigue Analysis

Many of the concepts mentioned above are applied in Sandia National Laboratories' "User's Manual for FAROW: Fatigue and Reliability of Wind Turbine Components," SAND94-2460, November 1994. FAROW is a computer program for the probabilistic analysis of large wind turbines, using structural reliability techniques to calculate the mean time to failure, probability of failure before a target lifetime, relative importance of each of the random inputs, and the sensitivity of the reliability to all input parameters. The method is useful whether extensive data are available or not (showing how much can be gained by reducing the uncertainty in each input). It helps one understand the fatigue reliability of a component and indicates how to improve the reliability. The sample figures (Figures 1.6.29 to 1.6.32) illustrate some of the key data and results for the machines and materials considered.

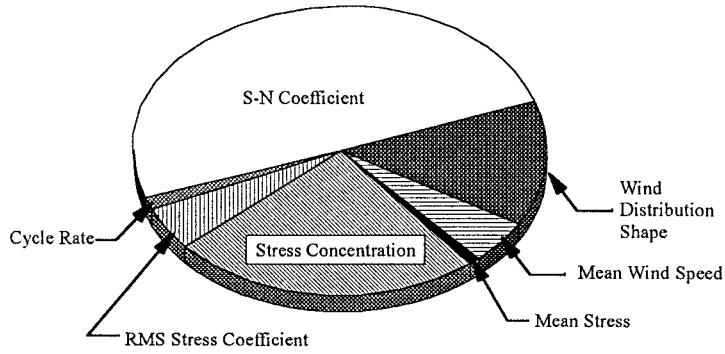

FIGURE 1.6.29 Relative importance factors as fractions of the total influence on the probability of failure. (Courtesy Sandia National Laboratories, Albuquerque, NM.)

Note especially a large discrepancy between mean lifetime and probability of failure in a few years. A mean lifetime of 600 years was calculated for a critical component, using the median values for all the random variables considered and using the constant values for all the other input parameters. However, the probability of the component failing in less than 5 years is estimated at 7.6% (Figure 1.6.32). This shows the uncertainty even in sophisticated fatigue life calculations because of reasonable uncertainty in the inputs and the sensitivity of fatigue life to parameter variation.

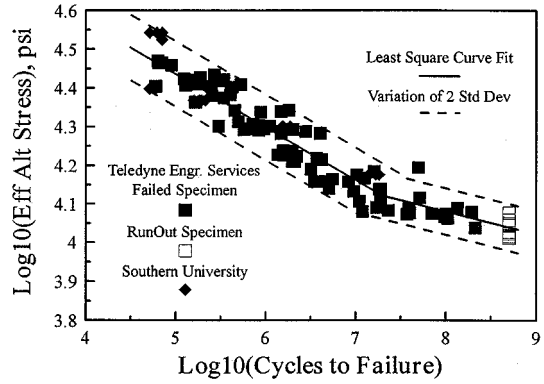

FIGURE 1.6.30 Fatigue life data for 6063 Al. (Courtesy Sandia National Laboratories, Albuquerque, NM.)

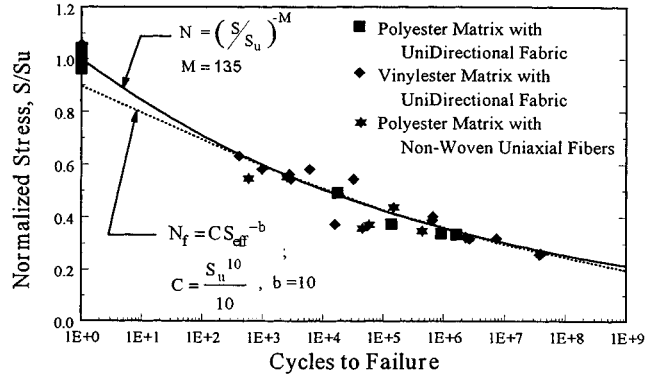

FIGURE 1.6.31 Fatigue life data for uniaxial fiberglass composite. (Courtesy Sandia National Laboratories, Albuquerque, NM.)

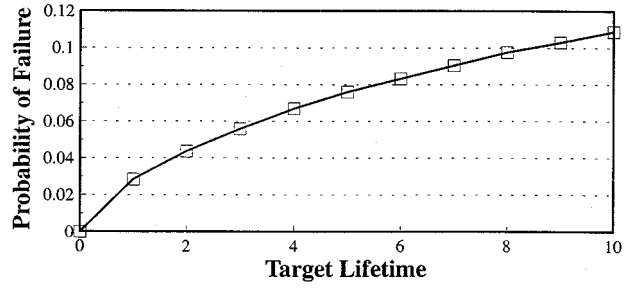

FIGURE 1.6.32 Example FAROW results for probability of premature failure as a function of target lifetime. (Courtesy Sandia National Laboratories, Albuquerque, NM.)

1.7 Comprehensive Example of Using Mechanics of Solids Methods

Richard C. Duveneck, David A. Jahnke, Christopher J. Watson, and Bela I. Sandor

A concise overview of an engineering project is presented to illustrate the relevance and coordinated application of several concepts and methods in this chapter. The sketchy outline is limited in breadth and depth, emphasizes modern methods, and is not aiming for completeness in any particular area.

The Project

Analyze the currently used A-shaped arm of the suspension system of a small, special-purpose ground vehicle. The goal is to redesign the component to save weight and, more importantly, reduce the cost of manufacturing, while assuring the product's reliability over its expected service life.

Concepts and Methods

Statics

Vectors
Free-body diagrams. Equilibrium
Two-force member: shock absorber
Frame components
Beams. Bending moments
Moments of inertia
Center of mass

Dynamics

Velocity, acceleration
Rigid-body dynamics
General plane motion
Relative motion

Vibrations

Natural frequency
Damping. Logarithmic decrement

Mechanics of Materials

Stress and strain. Transformation equations. Principal stresses. Maximum shear stress
Material properties. Material selection
Bending stresses. Beam optimization
Strain gages. Mechanical testing with closed-loop equipment

Durability

Stress concentrations. Finite element analysis
Cumulative fatigue damage. Cycle counting in random loading. Mean stresses. Goodman diagrams. Life prediction
Thermoelastic stress analysis

Illustrations

A few aspects of the project are graphically illustrated in Color Plate 16 and Figures 1.7.1 to 1.7.3.

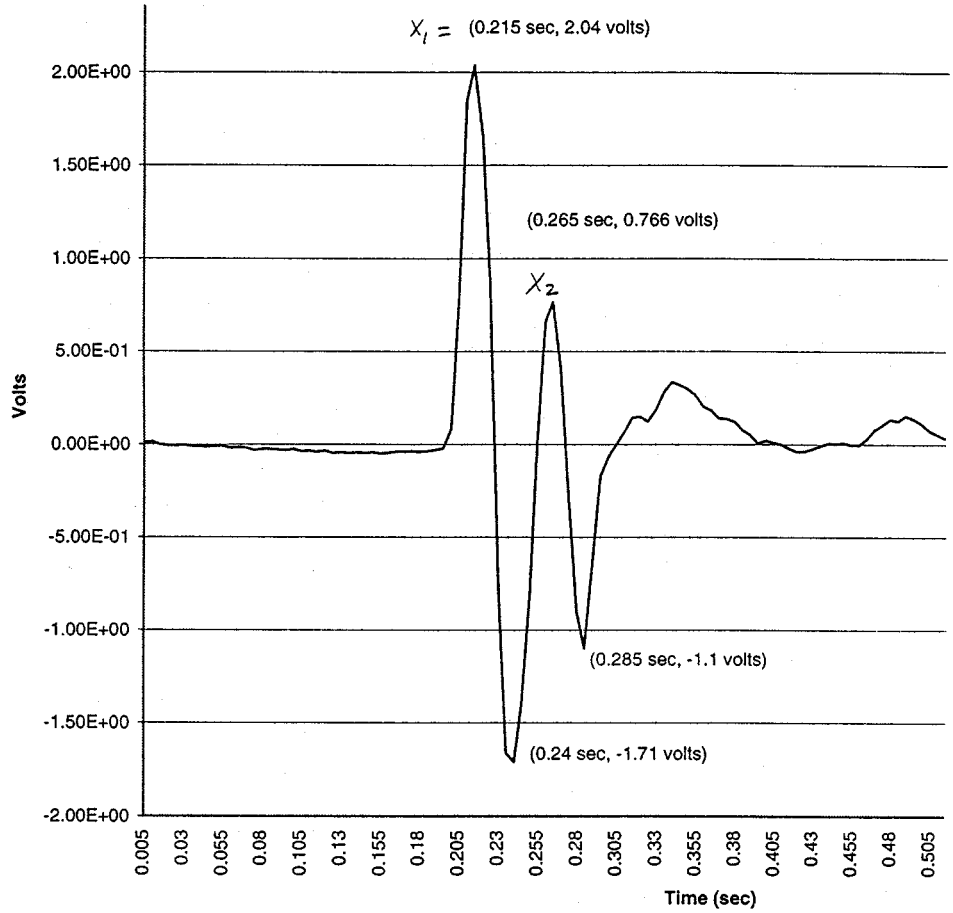

FIGURE 1.7.1 Accelerometer data from front suspension system of vehicle. Logarithmic decrement $\partial = \ln(x_1/x_2)$; damping ratio $\zeta = 0.16$.

Defining Terms

STATICS

Equilibrium: A concept used to determine unknown forces and moments. A rigid body is in equilibrium when the equivalent force-couple system of the external forces acting on it is zero. The general conditions of equilibrium are expressed in vector form ($\sum\mathbf{F} = 0$, $\sum\mathbf{M}_O = \sum[\mathbf{r} \times \mathbf{F}] = 0$) or scalar form ($\sum F_x = 0$, $\sum F_y = 0$, $\sum F_z = 0$, $\sum M_x = 0$, $\sum M_y = 0$, $\sum M_z = 0$).

Equivalent force-couple system: Any system of forces and moments acting on a rigid body can be reduced to a resultant force and a resultant moment. Transformations of a force-couple system involving chosen points of reference are easy to make. These are useful for determining unknown forces and moments and the critical locations in structural members.

Free-body diagram: A method of modeling and simplifying a problem for the efficient use of the equilibrium equations to determine unknown forces and moments. A body or group of bodies is imagined to be isolated from all other bodies, and all significant external forces and moments (known or unknown) are shown to act on the free-body model.

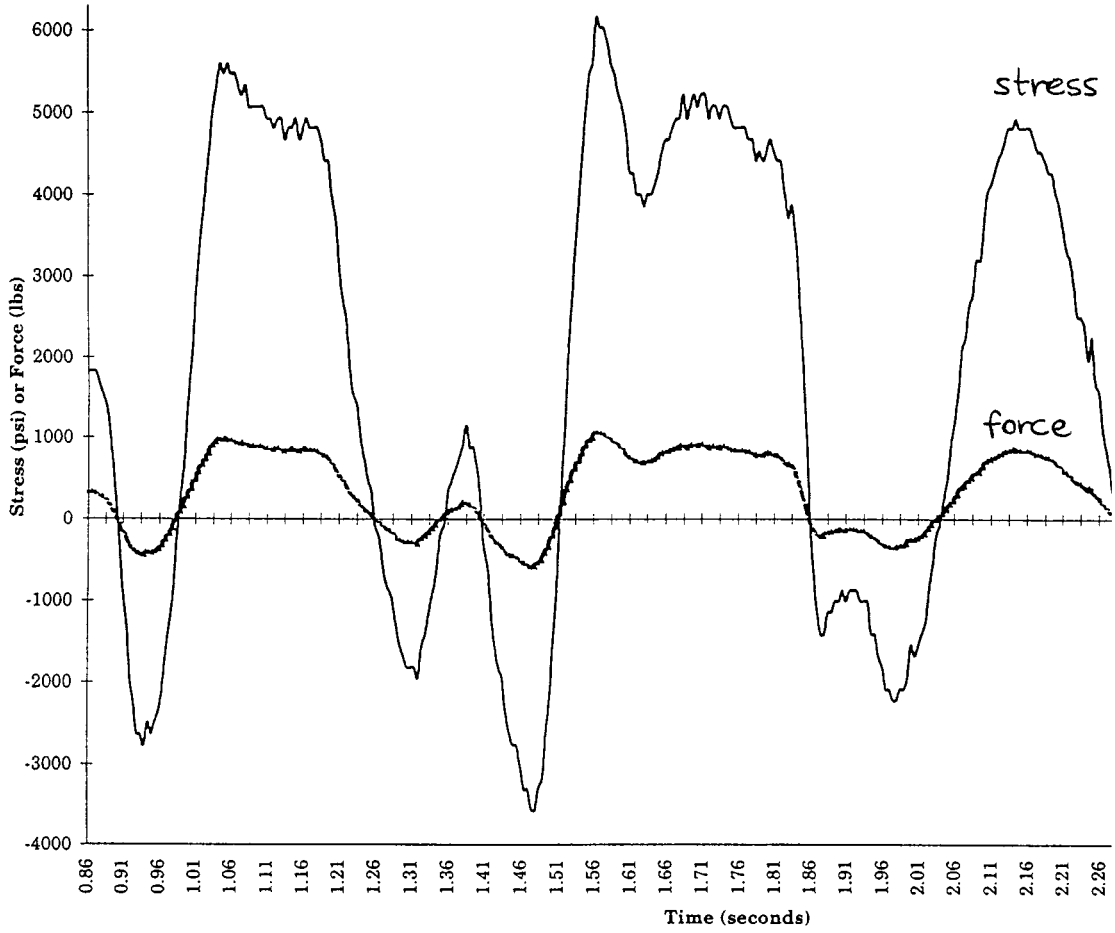

FIGURE 1.7.2 Axial stress and force vs. time in shock absorber shaft.

DYNAMICS

Equations of motion: Expressions of the acceleration of a body related to the forces acting on the body. The basic equation of motion for a particle of mass m is $\sum \mathbf{F} = m\mathbf{a}$. Many other equations of motion may be stated, depending on the dimensions of the body and its motion (such as two- or three-dimensional motion) and the coordinate system chosen.

Kinematics: The analysis of motion based on geometry and time-dependent aspects. Forces may or may not be associated with the motion, but the analysis does not involve considerations of forces. The parameters of interest in kinematics are position, displacement, velocity, acceleration, and time.

Kinetics: The analysis of motion based on kinematics and the effects of forces on masses.

VIBRATIONS

Forced vibration: Involves an exciting force applied periodically during the motion. A forced vibration may also be described in terms of the displacement of a foundation or primary mass that supports the vibrating system.

Free vibration: Occurs when only two kinds of forces are acting on a mass: (a) the elastic restoring force within the system and (b) the force of gravity or other constant forces that cause no displacement from the equilibrium configuration of the system.

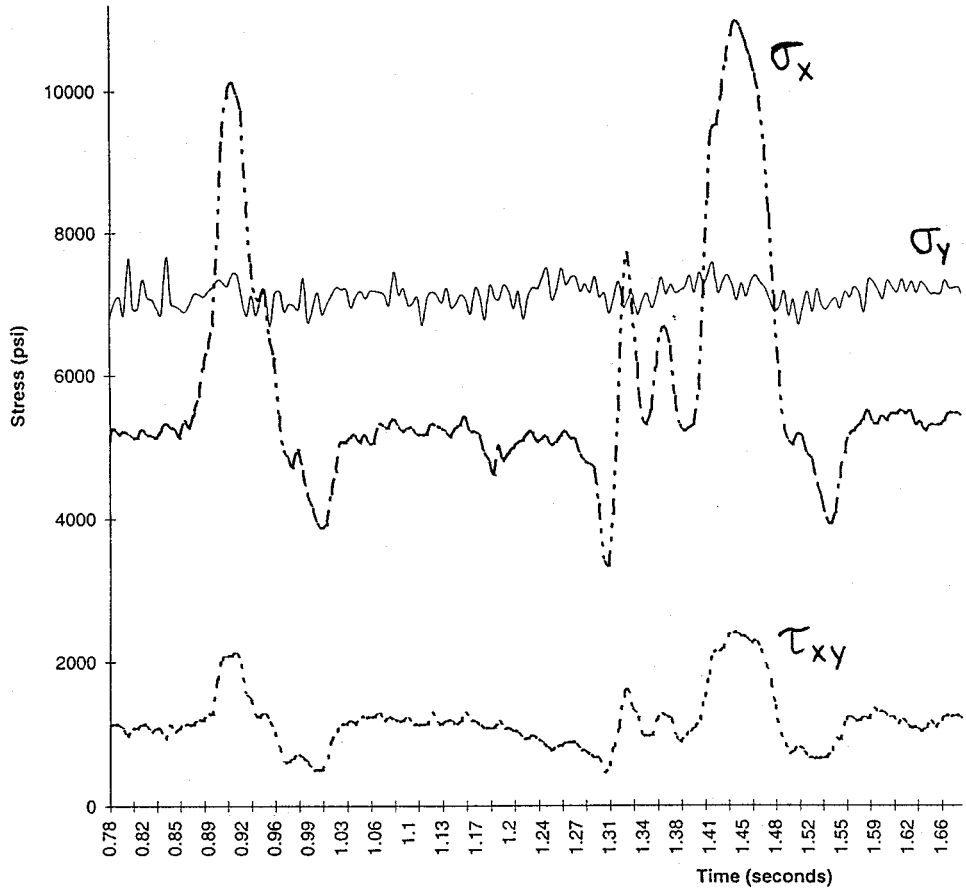

FIGURE 1.7.3 Stresses σ_x, σ_y, and τ_{xy} measured at one point of the A-arm by strain gages as the vehicle travels over bumps.

Resonance: A critical aspect of forced vibrations; it occurs when the forcing frequency equals the system's natural frequency. In this condition the amplitude of the displacements becomes infinite in theory, or dangerously large in practice when the damping is small. Near-resonance conditions may also be undesirable.

MECHANICS OF MATERIALS

Flexure formula: Used to calculate the bending stresses in beams. Must be applied with modifications if there are inelastic deformations, unsymmetric bending, or for composite beams and curved beams.

Hooke's law: Applicable for calculating uniaxial or multiaxial stress-strain responses when the material acts entirely elastically. Involves the modulus of elasticity E and Poisson's ratio v.

Principal stresses: The maximum and minimum normal stresses at a point, on an infinitesimal element. An important related quantity is the absolute maximum shear stress. These quantities can be determined (given an arbitrary state of applied stress) from stress transformation equations or from their graphical solution, Mohr's circle. Principal strains are determined in a similar way.

Stress-strain diagram: Shows the stress-strain response and many important mechanical properties for a material. These properties depend greatly on the material's chemical composition and several other factors of fabrication and service conditions. Monotonic (tension or compression) and cyclic loading conditions may result in grossly different mechanical behaviors even for a given material.

STRUCTURAL INTEGRITY AND DURABILITY

Rate of crack growth: A measure of damage evolution and remaining life of a member. In fatigue, the crack propagation rate *da/dN* depends on the stress intensity factor range ΔK and material properties. This relationship is the basis of the powerful, well-established damage-tolerant design method.

Stress concentration factor: The localized stress-raising effect of a geometric discontinuity. There are many, potentially confusing, forms of quantifying this effect. The most prominent factors are distinguished concisely:

a. Theoretical stress concentration factor, $K_t = \sigma_{max}/\sigma_{ave}$
   Depends on geometry of notch, not on material
   Has no engineering units
b. True stress concentration factor, $K_\sigma = \sigma_{max}/\sigma_{ave}$
   Depends on geometry of notch and material; $K_\sigma = K_t$ for perfectly elastic material, $K_\sigma < K_t$ for ductile material
   Has no engineering units
c. True strain concentration factor, $K_\varepsilon = \varepsilon_{max}/\varepsilon_{ave}$, $\varepsilon_{ave} = \sigma_{ave}/E$
   Depends on geometry of notch and material; $K_\varepsilon = K_t$ for perfectly elastic material, $K_\varepsilon > K_t$ for ductile material
   Has no engineering units

Stress intensity factor: A measure of the severity of a crack, or the intensity of the stress field near the crack tip. There are many, potentially confusing, forms of this factor, having identical engineering units of stress $\sqrt{\text{length}}$, but a variety of definitions and applications. A few are listed concisely:

a. Opening-mode stress intensity factor, K_I
   Depends on geometry of a crack and applied stress, not on material
   Units of stress $\sqrt{\text{length}}$
b. Plane strain fracture toughness, K_{IC}
   Depends on material but not on geometry above a certain thickness, and not on applied stress
   Units of stress $\sqrt{\text{length}}$
c. Stress intensity factor range, $\Delta K = K_{max} - K_{min}$
   Depends on geometry of a crack and applied cyclic stress, not on material
   Units of stress $\sqrt{\text{length}}$

References

STATICS AND DYNAMICS

Hibbeler, R. C. 1995. *Engineering Mechanics: Statics and Dynamics*, 7th ed. Prentice-Hall, Englewood Cliffs, NJ.

Sandor, B. I. 1987. *Engineering Mechanics Statics and Dynamics*, 2nd ed. Prentice-Hall, Englewood Cliffs, NJ.

VIBRATIONS

Harris, C. M. and Crede, C. E. 1988. *Shock and Vibration Handbook*, 3rd ed. McGraw-Hill, New York.

James, M. L., Smith, G. M., Wolford, J. C., and Whaley, P. W. 1994. *Vibration of Mechanical and Structural Systems*, 2nd ed. Harper Collins College Publishers, New York.

Wowk, V. 1991. *Machinery Vibration: Measurement and Analysis*. McGraw-Hill, New York.

Wowk, V. 1993. *Machinery Vibration: Balancing*. McGraw-Hill, New York.

MECHANICS OF MATERIALS

Dally, J. W. and Riley, W. F. 1991. *Experimental Stress Analysis*, 3rd ed. McGraw-Hill, New York.

Hibbeler, R. C. 1997. *Mechanics of Materials*, 3rd ed. Prentice-Hall, Englewood Cliffs, NJ.

Jawad, M. H. and Farr, J. R. 1989. *Structural Analysis and Design of Process Equipment*, 2nd ed. John Wiley & Sons, New York.

Kobayashi, A. S. (ed). 1993. *Handbook on Experimental Mechanics*, 2nd ed. Society for Experimental Mechanics, Bethel, CT.

Young, W. C. 1989. *Roark's Formulas for Stress and Strain*, 6th ed. McGraw-Hill, New York.

STRUCTURAL INTEGRITY AND DURABILITY

Anderson, T. L. 1994. *Fracture Mechanics: Fundamentals and Applications*, 2nd ed., CRC Press, Boca Raton, FL.

Boyer, J. E. 1986. *Atlas of Fatigue Curves*. American Society for Metals, Metals Park, OH.

Cook, R. D. 1995. *Finite Element Modeling for Stress Analysis*. John Wiley & Sons, New York.

Dowling, N. E. 1993. *Mechanical Behavior of Materials*. Prentice-Hall, Englewood Cliffs, NJ.

Fuchs, H. O. and Stephens, R. I. 1980. *Metal Fatigue in Engineering*. John Wiley & Sons, New York.

Gallagher, J. P. (ed). 1983. *Damage Tolerant Design Handbook*, 4 vols. Metals and Ceramics Information Ctr., Battelle Columbus Labs, Columbus, OH.

Murakami, Y. (ed). 1987. *Stress Intensity Factors Handbook*, 2 vols. Pergamon Press, Oxford, U.K.

Rice, R. C. (ed). 1988. *Fatigue Design Handbook*, 2nd ed. SAE Publ. No. AE-10. Society of Automotive Engineers, Warrendale, PA.

Further Information

Many technical societies are active in various areas of mechanics of solids, and they are excellent, steady sources of long-accepted and new information, some of which is available within hours. They also organize committee work, conferences, symposia, short courses, and workshops; establish codes and standards; and publish books, papers, journals, and proceedings, covering the latest developments in numerous specialties. A short list of societies is given here; note that they tend to have international breadth, regardless of the name. It is wise to belong to several relevant societies and at least scan their announcements.

ASM International (formerly American Society for Metals) (800-336-5152)
ASME — American Society for Mechanical Engineers (800-843-2763)
ASNT — American Society for Nondestructive Testing (800-222-2768)
ASTM — American Society for Testing and Materials (215-299-5585)
SAE — Society of Automotive Engineers (412-776-4841)
SEM — Society for Experimental Mechanics (203-790-6373)
SES — Standards Engineering Society (513-223-2410)

As a hint of the scope and magnitude of what is available from the large technical societies, here are selected offerings of ASTM:

- ASTM Staff Access/Tel: 215-299-5585; Fax: 215-977-9679; E-mail: infoctr@local.astm.org
- *ASTM Standardization News*, a monthly magazine; regularly presents information on "the development of voluntary full consensus standards for materials, products, systems and services and the promotion of related knowledge… the research, testing and new activities of the ASTM standards-writing committees… the legal, governmental and international events impacting on the standards development process" (quotes from the masthead).
- Over 50 volumes of ASTM Standards

  Samples of standards:

  Friction, wear, and abrasion (B611 on wear resistance of carbides; G77 on ranking of materials in sliding wear)

  Fracture mechanics (E399 on fracture toughness testing of metals)

  Fatigue (E466 on axial fatigue tests of metals; D671 on flexural fatigue of plastics)
- Training courses for ASTM Standards (215-299-5480)

- ASTM International Directory of Testing Laboratories
- ASTM Directory of Scientific & Technical Consultants & Expert Witnesses
- ASTM Special Technical Publications (STP) are books of peer-reviewed papers on recent research and developments

  Samples of STPs:

  STP 1198 — *Nondestructive Testing of Pavements and Backcalculation of Moduli*, Second Volume; 1995

  STP 1231 — *Automation in Fatigue and Fracture: Testing and Analysis*; 1995.

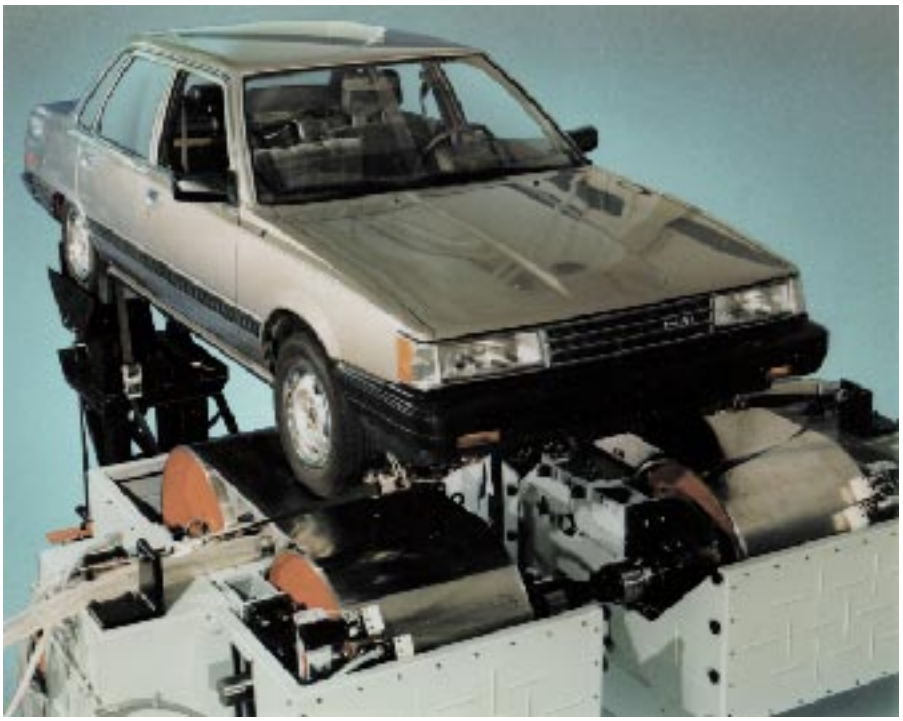

PLATE 1 Flat-Trac® Roadway Simulator, R&D 100 Award-winning system in 1993. (Photo courtesy MTS Systems Corp., Minneapolis, MN.)

PLATE 2 Spinning torque transducer with on-board preamplifier. An angular accelerometer is attached at the center of the torque cell. (Photo courtesy MTS Systems Corp., Minneapolis, MN.)

PLATE 3 Vibration screening of a circuit board using an electromagnetic shaker and a laser doppler vibration pattern imager. (Photo courtesy Ometron Inc., Sterling, VA.)

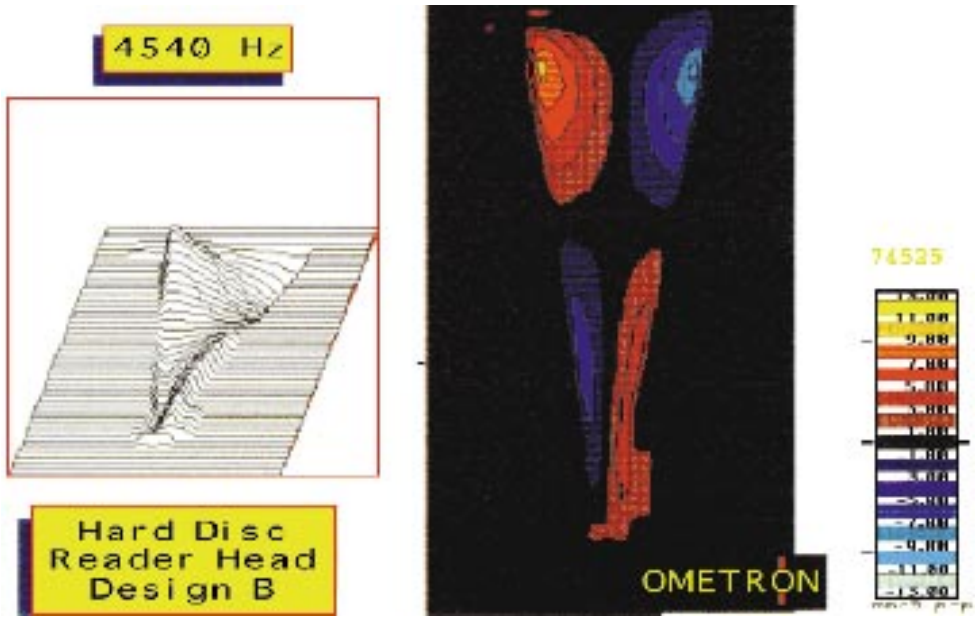

PLATE 4 Vibration patterns of a computer hard disc reader head at 4540 Hz. (Photo courtesy Ometron Inc., Sterling, VA.)

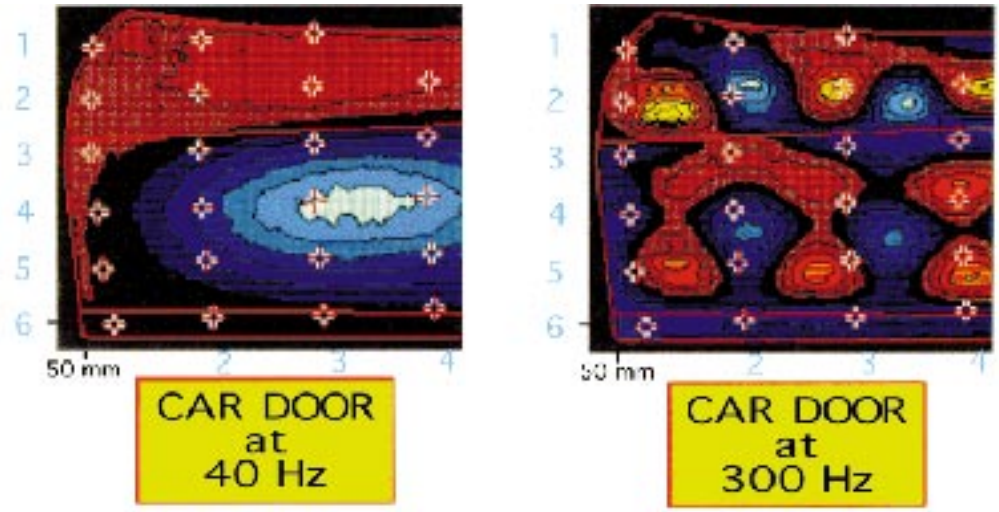

PLATE 5 Vibration patterns of a car door at 40 Hz and 300 Hz. (Photos courtesy Ometron Inc., Sterling, VA.)

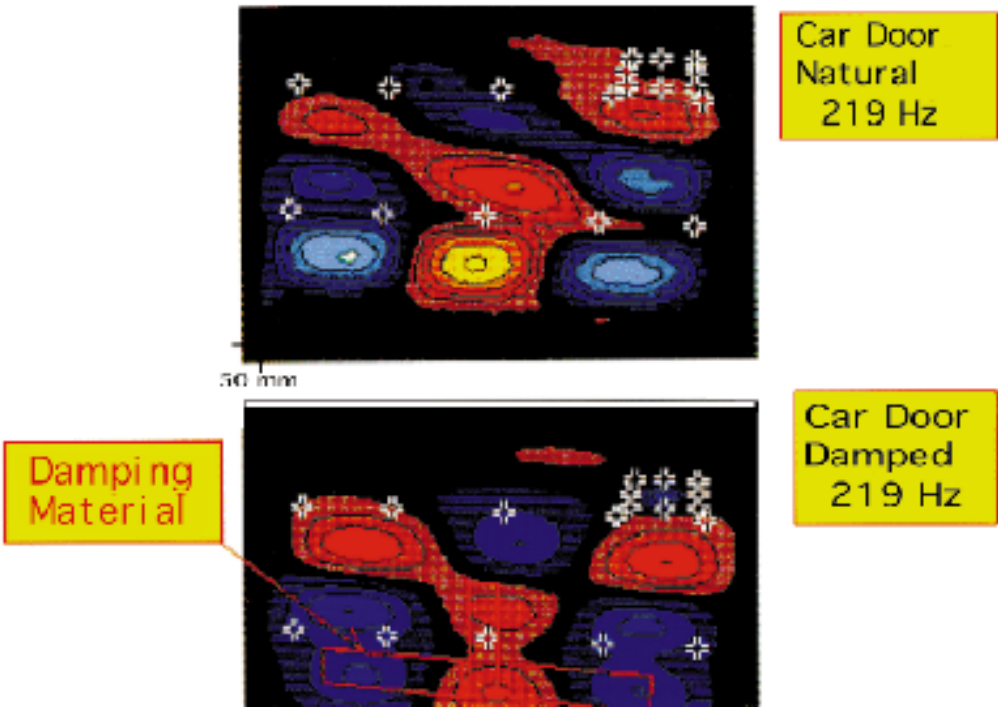

PLATE 6 Changes in the vibration patterns of a car door caused by the addition of damping material. (Photos courtesy Ometron Inc., Sterling, VA.)

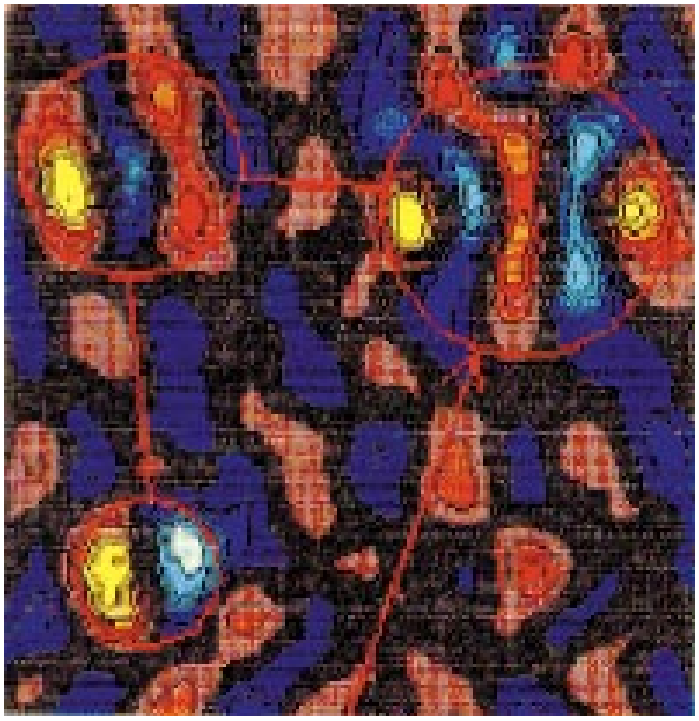

PLATE 7 Detection of delaminations in a foam-and-steel composite plate using vibration pattern imaging. (Photo courtesy Ometron Inc., Sterling, VA.)

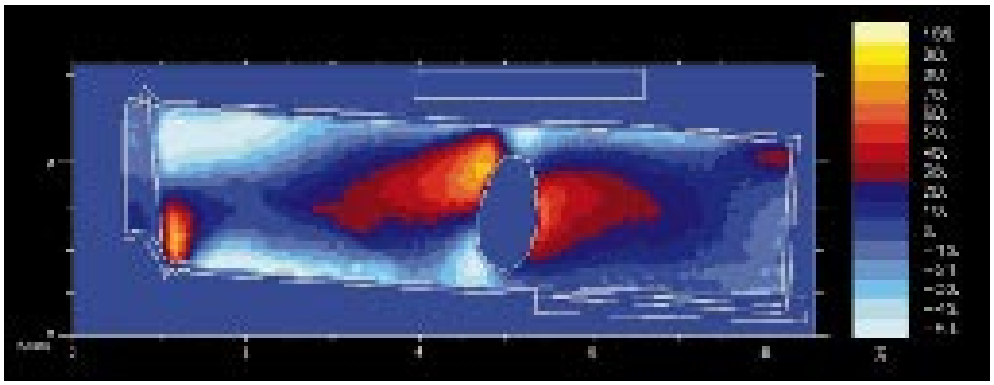

PLATE 8 Modal analysis of a vibrating turbine blade using Thermoelastic Stress Analysis. (Photo courtesy Stress Photonics Inc., Madison, WI.)

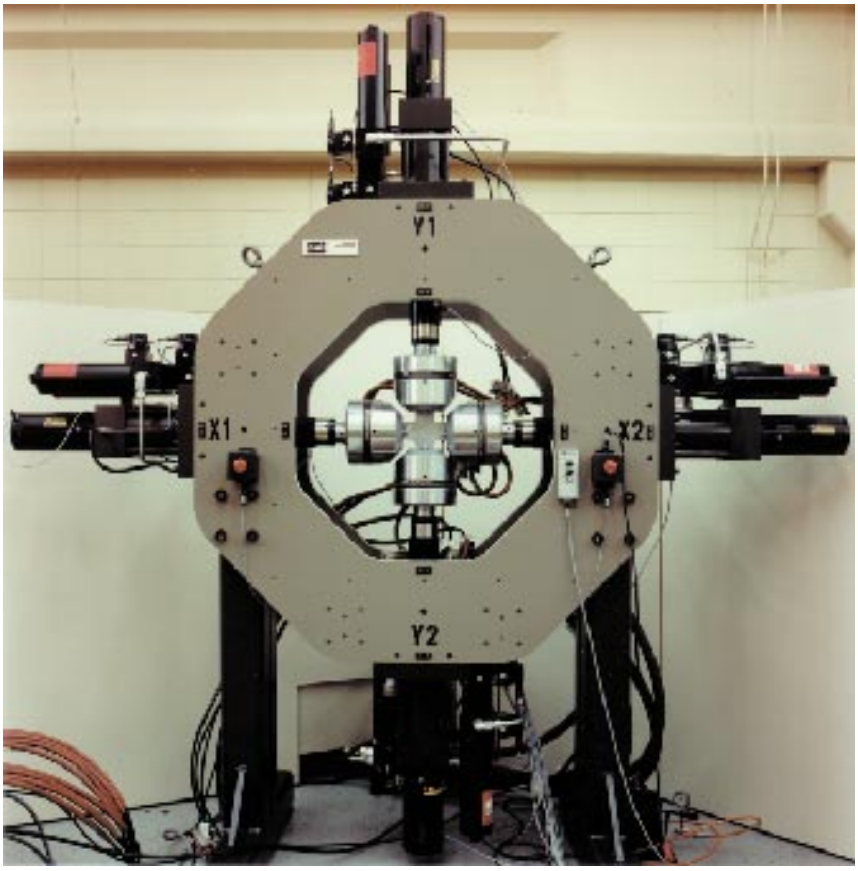

PLATE 9 Biaxial test setup. (Photo courtesy MTS Systems Corp., Minneapolis, MN.)

PLATE 10 Pressure vessel. (Photo courtesy Nooter Corp., St. Louis, MO.)

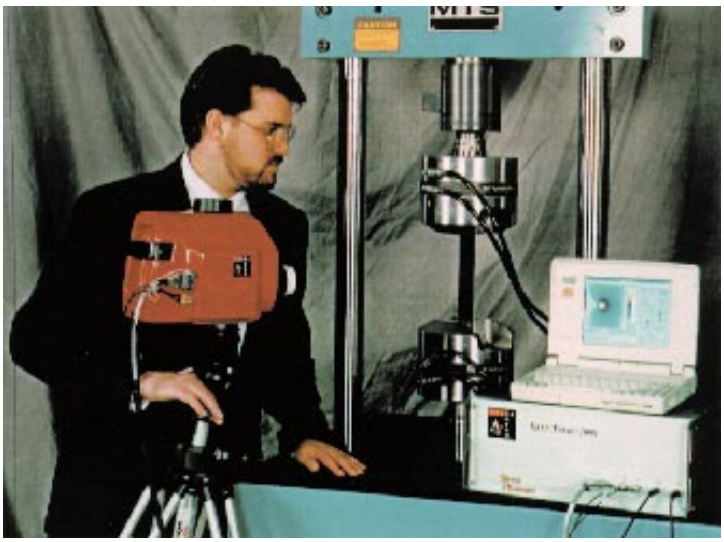

PLATE 11 Delta Therm 1000 Stress Imaging System with principal inventor Jon R. Lesniak. R&D 100 Award-winning instrument in 1994. (Photo courtesy Stress Photonics Inc., Madison, WI.)

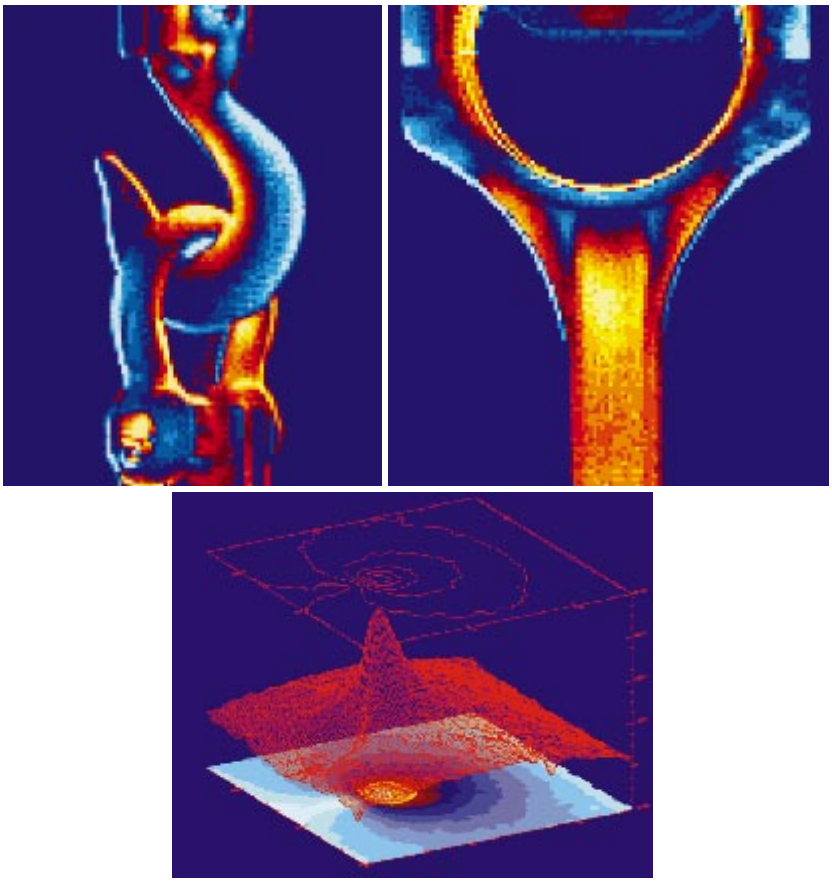

PLATE 12 TSA stress images and samples of data processing by Delta Therm instrument (Color Plate 11). (Photo courtesy Stress Photonics Inc., Madison, WI.)

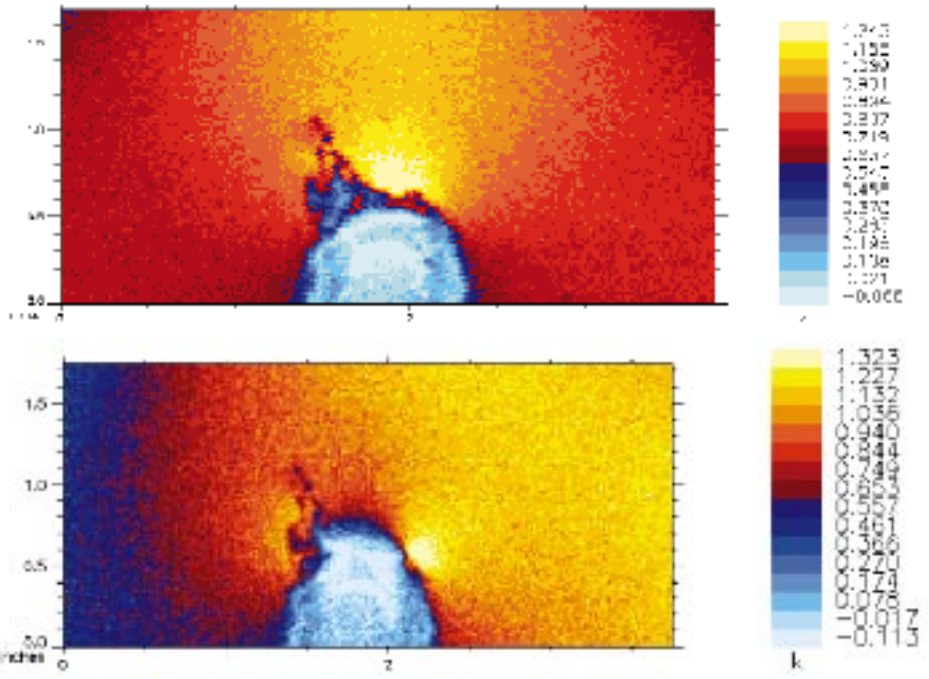

PLATE 13 TSA stress images showing damage evolution at a weld. Top: beginning of fatigue testing; yellow shows stress concentration at weld toe (no crack); dark blue spots represent lower stress at weld splatter. Bottom: gross and uneven stress redistribution to tips of crack (≈ 0.5 in. long) after 1 million cycles. (Photos courtesy Mark J. Fleming, University of Wisconsin-Madison.)

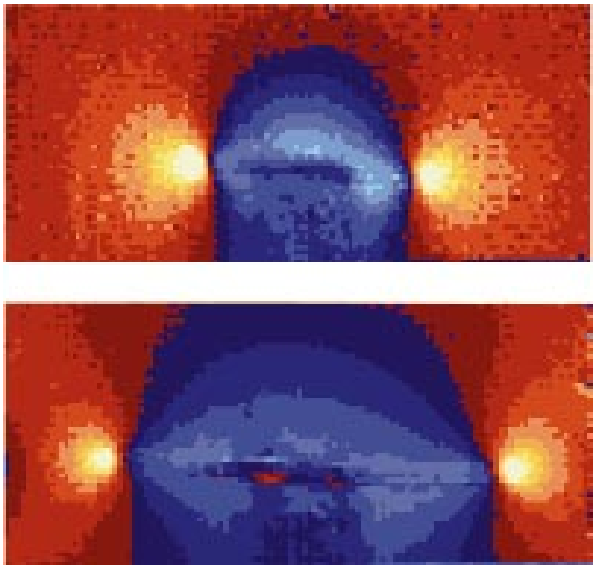

PLATE 14 Direct measurement of crack length and stress intensity factors by TSA stress imaging. Top: crack at 41,000 cycles. Bottom: crack at 94,000 cycles; light shows through the crack; blues show stress relief at crack faces and nearby. (Photos courtesy Mark J. Fleming, University of Wisconsin-Madison.)

PLATE 15 Closed-loop, electro-hydraulic mechanical testing systems. (Photo courtesy MTS Systems Corp., Minneapolis, MN.)

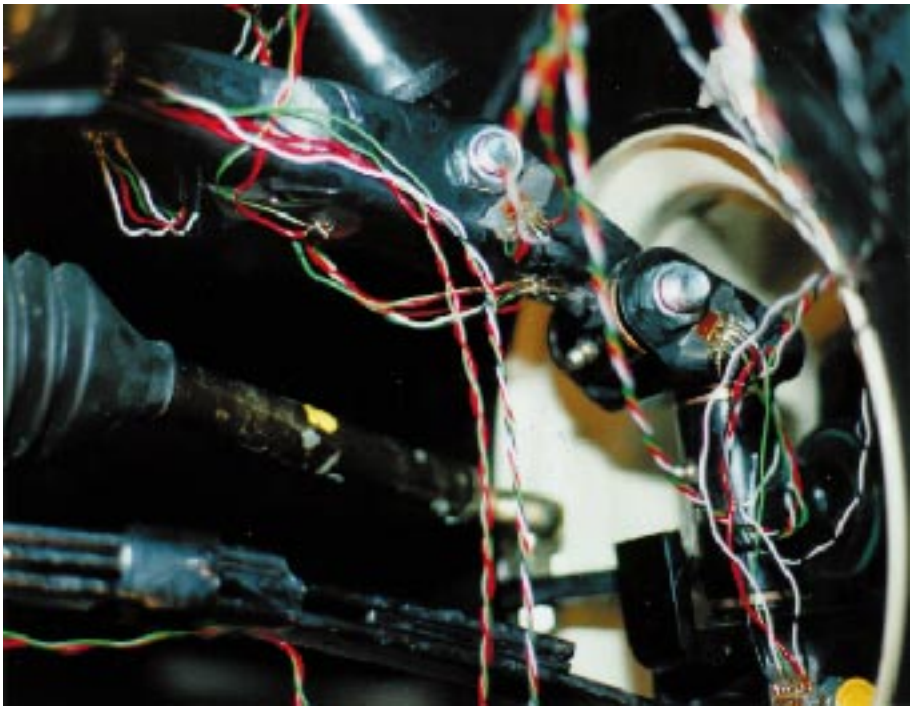

PLATE 16 Strain-gauging of a vehicle's suspension system in progress.